

**Nucleophilic Activation of Carbon Monoxide:
Synthesis, Characterization and Reactivity of
Intramolecular Group VI Metallaesters**

Thesis by

Thomas Smith Coolbaugh

**In Partial Fulfillment of the Requirements
for the Degree of
Doctor of Philosophy**

**California Institute of Technology
Pasadena, California**

1985

(Submitted June 20, 1984)

To Joye

Acknowledgement

I am grateful to Bob Grubbs for giving me the opportunity to do some organometallic chemistry in an amenable, if unrenovated, atmosphere. The Grubbs' group members (past and present) have been truly helpful and I'm glad I had the chance to work with them, even though it may have been more in spirit than in practice.

I would also like to thank Bernie Santarsiero and Bob Coots for their help in solving the crystal structures. I am also grateful to Professors Marsh and Schaefer for their helpful advice.

Finally, I would like to express my appreciation to my parents and Joye's for their offers of places to stay in the San Francisco and Boston areas during much needed escapes from the greater LA area.

Abstract

An investigation of the design and reactivity of bifunctional transition metal complexes pertinent to homogeneous reduction of carbon monoxide is presented. Oxygen nucleophiles were incorporated into Group VI metal carbonyl complexes *via* cyclopentadienyl ligands.

Neutral molybdenum dimers yield no intramolecular nucleophilic interaction between an alcohol, attached by different bridging arm lengths, and the metal carbonyl fragment. A crystal structure of the propanol substituted cyclopentadienyl molybdenum tricarbonyl dimer (space group $P\bar{1}$, $a = 7.487 \text{ \AA}$, $b = 7.713 \text{ \AA}$, $c = 10.902 \text{ \AA}$, $\alpha = 99.360^\circ$, $\beta = 81.460^\circ$, $\gamma = 115.260^\circ$, $V = 563.0 \text{ \AA}^3$, $Z = 1$) indicates only an intermolecular hydrogen bond between alcohols.

The synthesis of the cationic compounds, $[\text{CpRM}(\text{CO})_3\text{L}]^+\text{BF}_4^-$ is reported, where $M = \text{Mo}$, W and $R = -(\text{CH}_2)_n-\text{OH}$ with $n = 1-3$. Deprotonation of the alcohols leads to intramolecular metallaester formation for the methylene and ethylene bridged compounds. The equilibria established upon reaction with external alcohols are reported as are the thermodynamic parameters associated with the process.

Crystal structures of the metallaesters bridged by a methylene (space group $P2_1/n$, $a = 7.867 \text{ \AA}$, $b = 17.083 \text{ \AA}$, $c = 17.768 \text{ \AA}$, $\beta = 100.959^\circ$, $V = 2344.4 \text{ \AA}^3$, $Z = 4$) and ethylene group (space group $P2_1/n$, $a = 8.127 \text{ \AA}$, $b = 16.823 \text{ \AA}$, $c = 17.623 \text{ \AA}$, $\beta = 101.980^\circ$, $V = 2357.1 \text{ \AA}^3$, $Z = 4$) are presented. A comparison of the structures is given.

Reaction of the intramolecular metallaesters with molecular hydrogen produces no volatile products. Reaction with stoichiometric hydride sources yields

compounds of relevance to carbon monoxide reduction. Reactions with Me^+ and water are presented, the latter giving rise to a stoichiometric analog of the water-gas shift reaction.

Table of Contents

	<i>(Page)</i>
Chapter 1. Synthesis of Transition Metal Carbonyl Complexes Containing Intramolecular Nucleophiles	
Introduction	2.
Results and Discussion	11.
Experimental	23.
Notes and References	38.
Chapter 2. Synthesis, Characterization and Equilibrium Studies of Group VI-B Intramolecular Metallaesters	
Introduction	45.
Results and Discussion	46.
Experimental	78.
Notes and References	96.
Chapter 3. Reactivity of Group VI-B Intramolecular Metallaesters	
Introduction	103.
Results and Discussion	105.
Experimental	127.
Notes and References	134.

List of Tables

	(Page)
Chapter 1.	
Table 1.1. IR Stretching Frequencies of $[\eta^5\text{-C}_5\text{H}_4\text{-(CH}_2\text{)}_n\text{OH Mo(CO)}_3\text{]}_2$.	12.
Table 1.2. Best Least Square Plane and Torsion Angles	17.
Table 1.3. CO Stretching Frequencies of $[\text{Cp-(CH}_2\text{)}_n\text{OH M(CO)}_3\text{PPh}_3]^+$.	20.
Table 1.4. Hydroxyl Stretching Frequencies of $[\text{Cp-(CH}_2\text{)}_n\text{OH M(CO)}_3\text{PPh}_3]^+$ at High Dilution(ca. 10 mM)	22.
Table 1.5. Summary of Data Collection and Refinement Parameters . . .	34.
Table 1.6. Atom Coordinates ($\times 10^4$) and U_{eq} 's ($\text{\AA}^2 \times 10^4$)	35.
Table 1.7. Gaussian Amplitudes ($\times 10^4$)	36.
Table 1.8. Coordinates of Hydrogen Atoms ($\times 10^3$)	37.
Chapter 2.	
Table 2.1. IR Stretching Frequencies	47.
Table 2.2. ^1H and ^{31}P NMR Data	48.
Table 2.3. Best Least Square Plane and Torsion Angles for 2b	58.
Table 2.4. Thermodynamic Parameters for Intra to Intermolecular Equilibration	65.
Table 2.5. Lactone Hydrolysis Equilibria	69.
Table 2.6. Best Least Square Plane and Torsion Angles for 2g	75.
Table 2.7. Summary of Data Collection and Refinement Parameters for 2b	86.
Table 2.8. Bond Lengths and Angles for 2b	87.

Table 2.9. Atom Coordinates ($\times 10^4$) and U_{eq} 's ($\text{\AA}^2 \times 10^4$) for 2b	88.
Table 2.10. Gaussian Amplitudes for 2b ($\times 10^4$)	89.
Table 2.11. Coordinates of Hydrogen Atoms for 2b ($\times 10^3$)	90.
Table 2.12. Summary of Data Collection and Refinement	
Parameters for 2g	91.
Table 2.13. Bond Lengths and Angles for 2g	92.
Table 2.14. Atom Coordinates ($\times 10^4$) and U_{eq} 's ($\text{\AA}^2 \times 10^4$) for 2g	93.
Table 2.15. Gaussian Amplitudes for 2g ($\times 10^4$)	94.
Table 2.16. Coordinates of Hydrogen Atoms for 2g ($\times 10^3$)	95.
Chapter 3.	
Table 3.1. Hemiacetal to Hydroxy-Aldehyde Equilibria	116.

List of Figures

	(Page)
Chapter 1.	
Figure 1.1. Stereoview of ORTEP of $[(\eta^5\text{-C}_5\text{H}_4\text{-(CH}_2)_3\text{OHMo(C)}_3)_2]$. . .	14.
Figure 1.2. Atom labeling scheme for $[(\eta^5\text{-C}_5\text{H}_4\text{-(CH}_2)_3\text{OHMo(CO)}_3)_2]$. . .	15.
Figure 1.3. Selected bond lengths and angles for the structure of $[(\eta^5\text{-C}_5\text{H}_4\text{-(CH}_2)_3\text{OHMo(CO)}_3)_2]$	16.
Figure 1.4. ORTEP diagram showing the unitcell of $[(\eta^5\text{-C}_5\text{H}_4\text{-(CH}_2)_3\text{OHMo(CO)}_3)_2]$	18.
Chapter 2.	
Figure 2.1. 500 MHz ^1H NMR spectrum of 2d	49.
Figure 2.2. Difference NOE (500 MHz) spectrum of 2d upon irradiation of <i>ortho</i> protons of the p-tolyl groups	51.
Figure 2.3. Stereoview ORTEP diagram of 2b	53.
Figure 2.4. Atom labeling scheme for 2b	54.
Figure 2.5. Selected bond lengths for 2b	55.
Figure 2.6. Selected bond angles for 2b	56.
Figure 2.7. Stereoview ORTEP diagram of 2b viewed along C(1)–W–P	62.
Figure 2.8. van t'Hoff plot for the equilibration of 2 with MeOH	64.
Figure 2.9. Stereoview ORTEP diagram of 2g	71.
Figure 2.10. Atom labeling scheme for 2g	72.
Figure 2.11. Selected bond lengths for 2g	73.
Figure 2.12. Selected bond angles for 2g	74.

Figure 2.13. ORTEP diagram of **2g** showing the Cp orientation 76.

Figure 2.14. Stereoview of ORTEP diagram of **2g** viewed along C(1)–W–P 76.

Chapter 1

**Synthesis of Transition Metal Carbonyl Complexes
Containing Intramolecular Nucleophiles**

Introduction

Recently, much interest has been exhibited with respect to the synthesis of hydrocarbons from a mixture of carbon monoxide and hydrogen (synthesis gas).¹ While this has waned to some extent currently, it is expected that renewed concern for a synthetic approach will be shown in the not too distant future owing to the unstable world petroleum oil supply.

Serious study of catalytic hydrogen reduction of carbon monoxide began in the early 1900's when Sebatier and Senderens reported the synthesis of methane from CO and hydrogen utilizing a reduced nickel catalyst.² Following this a number of other processes were reported and in 1923, Fischer and Tropsch reported that an alkaline iron catalyst could be used for the formation of mostly oxygenated hydrocarbons at 100-150 atm CO/H₂ and 400-450°C.³ First known as the Synthol process, the Fischer-Tropsch synthesis (eq 1.1) enabled the Germans to produce 600,000 tons of fuels per year by 1944, a period when their petroleum resources were seriously curtailed.



Currently South Africa is using a heterogeneous iron catalyst at 25 atm and 220-240° C in a Fischer-Tropsch process.^{1a,4} South Africa possesses vast amounts of coal and essentially no oil reserves and as such, Fischer-Tropsch chemistry is attractive. Coal is readily transformed into a CO/H₂ mixture by steam reforming and although the mixture is generally not rich enough in hydrogen (being about 1:1), the ratio may be altered *via* the water-gas shift reaction

(1.2).⁵

Thus, synthesis gas (possibly coal derived) is a viable starting point in the production of hydrocarbons and their oxygenated derivatives.

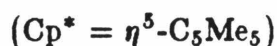
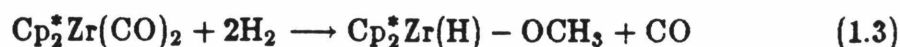
One of the principal aims of recent research has been the development of a homogeneous system that will catalyze Fischer-Tropsch type chemistry, the reason being that the classical catalysts exhibit low selectivity for any one desired product. With homogeneous systems it is often the case that better system control may be achieved and the active species may be more easily regulated.⁶ Also of importance is the fact that homogeneous systems may be studied more easily with standard techniques and the intermediates or their precursors (or their analogs) can sometimes be isolated and characterized unambiguously.^{7,8}

A number of approaches have been explored with respect to homogeneous catalysis of CO reduction. One of these has entailed the use of metal clusters since some investigators believe that these are required in order to mimic, to some extent, the activity that is seen on metal surfaces. It was believed that a mononuclear transition metal complex would not provide the requisite activation of carbon monoxide while allowing for the simultaneous (or subsequent) reaction with molecular hydrogen.

In fact, a number of clusters do catalyze the reduction of CO under reasonably mild conditions, e.g., $\text{Ir}_4(\text{CO})_{12}$ at 140°C and 2 atm pressure reduces CO to methane.⁹ However, low conversion was observed (1 % in 3-5 days) and it was not clear what the active species was. Introduction of Lewis acids as in the mixtures $\text{Ir}_4(\text{CO})_{12}/\text{NaCl-AlCl}_3$ and $\text{Os}_3(\text{CO})_{12}/\text{BBr}_3$ improved the activities

but again, the active species were apparently something other than the original metal clusters.^{10,11} The hydrogenation studies carried out by two groups using ruthenium carbonyl clusters have indicated that the active species may be derived from $\text{Ru}(\text{CO})_5$, thus pointing out the fact that mononuclear complexes may be involved.^{12,13}

While it appears that mononuclear species may be important, few unequivocal examples have been reported of the catalytic reduction of carbon monoxide with this type of complex. Generally the mononuclear cases have involved stoichiometric reactions using the oxophilicity of early transition metals as the driving force for the reduction (eqs 1.3 & 1.4).^{14,15}



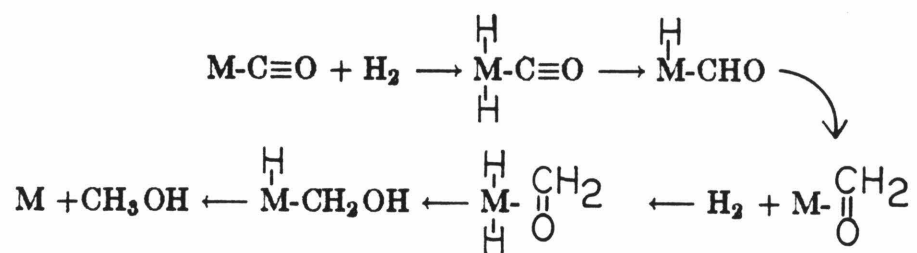
In the case of the Zr reaction, treatment of the methoxy hydride species with HCl yielded methanol, molecular hydrogen and permethylzirconocenedichloride.¹⁴ The titanium reaction is interesting in that substitution of H_2 with D_2 yields CD_4 but the reaction proceeds in the absence of CO since the only carbon source is apparently the initial carbonyl ligands since after 48 hours the blue inactive species shown on the right of eq 1.4 is the final titanium product.¹⁵

Stoichiometric hydrogen sources such as hydrides have been investigated as well. Among the first reported hydride reductions of coordinated carbon monoxide was the reaction of $[\text{CpMo}(\text{CO})_3\text{PPh}_3]^+$ with sodium borohydride to give the

neutral methyl complex, $\text{CpMo}(\text{CO})_2\text{PPh}_3(-\text{CH}_3)$.¹⁶ It is believed that the reduction proceeds first through formyl, then to the hydroxymethyl and finally on to the methyl species.¹⁷ Recently the synthesis of the formyl has been effected in high yield by treatment of the cation with hydride at low temperature.¹⁸ Similarly, the synthesis of the rhenium methyl complex, $\text{CpRe}(\text{CO})(\text{NO})-\text{CH}_3$, was carried out by reduction of a CO ligand by hydride.¹⁹ It was more recently shown that the individual reduction products (formyl, hydroxymethyl and methyl) could be observed separately.^{20,21,22} A number of hydroxymethyl complexes have now been reported in the literature.^{23,24,25}

The reason for the vigorous interest in the hydroxymethyl and formyl complexes is that they represent species that may be involved in the Fischer-Tropsch synthesis and as such may serve as valid models in the individual reaction steps of the process (Scheme 1.1).²⁶

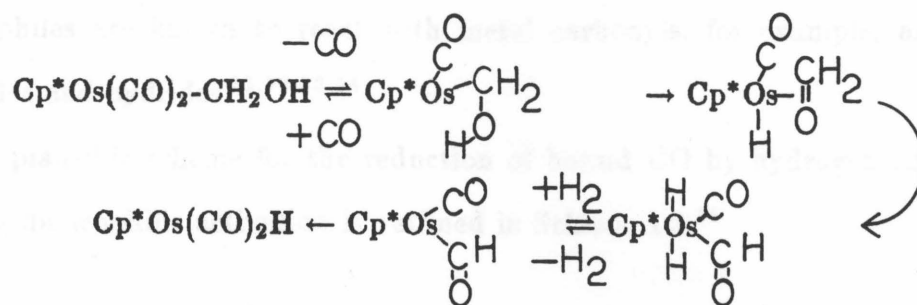
Scheme 1.1



While the forward reaction of the formal insertion of a carbonyl ligand into a metal hydride bond is not favored, recently the decomposition of a hydroxymethyl species $\text{Cp}^*\text{Os}(\text{CO})_2(-\text{CH}_2\text{OH})$, formed by NaBH_4 reduction of the tricarbonyl cation, has been observed to proceed with loss of CO and H_2 to ultimately give the hydride, $\text{Cp}^*\text{Os}(\text{CO})_2\text{H}$.²⁷ The decomposition gives the hydride

in good yield and based on the decomposition of the same compound with the hydroxymethyl ligand doubly deuterated on the methylene carbon, the reaction pathway shown in Scheme 1.2 was proposed.

Scheme 1.2



The final hydride ligand originates on the hydroxymethyl methylene since the deuterated compound affords the osmium deuteride and HD. Although the reverse of Scheme 1.2 may not be thermodynamically favorable, it does consist of a number of interesting, plausible steps that on the microscopic level are of relevance to the Fischer-Tropsch process (Scheme 1.1).²⁸

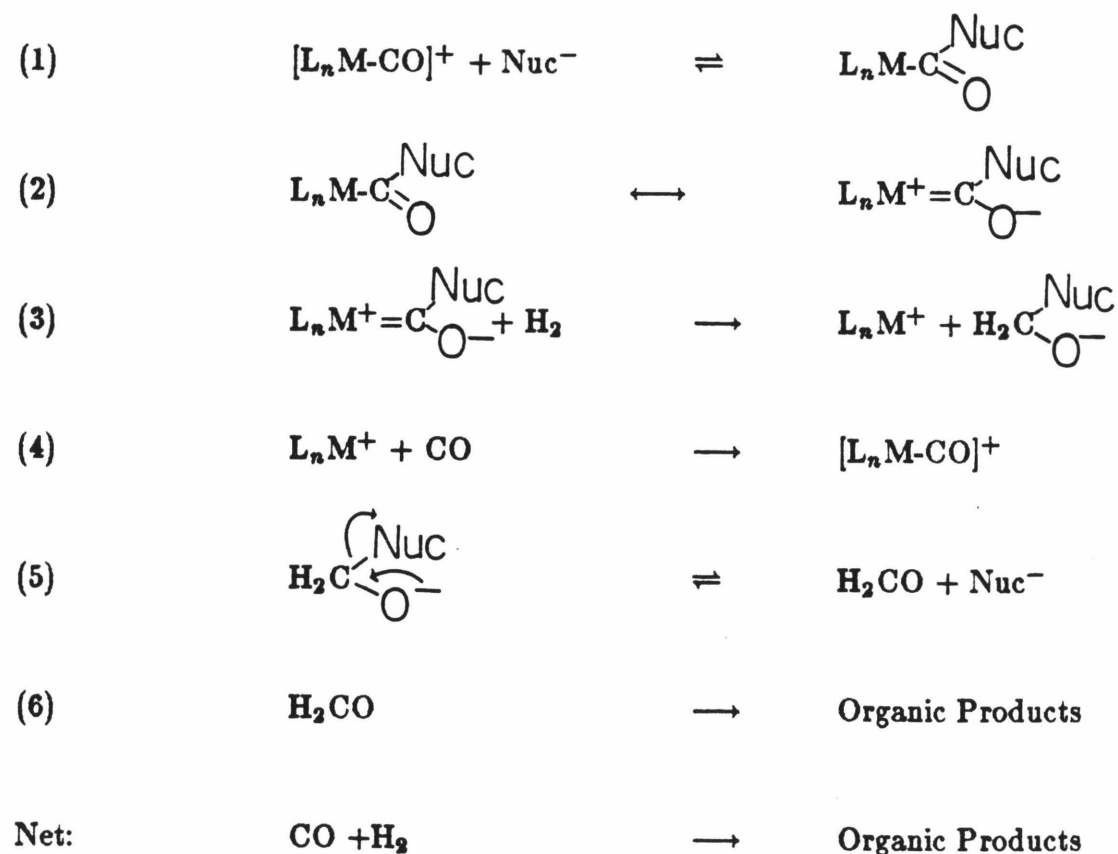
The importance of the formyl species has been suggested by a number of investigators.^{1a,7,29,30} While there are few examples of direct insertion of carbon monoxide into a metal-formyl bond, the formyl ligand is an attractive intermediate when one considers the synthesis of hydrocarbons from synthesis gas.^{1a} During hydrogen reduction of carbon monoxide CO bonds are broken and C-H bonds are formed, at which point the formyl ligand is one of the simplest early species that may be imagined.

Be that as it may, the research to be described entails an investigation of the possibility of obtaining a homogeneous system that will react with CO/H₂ catalytically under mild conditions to give Fischer-Tropsch type products. Two

modes of activating bound CO to reduction present themselves, the first being nucleophilic attack at carbon to reduce the CO bond order and the second is electrophilic attack at the CO oxygen. The electrophilic mode is well known and examples are the carbonyl cluster reactions with Lewis acids that were mentioned above. In the work to be described, the nucleophilic mode was chosen. Many nucleophiles are known to react with metal carbonyls, for example, amines, alkoxides and hydrides.^{31,32,33,34}

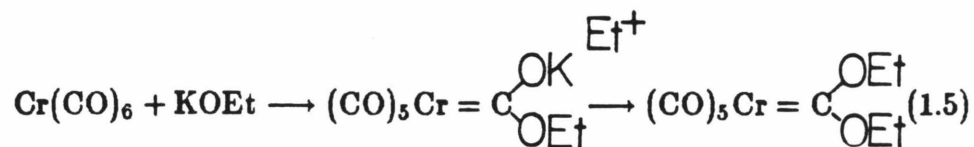
A plausible scheme for the reduction of bound CO by hydrogen and employing nucleophilic activation is outlined in Scheme 1.3.³⁵

Scheme 1.3

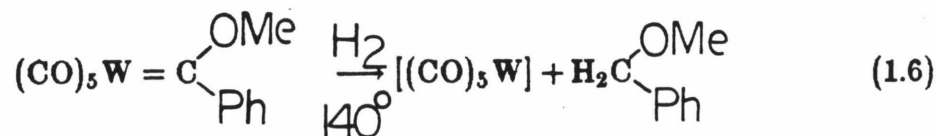


The overall thermodynamics should in all probability be favorable (e.g., for the formation of methanol, $\Delta G_f^\circ = -6.0 \text{ kcal/mol}$).³⁶ Even the unfavorable formation of formaldehyde ($\Delta G_f^\circ = 6.5 \text{ kcal/mol}$) may be mediated to some extent by coordination to the transition-metal center.^{36,37} Formaldehyde may serve as an intermediate to other products.

The reaction presented in (1) is commonplace (*vide supra*) and it is usually observed that the resonance shown in (2) is significant as evidenced by carbonyl stretches of metalloesters being displayed at about 1600 cm^{-1} , an energy region somewhat below that of their organic analogs.^{22,38,39} Additionally, the synthesis of Fischer carbenes frequently employs (1) followed by reaction with an alkyl cation which adds at the anionic oxygen of the right hand resonance form of (2) (eq 1.5).⁴⁰



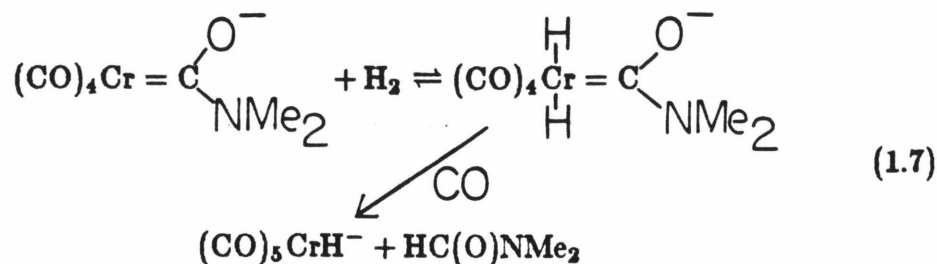
The subsequent reduction of the carbenoid ligand shown in (3) has precedent in the reaction of pentacarbonyltungsten-phenylmethoxy carbene with molecular hydrogen at 140° C in decalin to give benzylmethylether in 92 % yield (eq 1.6).⁴¹



Whether the reaction proceeds in one step or two (with a $\text{W}-(\text{CH}(\text{Ph})(\text{OMe}))$ species as intermediate) is not clear but it is known that H_2 is the hydrogen

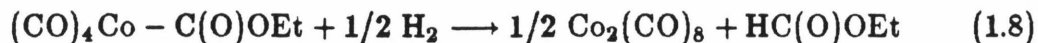
source since running the reaction in deuterated solvent did not give deuterated product (with the analogous diphenylcarbene).⁴¹

Also of interest with respect to (3) is the mechanism proposed for the formation of dimethylformamide from the reaction of an anionic carbene and hydrogen (eq 1.7).³⁵



Although the nucleophile used to activate CO is irretrievably lost to the product, the hydrogenation step is promising. This step may be the reductive elimination from the anionic carbamoyl resonance form, $(\text{CO})_4\text{Cr}^-(\text{H})_2(-\text{C}(\text{O})\text{NMe}_2)$.

An analogous reaction has been observed with a cobalt metalloester (eq 1.8).⁴² The reaction entails only partial reduction of the carbonyl and the effective nucleophile (EtO^-) remains part of the product.



The coordination of CO to the resulting unsaturated metal species (4) is expected and generation of formaldehyde while regenerating the nucleophile from the organic fragment (5) is quite reasonable since nucleophilic addition to formaldehyde (eg. with water) is generally reversible.⁴³ The scheme as out-

lined is a good starting point in an investigation of the homogeneously catalyzed reduction of carbon monoxide using a transition-metal complex.

In order to favor the nucleophilic attack of a base of moderate nucleophilicity, the possibility of intramolecular deployment presents itself as a means of keeping the effective concentration of nucleophile high by maintaining the two reacting groups in close proximity to each other. In this manner, the two equilibria shown in (1) and (5) may be more favored in the desired directions. An additional benefit may be that partially reduced products (*vide supra*) may have a further opportunity to react with H_2 since their proximity to the metal center will be greatly enhanced. Furthermore, bifunctional catalysts containing both nucleophile and a carbonyl ligand should provide information about the requirements for interaction between the two groups and as such, may serve as general models for the design of molecular systems while serving in the specific area of carbon monoxide reduction.

Results and Discussion⁴⁴

A reasonable means of incorporating a nucleophile into a transition metal carbonyl compound is by the use of substituted cyclopentadienyl complexes. Some work has been done utilizing substituted arene chromium tricarbonyl compounds but no evidence for intramolecular nucleophilic attack at CO was observed.⁴⁵ Additionally, reaction of the arene ligands was observed in one case to occur most probably *via* reductive coupling.⁴⁵ As such, cyclopentadienyl compounds were chosen because of their general stability upon metal complexation as well as there being numerous Cp complexes known that undergo nucleophilic attack at the carbonyl ligands.³¹ In another vein, the cyclopentadienyl complex is attractive in that numerous examples of the synthesis of substituted Cp ligands and their transition metal complexes exist.⁴⁶ The range of these Cp-transition metal compounds is quite wide, thus offering many avenues to explore.

In this work, the nucleophiles under consideration are oxygen containing. The first complexes examined were $[\text{CpRMo}(\text{CO})_3]_2$ compounds where R = $-(\text{CH}_2)_2\text{-OH}$ and $-(\text{CH}_2)_3\text{-OH}$.⁴⁷ The syntheses are straightforward and yield suitable amounts of the desired material (the yields are somewhat lower than that of the parent compound owing to the use of one equivalent of $\text{C}_5\text{H}_5\text{R}$ rather than excess). Unfortunately, the infra-red spectra in the carbonyl stretching range reveal nothing indicative of a nucleophilic interaction between the alcohol and the $\text{Mo}(\text{CO})_3$ fragment. In fact, the $\nu(\text{CO})$ region looks quite similar for the parent compound, the alcohol substituted compounds and the triphenylmethyl ether of the ethanol substituted complex (Table 1.1). It appears that no significant interaction has occurred.

Table 1.1. IR Stretching Frequencies $[(\eta^5\text{-C}_5\text{H}_4\text{-(CH}_2\text{)}_n\text{-OH)Mo(CO)}_3]_2$

n	$\nu(\text{CO}), \text{cm}^{-1}$		
Parent	2020(<i>w</i>)	1955(<i>s</i>)	1915(<i>s</i>)
2	2002(<i>w</i>)	1953(<i>s</i>)	1908(<i>s</i>)
3	2000(<i>w</i>)	1955(<i>s</i>)	1912(<i>s</i>)
2	2040(<i>w</i>)	1955(<i>s</i>)	1915(<i>s</i>)
(trityl ether)			

^a CH₂Cl₂ solution.

In an effort to generate a stronger nucleophile and thereby induce attack at the carbonyl, the hydroxyethyl-cyclopentadienyl compound was treated with bases such as sodium hydride and sodium methoxide. The only observed product was the tricarbonyl anion obtained from simple reductive cleavage of the metal-metal bond in a manner similar to the well known amalgam reduction.

Even though no direct nucleophilic interaction occurs, the substituted dimers provide a system in which the preferred orientation of an unconstrained substituted Cp in a "four-legged piano stool" complex may be examined. With this in mind, a single crystal of $[\text{Cp}-(\text{CH}_2)_3\text{-OH Mo}(\text{CO})_3]_2$ was obtained and an x-ray structure determined. The pertinent collection data are given in Table 1.5. Figure 1.1 shows a stereoview of the complex and Figures 1.2 and 1.3 show the atom labelling scheme and bond lengths and angles.

The structural framework is much the same as that of the parent compound.⁴⁸ The cyclopentadienyl ligand is tipped only slightly (1.61°) with respect to the Cp centroid-Mo axis and there is little deviation of the ring carbons ($\leq .003 \text{ \AA}$) or C(6) ($.136 \text{ \AA}$) from planarity (Table 1.2). Additionally, the pendant arm has adopted a low energy staggered conformation with a C(7)-C(6)-C(5)-C(4) torsion of $179.0(4)^\circ$ (Table 1.2).

The hydroxyl groups form an intermolecular chain with hydrogen bonds directed approximately parallel to the x axis and $\text{O}\cdots\text{O}'$ contacts ranging from 2.69 to 3.38 \AA (Figure 1.4).⁴⁹ A three-fold disorder is associated with the alcohol oxygen (O(4)) and refinement was carried out using initial populations and coordinates obtained from a difference Fourier map.

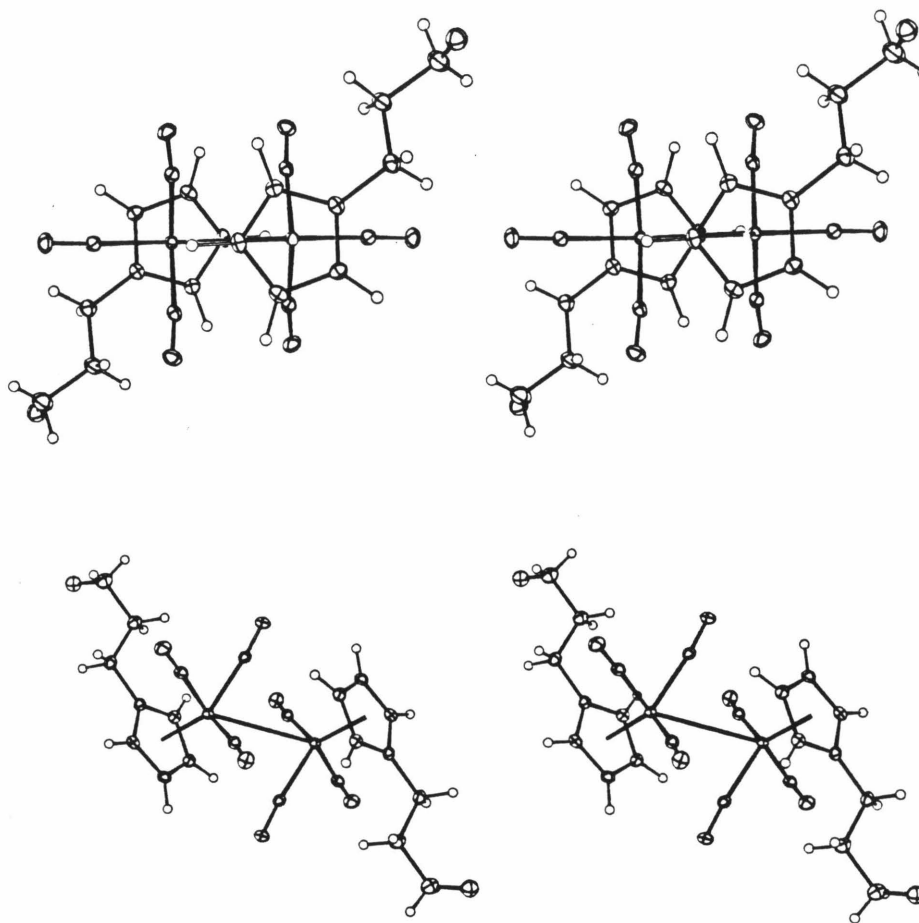


Figure 1.1. Stereoview of ORTEP of $[(\eta^5\text{-C}_5\text{H}_4\text{-(CH}_2\text{)}_3\text{OH Mo(CO)}_3)_2]$. Non-hydrogen atoms are represented by their 50 % probability ellipsoids.

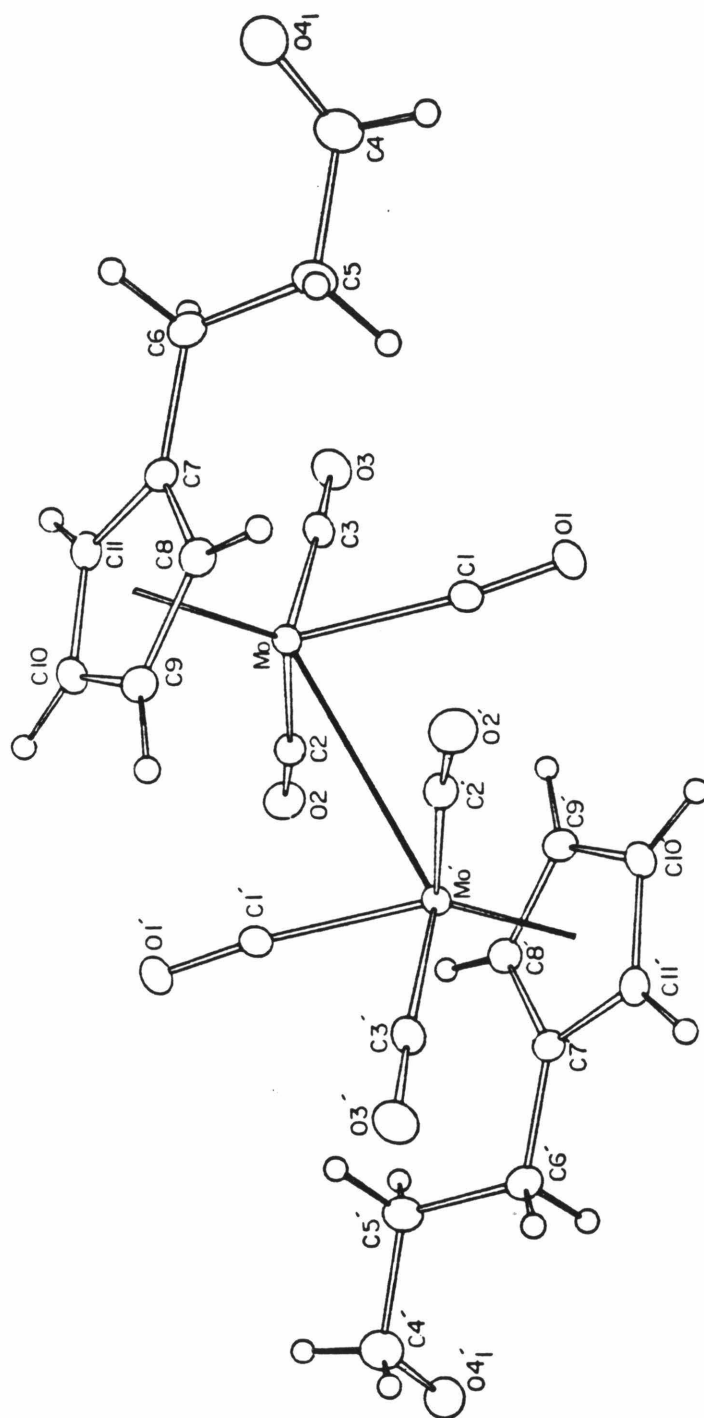


Figure 1.2. Atom labeling scheme for $[(\eta^5\text{-C}_5\text{H}_4\text{-(CH}_2)_3\text{OHMo(CO)}_3)_2]$.

Table 1.2. Best Least Square Plane and Torsion Angles

Atom	Dev ^a
C(7)	0.003
C(8)	-0.002
C(9)	0.001
C(10)	0.000
C(11)	-0.002
Mo	-2.013
C(6)	0.136

Atoms	Angle(°)
C(8)-C(7)-C(6)-C(5)	-33.4(6)
C(11)-C(7)-C(6)-C(5)	153.7(4)
C(7)-C(6)-C(5)-C(4)	-179.0(4)
C(6)-C(5)-C(4)-O(41)	-69.7(7)
C(6)-C(5)-C(4)-O(42)	67.5(9)
C(6)-C(5)-C(4)-O(43)	168.1(12)

^aDeviation in Å from best Cp plane (C(7) through C(11)).

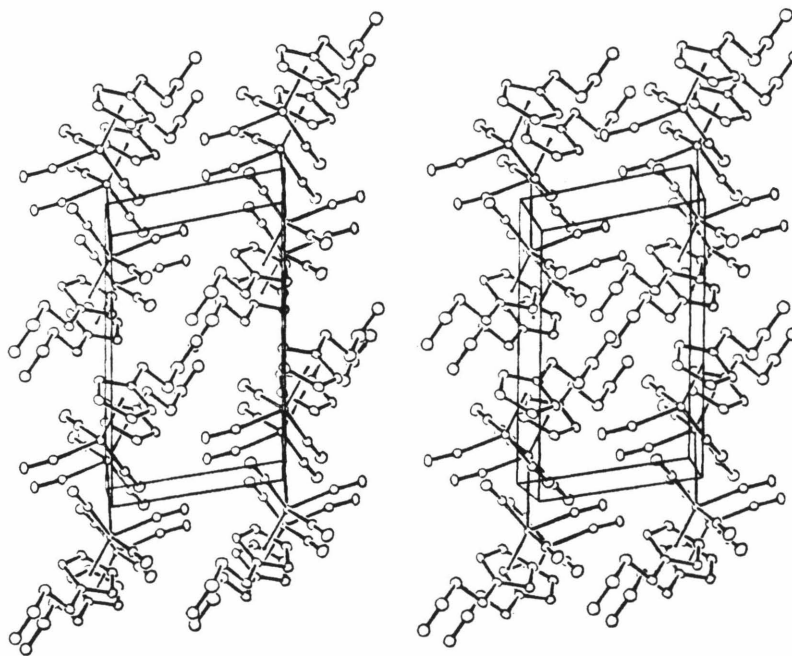


Figure 1.4. ORTEP diagram showing the unitcell of $[(\eta^5\text{-C}_5\text{H}_4\text{-(CH}_2\text{)}_3\text{OH)Mo(CO)}_3]_2$.

In any event, it is clear that the arm connecting the alcohol to the Cp possesses sufficient length to span the distance to the carbonyl ligands. It simply seems that the driving force is insufficient to induce nucleophilic attack. A means of altering this is to make the carbonyl ligands more electrophilic by putting positive charge on the metal center.

Using the substituted molybdenum dimers it is possible to generate $[\text{CpR Mo}(\text{CO})_3\text{L}]^+\text{BF}_4^-$ complexes by protonation of the tricarbonylanions followed by treatment with triphenylcarbenium tetrafluoroborate to remove the hydrogen as a hydride. Finally, introduction of L (CO, PR_3) gives the final eighteen electron cation in good yield.⁵⁰ Alternatively, the tricarbonyl anion may be formed by reaction of $\text{M}(\text{CO})_6$ and the sodium salt of the substituted cyclopentadienyl anion, thus making the synthesis of tungsten compounds possible as well. The synthesis where $n=1$ in the $\text{Cp}-(\text{CH}_2)_n\text{-OH}$ compounds first requires the reaction of formylcyclopentadienide with $\text{W}(\text{CO})_6$ to give the formyl substituted $\text{CpRW}(\text{CO})_3$ anion.⁵¹ This was subsequently reduced with sodium borohydride in ethanol to give the hydroxymethyl-Cp tungsten tricarbonyl anion from which the synthesis proceeded as in the other complexes.

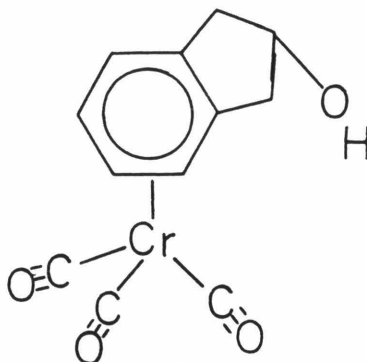
The infra-red spectra indicate that the carbonyls are more electron deficient by their shift to a higher energy region (Table 1.3). As a result, they should be more susceptible to nucleophilic attack.⁵³ Nevertheless, the CO stretches are not sufficiently different from those of the parent cations to indicate any strong interaction of the alcohol with the carbonyls. It has however been observed in chromium tricarbonyl complexes (Figure 1.5) that intramolecular hydrogen bonding may occur between the alcohol and the $\text{M}(\text{CO})_3$ fragment.^{52,53}

Table 1.3. CO Stretching Frequencies of $[\text{Cp}-(\text{CH}_2)_n\text{OH M}(\text{CO})_3\text{PPh}_3]^+$

M	n	$\bar{\nu}\text{CO}(cm^{-1})^a$
Mo	parent	2053(<i>s</i>), 1997(<i>m</i>), 1975(<i>s</i>)
W	parent	2050(<i>s</i>), 1984(<i>m</i>), 1962(<i>s</i>)
W	1	2050(<i>s</i>), 1985(<i>m</i>), 1957(<i>s</i>)
W	2	2050(<i>s</i>), 1980(<i>m</i>), 1960(<i>s</i>)
Mo	2	2056(<i>s</i>), 1995(<i>sh</i>), 1969(<i>s</i>)
W	3	2050(<i>s</i>), 1980(<i>m</i>), 1960(<i>s</i>)
Mo	3	2050(<i>s</i>), 1996(<i>sh</i>), 1970(<i>s</i>)

^a CH_2Cl_2 solution.

Figure 1.5



Therefore, a dilution study of the OH stretch in the IR was conducted. From the results shown in Table 1.4 it is clear that the cations exhibit a free OH stretch as well as a lower energy stretch that is invariant with dilution while the ethanol substituted dimer displays only a stretch that may be attributed to free OH.⁵⁴ It appears that while the cationic charges do not generate a covalent interaction they do induce a weak hydrogen bonding interaction between the alcohols and the $M(CO)_3L$ fragments. Interestingly the hydroxymethyl substituted tungsten cation displays mostly the H bonded stretch while the propanol substituted compound displays approximately a 1:1 mixture of free and H bonded species. It is apparent then that the compounds being studied offer promise in that they do possess the requisite length with the pendant alcohol to interact at least weakly with the carbonyl ligands. Additionally, changing the arm length changes the character of the interaction to some degree. Thus, the complexes offer exciting possibilities in the study of the requirements of catalyst design.

Table 1.4. Hydroxyl Stretching Frequencies of $[\text{Cp}-(\text{CH}_2)_n\text{OH M}(\text{CO})_3\text{PR}_3]^+$ at High Dilution (ca. 10mM)

M	n	PR ₃	$\nu\text{OH}(cm^{-1})^a$
W	1	Ph	3630, 3570
W	2	p-tolyl	3615, 3530
Mo	2	Ph	3600, 3530
Mo	3	Ph	3620, 3570
Mo	2	dimer	3615

^a CH₂Cl₂ solution.

Experimental

$W(CO)_6$ and $Mo(CO)_6$ were purchased from Pressure Chemical Company and tri-*para*-tolyl phosphine was purchased from Strem Chemicals and used as received. Sodium borohydride was purchased from Alfa.

All reactions were carried out using standard Schlenk techniques. Argon used in Schlenk work was purified by passage through columns of BASF RS-11 (Chemalog) and Linde 4Å molecular sieves. Manipulations were also performed using a Vacuum Atmospheres dry box with nitrogen atmosphere. Toluene, benzene and THF were vacuum transferred from sodium-benzophenone ketyl. Methylene chloride was stirred over P_2O_5 and acetone was dried over 4Å molecular sieves prior to use. Infra-red spectra were obtained from a Perkin-Elmer 257 grating instrument and a Beckman model IR 4240 spectrometer referenced to the 1601 cm^{-1} stretch of polystyrene. FT IR spectra obtained for the dilution study were recorded on a Mattson Sirius 100 instrument. Continuous wave NMR spectra were recorded on a Varian EM-390 instrument with an ambient probe temperature of 34° C . Fourier transform ^{31}P and ^1H spectra were taken on a JEOL FX-90Q spectrometer operating at 36.2 and 89.56 MHz respectively with a probe temperature of 25° C . All ^{31}P NMR spectra were referenced to an external sample of the appropriate free phosphine in the relevant solvent. Melting points were obtained from a Büchi melting point apparatus with all samples placed in glass capillaries under a nitrogen atmosphere and sealed. No temperature corrections were made. Elemental analyses were performed by Schwarzkopf Microanalytical of Woodside, New York, Dornis und Kolbe of Mannheim, West Germany and the analytical facility of the California Institute of Technology.

The parent compounds: $[\text{CpMo}(\text{CO})_3]^- \text{Na}^+$,⁵⁵ $[\text{CpW}(\text{CO})_3]^- \text{Li}^+$,⁵⁶ $\text{Cp-Mo}(\text{CO})_3\text{H}$,⁵⁷ $\text{CpW}(\text{CO})_3\text{H}$,^{57a,59} and $[\text{CpM}(\text{CO})_3\text{PR}_3]^+ \text{BF}_4^-$ ⁵⁰ were prepared according to literature methods.

2 Hydroxyethylcyclopentadiene

The method of Schröder was used with the substitution of potassium *tert*-butoxide for potassium in *tert*-butanol.⁶⁰

To a mixture of 5.61 g of potassium *t*-butoxide (0.05 mol) in 100 mL of *t*-butanol (dried over MgSO_4) in a large Schlenk flask under argon was added 0.5 mol of freshly distilled cyclopentadiene (41.14 mL). To this mixture, one equivalent of ethylene oxide in 20 mL of *t*-butanol was slowly added, the temperature of the reaction mixture being maintained at 20 – 25°C by means of a water bath. The mixture was then stirred at room temperature for 4h, during which time the color changed from red to dark gray. Following this, the reaction mixture was neutralized with 5% H_2SO_4 and extracted twice with 50 mL of petroleum ether. The extracts were then washed once with water and dried over Na_2SO_4 . A yellow solution was obtained. Solvent was then removed under reduced pressure and the resulting yellow oil was purified by kugelrohr. The desired product was collected at 40°C and 5 μ of Hg (5.6g, 10.2%): ^1H NMR (CDCl_3), $\text{C}_5\text{H}_5\text{R}$ (alkenyl) 6.5-6.0 (m, 3H), $-\text{CH}_2-\text{O}$ 3.7 (t, 2H), $\text{C}_5\text{H}_5\text{R}$ (alkyl) 2.9 (d, 2H), $\text{C}_3\text{H}_5\text{CH}_2-$ 2.6 (m, 2H), $-\text{OH}$ variable (s, 1H).

3 Hydroxypropylcyclopentadiene

To a mixture of .5 mol of NaH (20 g of 60 % dispersion in oil) in 150 mL of THF in a large Schlenk flask under argon was added one equivalent of freshly distilled cyclopentadiene (41.1 mL). The mixture was stirred and cooled during the addition. One equivalent of 3-bromopropanol (45.2 mL) was then added to the NaCp mixture as quickly as possible while continuing stirring and cooling. The mixture was then stirred for 2 h at room temperature after which 150 mL of petroleum ether were added followed by slow addition of 150 mL of water. The two layers were separated and the aqueous layer was extracted twice with 50 mL of petroleum ether, these being added to the original petroleum ether layer. The combined petroleum ether fraction was then washed twice with 50 mL of water and dried over Na₂SO₄. Solvent was then removed under reduced pressure and the resulting material was vacuum distilled. The desired product was collected at 70°C and 1μ of Hg (9.3 g, 15 %): ¹H NMR (CDCl₃), C₅H₅R (alkenyl) 6.5-5.9 (m, 3H), -CH₂-O 3.6 (t, 2H), C₅H₅R (alkyl) 2.9 (d, 2H), C₅H₅-CH₂- 2.4 (m, 2H), -CH₂- 1.8 (m, 2H), -OH variable (s, 1H).



(n = 2,3)

The method of King was followed with the substitution of one equivalent of the substituted cyclopentadiene for excess cyclopentadiene.⁶¹ The synthesis where n = 2 is given below.

One equivalent of $\text{Mo}(\text{CO})_6$ and 2-hydroxyethylcyclopentadiene were refluxed in toluene under argon with stirring for 2.5 h. The mixture was then cooled to room temperature and the resulting liquid phase was transferred to another flask *via* cannula, leaving unreacted hexacarbonyl behind. Solvent was removed under reduced pressure at which point more hexacarbonyl sublimed out of the mixture. The resulting red oil was dissolved in a minimal amount of THF. Methylene chloride was then added (four times the THF volume) and the mixture was cooled to -20°C overnight. The resulting red powder was isolated by Schlenk filtration and washed with CH_2Cl_2 followed by diethyl ether. Remaining solvent was removed under reduced pressure leaving the product as a fine red powder (1.81 g, 17%):

$n = 2$ MP = $155-157^\circ\text{C}$: $^1\text{H NMR}$ ($(\text{CD}_3)_2\text{CO}$), CpR 5.37 (broad d, 4H), $-\text{CH}_2-\text{O}$ 3.62 (t, 2H), Cp- CH_2- 2.54 (t, 2H), $-\text{OH}$ variable (s, 1H); IR (CH_2Cl_2) νCO , 2002 (w), 1953 (s), 1908 (s).

Anal. Calcd. for $\text{C}_{20}\text{H}_{18}\text{Mo}_2\text{O}_8$: C 41.54; H 3.14. Found: C 41.21; H 3.26.

$n = 3$ MP = $126-130^\circ\text{C}$: $^1\text{H NMR}$ ($(\text{CD}_3)_2\text{CO}$), CpR 5.40 (broad d, 4H), $-\text{CH}_2-\text{O}$ 3.57 (t, 2H), Cp- CH_2- 2.53 (t, 2H), $-\text{CH}_2-$ 1.72 (m, 2H), $-\text{OH}$ variable (s, 1H); IR (CH_2Cl_2) νCO , 1955 (s), 1910 (s).

Anal. Calcd. for $\text{C}_{22}\text{H}_{22}\text{Mo}_2\text{O}_8$: C 43.58; H 3.71. Found: C 43.93; H 3.86.

$n = 2$, trityl ether⁶² MP = $197-199^\circ\text{C}$: $^1\text{H NMR}$ (C_6D_6), Ph 7.60-6.99 (m, 15H), CpR 4.84 (d of d, 4H), Cp- CH_2- 3.05 (t, 2H), $-\text{CH}_2-$ 2.35 (t, 2H), $-\text{OH}$ variable (s, 1H); IR (CHCl_3) νCO , 1955 (s), 1915 (s).

Anal. Calcd. for $\text{C}_{58}\text{H}_{46}\text{Mo}_2\text{O}_8$: C 65.54; H 4.33. Found: C 65.59; H 4.62.



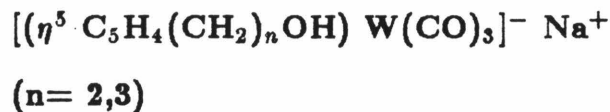
($n = 2, 3$)

The synthesis where $n = 2$ is given below.

A solution of 300 mgs of $[(\text{CpCH}_2\text{CH}_2\text{OH})\text{Mo}(\text{CO})_3]_2$ (0.52 mmol) in 60 mL of THF was stirred over excess sodium amalgam (2.1 mmol of Na in 1.5 mL of Hg) under argon at room temperature. After 75 min, the red solution had changed to a pale gold. The solution was transferred away from the amalgam *via* cannula and filtered on a Schlenk frit. A clear yellow filtrate was obtained from which solvent was removed under reduced pressure. The remaining brown solid was dissolved in 5 mL of THF after which 30 mL of diethyl ether were added causing a pale precipitate to form. This was isolated by cannula filtration and upon removal of remaining solvent under reduced pressure, 231 mgs of the desired product were obtained (75%):

$n = 2$ ^1H NMR ($(\text{CD}_3)_2\text{CO}$), CpR 4.90 (AA'BB', 4H), $-\text{CH}_2\text{-O}$ 3.55 (t, 2H), Cp- CH_2 - 2.46 (t, 2H), $-\text{OH}$ variable (s, 1H); IR (THF) νCO , 1900 (s), 1795 (s), 1750 (s).

$n = 3$ ^1H NMR ($(\text{CD}_3)_2\text{CO}$), CpR 4.88 (AA'BB', 4H), $-\text{CH}_2\text{-O}$ 3.57 (t, 2H), Cp- CH_2 - 2.32 (t, 2H), $-\text{CH}_2$ - 1.75 (m, 2H), $-\text{OH}$ variable (s, 1H); IR (THF) νCO , 1900 (s), 1795 (s), 1742 (s).



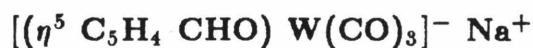
The synthesis where $n = 2$ is given below.

An equimolar (22.5 mmol) mixture of $\text{W}(\text{CO})_6$ and $\text{NaCpCH}_2\text{CH}_2\text{OH}$ (made freshly from NaH and hydroxyethylcyclopentadiene in THF) was refluxed in 14 mL of THF under argon with stirring. After 12 h, the mixture was cooled

to room temperature and filtered. Solvent was removed from the filtrate under reduced pressure until approximately one-half remained. Twenty mL of benzene were then added at which point yellow solid began to precipitate. This material was isolated by filtration and remaining solvent was removed under reduced pressure. The filtrate was again reduced in volume (to one-fourth) under reduced pressure after which 16 mL of diethyl ether were added causing additional precipitate to form for a total yield of 2.3 g (25.5%):

$n = 2$ $^1\text{H NMR}$ ($(\text{CD}_3)_2\text{CO}$), CpR 4.92 (AA' BB', 4H), $-\text{CH}_2\text{-O}$ 3.54 (t, 2H), Cp- CH_2 - 2.52 (t, 2H), $-\text{OH}$ variable (s, 1H); IR (THF) νCO , 1895 (s), 1793 (s), 1742 (s).

$n = 3$ $^1\text{H NMR}$ ($(\text{CD}_3)_2\text{CO}$), CpR 4.92 (AA'BB', 4H), $-\text{CH}_2\text{-O}$ 3.53 (t, 2H), Cp- CH_2 - 2.36 (t, 2H), $-\text{CH}_2$ - 1.74 (m, 2H), $-\text{OH}$ variable (s, 1H); IR (THF) νCO , 1900, 1795, 1745.



The same procedure as that for the alcohol substituted compounds was followed, with the use of formyl cyclopentadienide as the functionalized Cp (43 % yield of the THF solvate based on starting $\text{W}(\text{CO})_6$):⁵¹

$^1\text{H NMR}$ ($(\text{CD}_3)_2\text{CO}$), CpR (H_2 & H_5) 5.52 (AA'BB', $J = 2.4$ Hz, 2H), CpR (H_3 & H_4) 5.11 (AA'BB', $J = 2.4$ Hz, 2H), $-\text{CHO}$ 9.28 (s, 1H); IR (THF) νCO , 1910 (s), 1810 (s), 1775 (m), 1740(sh).



Using the precedent of other borohydride reductions of formyl Cp complex-

es,^{63,64} 1.16 g of $[\text{CpCHO W}(\text{CO})_3]^- \text{Na}^+$ (2.5 mmol) were dissolved in 10 mL of dry, degassed ethanol in a small Schlenk tube. One-half of one equivalent of NaBH_4 (48 mg) was added and the mixture was stirred at room temperature for 2 h. Solvent was then removed under reduced pressure yielding a quantitative amount of the product as a tan powder (as the ethanol solvate):

$^1\text{H NMR}$ ($(\text{CD}_3)_2\text{CO}$), CpR (H_2 & H_5) 5.09 (AA'BB', J= 2.0 Hz, 2H), CpR (H_3 & H_4) 4.90 (AA'BB', J= 2.4 Hz, 2H), Cp-CH₂- 4.04 (s, 2H), -OH variable (s, 1H); IR (THF) νCO , 1895 (vs), 1792 (vs), 1743 (vs).

$(\eta^5\text{-C}_5\text{H}_4(\text{CH}_2)_n\text{OH}) \text{M}(\text{CO})_3\text{H}$
(M=Mo, W; n= 1,2,3)

One equivalent of CH_3COOH was added to $[(\eta^5\text{-C}_5\text{H}_4(\text{CH}_2)_n\text{OH}) \text{M}(\text{CO})_3]^- \text{Na}^+$ in THF (typically 0.5 mmol in 3 mL of THF) under argon with stirring at room temperature. After 10 min, solvent was removed under reduced pressure and the resulting mixture was extracted with benzene (typically 8 times with 2 mL). Solvent was then removed from the combined extracts under reduced pressure giving the product as a gold oil at room temperature (100%). Thermal instability has precluded elemental analysis:

M= W n= 1 $^1\text{H NMR}$ (C_6D_6), CpR 4.66 (AA'BB', ,4H), -CH₂-O 3.78 (s, 2H), W-H -7.07 (s w/ small d, J=37.6 Hz, 1H), -OH variable (s, 1H); IR (C_6D_6) νCO , 2018 (s), 1925 (vs).

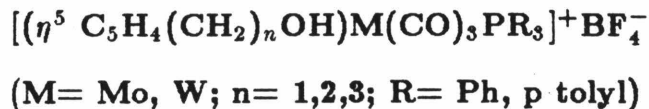
M=Mo n= 2 $^1\text{H NMR}$ (C_6D_6), CpR 4.75 (AA'BB', ,4H), -CH₂-O 3.22 (t, 2H), Cp-CH₂- 2.04 (t, 2H), Mo-H -5.30 (s, 1H), -OH variable (s, 1H); IR (C_6D_6) νCO , 2013 (s), 1981 (w), 1932 (s).

M=W n= 2 $^1\text{H NMR}$ (C_6D_6), CpR 4.70 (AA'BB', 4H), -CH₂- 3.29 (t, 2H),

Cp-CH₂- 2.13 (t, 2H), W-H -7.02 (s w/ small d, J_{WH} = 37.6 Hz, 1H), -OH variable (s, 1H); IR (C₆H₆) νCO, 2020 (s), 1925 (s).

M=Mo, n= 3 ¹H NMR (C₆D₆), CpR 4.63 (AA'BB', 4H), -CH₂-O 3.15 (t, 2H), Cp-CH₂- 2.00 (t, 2H), -CH₂- 1.02 (m, 2H), Mo-H -5.30 (s, 1H), -OH variable (s, 1H); IR (C₆D₆) νCO, 2020 (s), 1930 (vs).

M=W, n= 3 ¹H NMR (C₆D₆), CpR 4.61 (AA'BB', 4H), -CH₂-O 3.13 (t, 2H), Cp-CH₂- 2.01 (t, 2H), -CH₂- 1.1, W-H -6.99 (s w/ small d, J_{WH} = 37.6 Hz, 1H), -OH variable (s, 1H); IR (C₆H₆) νCO, 2017 (s), 1922 (s).



The method of Beck and Schloter was used.⁵⁰ As an example, the synthesis of [(CpCH₂CH₂OH)W(CO)₃PPh₃]⁺BF₄⁻ is given.

A solution of 172.5 mgs of (CpCH₂CH₂OH)W(CO)₃H (0.46 mmol) in 4 mL of CH₂Cl₂ under argon was cooled to -30°C. To this was added one equivalent of Ph₃C⁺BF₄⁻ (152 mg). Immediately, a dark purple solution was obtained. This was allowed to sit for 5 min after which one equivalent of triphenylphosphine (121 mgs) was added. The solution immediately changed to a red-violet color. The mixture was kept at -30°C for 1 h with occasional agitation. Following this, the mixture was warmed to room temperature at which point yellow crystalline solids began to form. Diethyl ether (8 mL) was added causing more yellow solids to precipitate. The solid was isolated by filtration and washed 6 times with 2 mL of diethyl ether after which remaining solvent was removed under reduced pressure leaving the product as bright yellow crystalline material (258

mgs, 78.3%):

M=W, n=1, R=Ph ^1H NMR ($(\text{CD}_3)_2\text{CO}$), PPh_3 8.27 – 7.11 (m, 15H), CpR 6.15 (AA'BB', 4H), $-\text{CH}_2\text{-O}$ 4.57 (s, 2H), $-\text{OH}$ variable (s, 1H); ^{31}P NMR ($(\text{CD}_3)_2\text{CO}$) 19.45 (s w/ small d, $J_{\text{WP}} = 192.9$ Hz); IR (CH_2Cl_2) νCO , 2050 (s), 1985 (m), 1957 (s).

M=Mo, n=2, R=Ph MP: 200 – 206°C (d); ^1H NMR ($(\text{CD}_3)_2\text{CO}$), PPh_3 7.81 – 7.31 (m, 15H), CpR 6.00 (AA'BB', 4H), $-\text{CH}_2\text{-O}$ 3.71 (t, 2H), Cp- $\text{CH}_2\text{-}$ 2.64 (t, 2H), $-\text{OH}$ variable (s, 1H); ^{31}P NMR ($(\text{CD}_3)_2\text{CO}$), 50.18 (s); IR (CH_2Cl_2) νCO , 2056 (s), 1995 (sh), 1969 (s).

Anal. Calcd. for $\text{C}_{28}\text{H}_{24}\text{B}_1\text{F}_4\text{Mo}_1\text{O}_4\text{P}_1$: C 52.70; H 3.79. Found: C 52.76; H 3.78.

M=W, n=2, R=Ph MP: 211 – 215°C (d); ^1H NMR ($(\text{CD}_3)_2\text{CO}$), PPh_3 7.79 – 7.24 (m, 15H), CpR 6.13 (AA'BB', 4H), $-\text{CH}_2\text{-O}$ 3.72 (t, 2H), Cp $\text{CH}_2\text{-}$ 2.56 (t, 2H), $-\text{OH}$ variable (s, 1H); ^{31}P NMR ($(\text{CD}_3)_2\text{CO}$) 19.92 (s w/ small d, $J_{\text{WP}} = 192.9$ Hz); IR (CH_2Cl_2) νCO , 2050 (s), 1980 (m), 1960 (s).

Anal. Calcd. for $\text{C}_{28}\text{H}_{24}\text{B}_1\text{F}_4\text{O}_4\text{P}_1\text{W}_1$: C 46.32; H 3.33. Found: C 46.15; H 3.41.

M=Mo, n=2, R=p tolyl MP: 230 – 235°C (d); ^1H NMR ($(\text{CD}_3)_2\text{CO}$), $\text{P}(\text{p-tolyl})_3$ (aryl) 7.89 – 7.15 (m, 12H), CpR 5.95 (AA'BB', 4H), $-\text{CH}_2\text{-O}$ 3.71 (t, 2H), Cp- $\text{CH}_2\text{-}$ 2.63 (t, 2H), $-\text{CH}_3$ 2.43, $-\text{OH}$ not directly observed; ^{31}P NMR ($(\text{CD}_3)_2\text{CO}$), 50.01 (s); IR (CH_2Cl_2) νCO , 2055 (s), 1960 (s), 1971 (vs).

Anal. Calcd. for $\text{C}_{31}\text{H}_{30}\text{B}_1\text{F}_4\text{Mo}_1\text{O}_4\text{P}_1$: C 54.73; H 4.44. Found: C 54.35; H 4.47.

M=W, n=2, R=p tolyl MP: 252 – 254°C (d); ^1H NMR ($(\text{CD}_3)_2\text{CO}$), $\text{P}(\text{p-tolyl})_3$ (aryl) 7.57 – 7.14 (m, 12H), CpR 6.07 (AA'BB', 4H), $-\text{CH}_2\text{-O}$ 3.72 (t, 2H), Cp $\text{CH}_2\text{-}$ 2.73 (t, 2H), $-\text{CH}_3$ 2.44 (s, 9H), $-\text{OH}$ not directly observed; ^{31}P

NMR ($(\text{CD}_3)_2\text{CO}$), 19.79 (s w/ small d, $J_{WP} = 190.4$ Hz); IR (CH_2Cl_2) νCO , 2043 (s), 1974 (sh), 1956 (s).

Anal. Calcd. for $\text{C}_{31}\text{H}_{30}\text{B}_1\text{F}_4\text{O}_4\text{P}_1\text{W}_1$: C 48.47; H 3.94. Found: C 48.13; H 4.19.

M=Mo, n=3, R=Ph MP: 189-191°C (d); ^1H NMR ($(\text{CD}_3)_2\text{CO}$), P- PH_3 7.82-7.28 (m, 15H), CpR 6.01 (AA'BB', 4H), $-\text{CH}_2\text{-O}$ 3.56 (t, 2H), Cp- $\text{CH}_2\text{-}$ 2.57 (t, 2H), $-\text{CH}_2\text{-}$ 1.77 (m, 2H), $-\text{OH}$ variable (s, 1H); ^{31}P NMR ($(\text{CD}_3)_2\text{CO}$), 49.86 (s); IR (CH_2Cl_2) νCO , 2050 (s), 1996 (sh), 1970 (s).

M=W, n=3, R=Ph MP: 142-145°C; ^1H NMR ($(\text{CD}_3)_2\text{CO}$), PPh₃ 7.79-7.07 (m, 15H), CpR 6.13 (m, 4H), $\text{CH}_2\text{-O}$ 3.56 (t, 2H), Cp- $\text{CH}_2\text{-}$ 2.66 (t, 2H), $-\text{CH}_2\text{-}$ 1.74 (m, 2H), $-\text{OH}$ variable (s, 1H); ^{31}P NMR ($(\text{CD}_3)_2\text{CO}$), 19.65 (s w/ small d, $J_{WP} = 190.4$ Hz); IR (CH_2Cl_2) νCO , 2050 (m), 1980 (sh), 1960 (s).

X ray Structure Determination

A thin triangular crystalline plate of $[(\eta^5\text{-C}_5\text{H}_4\text{-(CH}_2)_3\text{-OH)Mo(CO)}_3]_2$ ($0.05 \times 0.25 \times 0.80\text{mm}$), obtained after allowing a reaction mixture to stand at room temperature under argon for a period of twelve months, was mounted in a glass capillary under N_2 . A series of oscillation and Weissenberg photographs indicated triclinic symmetry and the space group was assumed to be $P\bar{1}$; data were collected on a locally-modified Syntex $P2_1$ diffractometer with graphite monochromator and $\text{MoK}\alpha$ radiation. The unit cell parameters (Table 1.5) were obtained by least-squares refinement of twelve reflections ($30^\circ < 2\theta < 34^\circ$). The three check reflections indicated no decomposition. The data were reduced to F_o^2 ; the form factors for H were from Stewart *et al.*⁶⁵ and those for the other atoms were from the *International Tables for X-Ray Crystallography*⁶⁶

The values for Mo were corrected for anomalous dispersion. The details of data collection are included in Table 1.5.

The position of the Mo atom was derived from the Patterson map, and the Fourier map phased on Mo revealed the remainder of the complex. All H-atoms (except on OH) were introduced into the model with fixed coordinates at idealized positions and isotropic $U = 0.076 \text{ \AA}^2$. The alcohol oxygen (O4) was found to be three-fold disordered. The populations and coordinates of the three oxygen positions were obtained from difference Fourier maps. Least-squares refinement of the non-hydrogen atoms with anisotropic U_{ij} 's (O4 was refined with isotropic parameters), minimizing $\Sigma w[F_o^2 - (F_c/k)^2]^2$,⁶⁷ using all the data (3283 reflections) led to $S(\text{goodness of fit}) = 1.47$ and $R_F = 0.057$; final shift/errors < 0.01 . The maximum deviations found in the $\Delta\rho$ map are close to Mo and are about $0.9 e \text{ \AA}^{-3}$. Atom coordinates of non-hydrogen atoms and their Gaussian amplitudes are given in Tables 1.6 and 1.7. The hydrogen atom coordinates are given in Table 1.8. All calculations were carried out on a VAX 11/780 computer using the CRYRM system of programs.

Table 1.5. Summary of Data Collection and Refinement Parameters

Formula	$C_{22}H_{22}O_8Mo_2$	
Formula weight	606.30	
Space group	$P\bar{1}$	
a	7.487(3) Å	
b	7.713(3) Å	
c	10.902(7) Å	
α	99.36(4)°	
β	81.46(4)°	
γ	115.26(3)°	
V	563.0(10) Å ³	
Z	1	
D_{calc}	1.789 g/cm ³	
Crystal size	0.050 × 0.250 × 0.800 mm	
λ	0.71073 Å	
μ	5.10 mm ⁻¹	
2θ limits	4 — 56°	56 — 60°
Scan rate	2.02°/min	0.99°/min
Bkgrd-to-scan time ratio	1.0	0.5
Scan width	1.1°	1.2° above $K\alpha_2$
	1.1°	1.2° below $K\alpha_1$
Number of reflections	5780	1198
Total number of averaged data	3283	
Final agreement ^a		
R_F	0.057 (3087)	
R'_F	0.039 (2374)	
S	1.47 (3283)	

^aDefined in footnote 67; number of reflections given in parentheses.

Table 1.6. Atom Coordinates ($\times 10^4$) and U_{eq} 's (\AA^2 , $\times 10^4$)

	<i>x</i>	<i>y</i>	<i>z</i>	<i>U_{eq}</i>
Mo	4111.5(4)	126.9(4)	1430.3(3)	370
C(1)	1849(5)	-1132(5)	383(3)	450
O(1)	439(4)	-1904(4)	-134(2)	637
C(2)	5625(5)	2738(5)	908(3)	468
O(2)	6485(4)	4330(4)	728(2)	651
C(3)	2441(5)	1453(5)	2194(3)	485
O(3)	1493(4)	2259(4)	2685(3)	720
C(4)	-2508(8)	-4042(9)	4028(5)	965
O(41)	-2765(10)	-5098(10)	4870(7)	807*
O(42)	-3082(15)	-2813(15)	4362(9)	954*
O(43)	-4023(27)	-4827(24)	3627(16)	908*
C(5)	-522(6)	-3512(7)	3233(4)	771
C(6)	1203(6)	-2157(6)	3933(3)	582
C(7)	3192(5)	-1573(5)	3171(3)	474
C(8)	3801(5)	-2693(5)	2187(3)	491
C(9)	5835(6)	-1640(6)	1848(3)	513
C(10)	6497(5)	126(6)	2602(4)	534
C(11)	4878(6)	179(5)	3417(3)	521

* Refined Using Isotropic U's. The populations were: O41, 44.0 %; O42, 35.7 %; O43, 20.3 %.

Table 1.7. Gaussian amplitudes ($\times 10^4$)

	U_{11}	U_{22}	U_{33}	U_{12}	U_{13}	U_{23}
Mo	352(2)	364(2)	409(2)	159(1)	-36(1)	52(1)
C(1)	416(20)	491(22)	490(22)	233(18)	18(17)	105(17)
O(1)	416(15)	763(19)	664(18)	153(14)	-148(14)	65(15)
C(2)	487(22)	472(22)	455(22)	215(19)	-54(17)	18(18)
O(2)	793(20)	343(14)	709(19)	153(14)	-6(15)	52(14)
C(3)	458(21)	476(22)	547(24)	215(18)	-103(18)	10(18)
O(3)	655(19)	813(21)	807(21)	488(17)	-40(16)	-103(16)
C(4)	691(36)	1104(47)	855(40)	154(34)	28(31)	151(35)
C(5)	547(27)	841(33)	704(31)	106(25)	49(23)	97(26)
C(6)	613(26)	613(26)	497(24)	220(22)	24(20)	157(20)
C(7)	491(22)	570(23)	425(21)	248(19)	1(17)	180(18)
C(8)	580(24)	416(20)	553(24)	250(19)	-47(19)	132(18)
C(9)	561(24)	640(26)	506(23)	395(21)	21(19)	165(20)
C(10)	429(21)	643(26)	581(25)	213(20)	-106(19)	176(21)
C(11)	558(24)	539(24)	477(22)	217(20)	-160(19)	12(18)

Table 1.8. Atom Coordinates ($\times 10^3$) of Hydrogen Atoms

	<i>x</i>	<i>y</i>	<i>z</i>
H(411)	-3432	4916	3434
H(412)	-2641	-3019	4326
H(421)	-2339	-4670	4694
H(422)	-3419	-5126	3495
H(431)	-2481	-3008	4455
H(432)	-2388	-4956	4541
H(51)	-369	-4778	2947
H(52)	-473	-2954	2430
H(61)	1211	-2787	4683
H(62)	951	-962	4283
H(8)	2916	-4043	1793
H(9)	6694	-2085	1164
H(10)	7901	1193	2566
H(11)	4889	1300	4077

Notes and References

- (1) (a) Muetterties, E.L.; Stein, J. *Chem. Rev.* **1979**, *79*, 479. (b) Rofer-DePorter, C.K. *Chem. Rev.* **1981**, *81*, 447. (c) Vannice, M.A. *Catal. Rev. Sci. Eng.* **1976**, *14*, 153. (d) Biloen, P.; Sachtler, W.M.H. *Adv. Cat.* **1981**, *30*, 165. (e) Pruett, R.L. *Science* **1981**, *211*, 11.
- (2) Sebatier, P.; Senderens, J.B. *Comp. Rend.* **1902**, *134*, 514.
- (3) Fischer, F.; Tropsch, H. *Brennstoff. Chemie* **1923**, *4*, 276.
- (4) "New Syntheses with Carbon Monoxide," Falbe, J., ed.; Springer-Verlag: Berlin (1980).
- (5) Storch, H.H.; Golumbic, N.; Anderson, R.B., "The Fischer-Tropsch and Related Syntheses;" Wiley: New York (1951).
- (6) Parshall, G.W., "Homogeneous Catalysis;" Wiley: New York (1980).
- (7) Masters, C. *Adv. Organomet. Chem.* **1979**, *17*, 61.
- (8) For example, the study of Wilkinson's Catalyst by Halpern: (a) Halpern, J. *Trans. Am. Crystall. Assoc.* **1978**, *14*, 59. (b) Halpern, J.; Wong, C.S. *Chem. Commun.* **1973**, 629.
- (9) Thomas, M.G.; Beier, B.F.; Muetterties, E.L. *J. Am. Chem. Soc.* **1976**, *98*, 1296.
- (10) Wang, H.-K.; Choi, H.W.; Muetterties, E.L. *Inorg. Chem.* **1981**, *20*, 2661.
- (11) Choi, H.W.; Muetterties, E.L. *Inorg. Chem.* **1981**, *20*, 2664.
- (12) Bradley, J.S. *J. Am. Chem. Soc.* **1979**, *101*, 7419.
- (13) Dombek, B.D. *J. Am. Chem. Soc.* **1980**, *102*, 6857.
- (14) Manriquez, J.M.; McAlister, D.R.; Stanner, R.D.; Bercaw, J.E. *J. Am.*

Chem. Soc. **1976**, *98*, 6733.

(15) Huffmann, J.C.; Stone, J.G.; Krussell, W.C.; Caulton, K.G. *J. Am. Chem. Soc.* **1977**, *99*, 5829.

(16) Treichel, P.M.; Shubkin, R.L. *Inorg. Chem.* **1967**, *6*, 1328.

(17) The synthesis of the formyl was reported but it was found to be unstable at -41° C in the solvent employed: Tam, W.; Lon, G.-Y.; Gladysz, J.A. *Organometallics* **1982**, *1*, 525.

(18) Gibson, D.H.; Owens, K.; Ong, T.-S. *J. Am. Chem. Soc.* **1984**, *106*, 1125.

(19) Stewart, R.P.; Okamoto, N.; Graham, W.A.G. *J. Organomet. Chem.* **1972**, *42*, C32.

(20) Sweet, J.R.; Graham, W.A.G. *J. Organomet. Chem.* **1979**, *173*, C9.

(21) Tam, W.; Wong, W.-K.; Gladysz, J.A. *J. Am. Chem. Soc.* **1979**, *101*, 1589.

(22) Casey, C.P.; Andrews, M.A.; McAlister, D.R.; Rinz, J.E. *J. Am. Chem. Soc.* **1980**, *102*, 1927.

(23) Lin, Y.C.; Milstein, D.; Wreford, S.S. *Organometallics* **1983**, *2*, 1461.

(24) Sweet, J.R.; Graham, W.A.G. *Organometallics* **1982**, *1*, 982.

(25) Nelson, G.O. *Organometallics* **1983**, *2*, 1474.

(26) The scheme is quite analogous to mechanism proposed in heterogeneous systems, the main difference lies in the placement of coordinated CO and H on the same metal center: See ref 1b.

(27) May, C.J.; Graham, W.A.G. *J. Organomet. Chem.* **1982**, *234*, C49.

(28) The transformation of coordinated formaldehyde to a hydrido-formyl species upon thermolysis of $\text{Os}(\text{CO})_2\text{L}_2(\eta^2\text{-CH}_2\text{O})$ has recently been reported; the hydrido formyl is unstable in solution and reductively eliminates H_2 yielding

- $\text{Os}(\text{CO})_3\text{L}_2$: Brown, K.L.; Clark, G.R.; Headford, C.E.L.; Marsden, K.; Roper, W.R. *J. Am. Chem. Soc.* **1979**, *101*, 503.
- (29) Blackborrow, J.R.; Daroda, R.J.; Wilkinson, G. *Coord. Chem. Rev.* **1982**, *49*, 17.
- (30) Henrici-Olivé, G.; Olivé, S. *Angew. Chem. Intl. Ed. Eng.* **1976**, *15*, 136.
- (31) Kang, H.; Mauldin, C.H.; Cole, T.; Slegeir, W.; Cann, K.; Pettit, R. *J. Am. Chem. Soc.* **1977**, *99*, 8323.
- (32) Busetto, L.; Angelici, R.J. *Inorg. Chim. Acta* **1968**, 391.
- (33) Angelici, R.J. *Accts. Chem. Res.* **1972**, *5*, 335.
- (34) Angelici, R.J.; Blacik, L.J. *Inorg. Chem.* **1972**, *11*, 1754.
- (35) Doxsee, K.M.; Grubbs, R.H. *J. Am. Chem. Soc.* **1981**, *103*, 7696.
- (36) Stull, D.R.; Westrum, E.F.; Sinke, G.C., "The Chemical Thermodynamics of Organic Compounds," Wiley: New York (1969).
- (37) A number of formaldehydo complexes are known see for example: Berke, H.; Huttner, G.; Weiler, G.; Zsolnai, L. *J. Organomet. Chem.* **1981**, *219*, 353, for an iron complex; Gambarotta, S.; Floriani, C. *J. Am. Chem. Soc.* **1982**, *104*, 2019, for a vanadium complex and Ref. 28 for an osmium complex.
- (38) King, R.B.; Bisnette, M.B.; Fronzaglia, A. *J. Organomet. Chem.* **1966**, *5*, 341.
- (39) Additionally, acyl complexes of the form $\text{CpM}(\text{CO})_2\text{L}(-\text{C}(\text{O})\text{R})$ display $\text{C}=\text{O}$ stretches at about 1600 cm^{-1} : see for example ref 61.
- (40) Fischer, E.O.; Scherzer, K.; Kreissl, F.R. *J. Organomet. Chem.* **1976**, *118*, C33.
- (41) Casey, C.P.; Neumann, S.M. *J. Am. Chem. Soc.* **1977**, *99*, 1651.
- (42) Ungváry, F.; Markó, L. *Organometallics* **1983**, *2*, 1608.

- (43) Hendrickson, J.B.; Cram, D.J.; Hammond, G.S., "Organic Chemistry," 3rd ed., McGraw-Hill: New York (1970).
- (44) Significant proportions of this material have been submitted for publication: Metal dimers, Coolbaugh, T.S.; Coots, R.J.; Santarsiero, B.D.; Grubbs, R.H. *Inorg. Chim. Acta.* Cationic Complexes, Coolbaugh, T.S.; Santarsiero, B.D.; Grubbs, R.H. *J. Am. Chem. Soc.*
- (45) Doxsee, K.M., Ph.D. Thesis, California Institute of Technology (1983).
- (46) See for example, Macomber, D.W.; Hart, W.P.; Rausch, M.D. *Adv. Organomet. Chem.* **1982**, *21*, 1.
- (47) Group VI is a viable choice since numerous examples of Cp compounds, including those containing carbenes, are known. Recently several bimetallic compounds containing a carbene were reported including the complex, $\text{Cp}(\text{CO})_3\text{Mo}-\text{MoCp}(\text{CO})_2(=\overline{\text{CO}-(\text{CH}_2)_3})$: Adams, H.; Bailey, N.A.; Winter, M.J. *J. Chem. Soc. Dalton* **1984**, 273.
- (48) Wilson F.C.; Shoemaker, D.P. *J. Chem. Phys.* **1957**, *27*, 809.
- (49) Stout, G.H.; Jensen, L.H., "X-Ray Structure Determination," Macmillan: New York (1968).
- (50) Beck, W.; Schloter, K. *Z. Naturforsch. B.: Anorg. Chem. Org. Chem.* **1978**, *33B*, 1214.
- (51) The synthesis of formyl-Cp followed the method of : Rogers, R.D.; Atwood, J.L.; Rausch, M.D.; Macomber, D.W.; Hart, W.P. *J. Organomet. Chem.* **1982**, *238*, 79.
- (52) Jackson, W.R.; McMullen, C.H. *J. Chem. Soc.* **1965**, 1170.
- (53) Caro, B.; Jaouen, G. *J. Organomet. Chem.* **1981**, *220*, 309.
- (54) Normally free -OH exhibits a stretch at $3650\text{-}3584\text{ cm}^{-1}$ according to: Sil-

verstein, R.M.; Bassler, G.C.; Morrill, T.C., "Spectrophotometric Identification of Organic Compounds," 3rd ed., Wiley: New York (1974).

(55) Watson, P.L.; Bergman, R.G. *J. Am. Chem. Soc.* **1979**, *101*, 2055.

(56) The synthesis employed was adapted from references 57a and b with the substitution fo $W(CH_3CN)_3(CO)_3$ ⁵⁸ for $W(CO)_6$.

(57) (a) Piper, T.S.; Wilkinson, G. *J. Inorg. Nucl. Chem.* **1956**, *9*, 104. (b) Fischer, E.O.; Hafner, W.; Stahl, H.O. *Z. Anorg. Allg. Chem.* **1955**, *282*, 47.

(58) Tate, D.P.; Knipple, W.R.; Augl, J.M. *Inorg. Chem.* **1962**, *1*, 433.

(59) King, R.B.; Fronzaglia, A. *Inorg. Chem.* **1966**, *5*, 1837, with the substitution of $W(CH_3CN)_3(CO)_3$ ⁵⁸ for $W(CO)_6$.

(60) Schröder, V.R.; Striegler, A.; Zimmerman, G.; Mühlstädt, M. *J. Prakt. Chem.* **1973**, *315*, 958.

(61) King, R.B., "Organometallic Syntheses," Vol.I, Academic: New York (1965).

(62) The trityl ether of the starting substituted cyclopentadienyl was a gift from K.M. Doxsee.

(63) Tirosh, N.; Modiano, A.; Cais, M. *J. Organomet. Chem.* **1966**, *5*, 357.

(64) Macomber, D.W.; Rausch, M.D. *Organometallics* **1983**, *2*, 1523.

(65) Stewart, R.F.; Davidson, E.R.; Simpson, W.T. *J. Chem. Phys.* **1965**, *42*, 3175.

(66) "International Tables for X-Ray Crystallography," Vol IV, Kynoch Press: Birmingham, England (1974).

(67) The weights, $w = [s + r^2b + (.02 \times s)^2]^{-1}(Lp/k^2)^2$, s = scan counts, r = scan-to-background time ratio, b = total background counts, k = scale factor of F ; $R_F = \Sigma |F_o - |F_c|| / \Sigma |F_o|$ (sums of reflections with $I > 0$); $R'_F = R_F$ (sums of reflections with $I > 3\sigma_I$); $S = [\Sigma w(F_o^2 - (F_c/k)^2)^2 / (n - v)]^{1/2}$, n = number of

reflections, v = number of parameters.

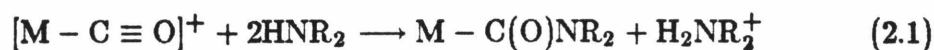
Chapter 2

**Synthesis, Characterization and Equilibrium
Studies of Group VI B Intramolecular Metallaesters**

Introduction

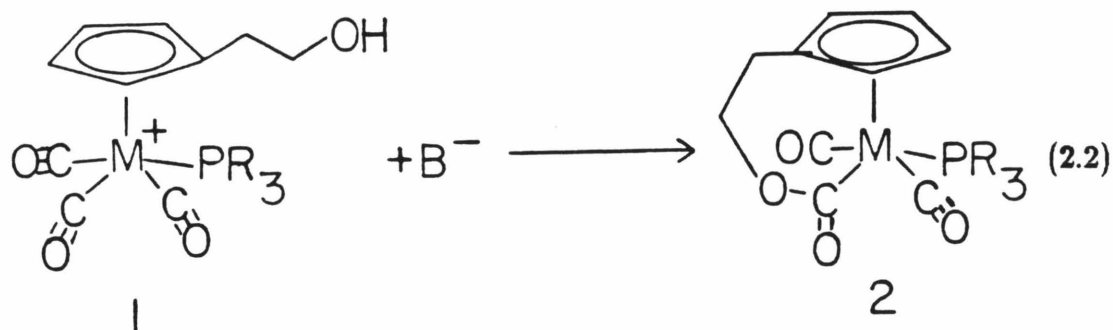
The possibility of intramolecular nucleophilic activation of carbon monoxide as a means of enhancing the reactivity of the carbonyl ligand toward reduction was discussed in Chapter 1. While a number of bifunctional complexes were synthesized containing both alcohol and carbonyl functionalities, no interaction other than an intramolecular hydrogen bond in the case of $[\text{Cp}-(\text{CH}_2)_n\text{-OH M}(\text{CO})_3\text{PR}_3]^+$ complexes was observed. While the CO stretching frequencies were in the range usually observed for complexes that react with amines or other nucleophiles to give carbamoyl or analogous compounds, the alcohol group does not display the requisite nucleophilicity to attack the carbonyl.¹

The reaction with amines (eq 2.1) requires two equivalents of primary or secondary amines.² This allows for the formation of an amide, the species that attacks at the carbonyl carbon to yield the carbamoyl complex. Hence, the use of anionic nucleophiles is suggested.



Results and Discussion ³

Initial investigation was focused on the compounds with the bridging arm length $-(\text{CH}_2)_2-$ due to the fact that this intermediate arm length looked quite promising as a bridging group and because of its relative ease of synthesis.⁴ Treatment of the cations, $[\text{Cp}-(\text{CH}_2)_2-\text{OHM}(\text{CO})_2\text{PR}_3]^+$, (**1 a-d**) with base cleanly generated the intramolecular metallalaesters (**2**) shown in eq 2.2.⁵



1 & 2: a, M=Mo, R=Ph

b, M=W, R=Ph

c, M=Mo, R=p-tolyl

d, M=W, R=p-tolyl

Comparison of the IR, ^1H and ^{31}P NMR data indicates that the metallalaesters (**2**) are analogous to the products formed by methoxide or PhCH_2O^- attack on the parent cations (**3,4**) (Tables 2.1 and 2.2). One major difference is the formation of only one isomer as indicated by ^{31}P and ^1H NMR. The proton NMR (Figure 2.1), and the fact that the asymmetric carbonyl stretch is more

Table 2.1. IR Stretching Frequencies^a

Compound			
$(\eta^5\text{-C}_5\text{H}_4)\text{-CH}_2\text{CH}_2\text{-O}_2\text{C-M(CO)}_2\text{PR}_3$			
M	R	$\nu(\text{CO}), \text{cm}^{-1}$	$\nu(\text{C=O}), \text{cm}^{-1}$
Mo, 2a	Ph	1970(<i>s</i>), 1881(<i>vs</i>)	1613(<i>m</i>)
W, 2b	Ph	1961(<i>s</i>), 1868(<i>vs</i>)	1610(<i>m</i>)
Mo, 2c	p-tolyl	1968(<i>s</i>), 1876(<i>vs</i>)	1610(<i>m</i>)
W, 2d	p-tolyl	1961(<i>s</i>), 1870(<i>vs</i>)	1610(<i>m</i>)
$(\eta^5\text{-C}_5\text{H}_5)\text{M(CO)}_2\text{PPh}_3\text{-CO}_2\text{Me}^b$			
Mo, 3a		1960(<i>s</i>), 1875(<i>vs</i>)	1610(<i>m</i>)
W, 3b		1950(<i>s</i>), 1863(<i>vs</i>)	1608(<i>m</i>)
$(\eta^5\text{-C}_5\text{H}_5)\text{W(CO)}_2\text{PPh}_3\text{-CO}_2\text{Bz}$			
W, 4		1957(<i>s</i>), 1866(<i>vs</i>)	1610(<i>m</i>)

^a CH₂Cl₂ solution. ^b A mixture of the *cis* and *trans* compounds.

Table 2.2. ^1H and ^{31}P NMR Data^a

Compound		^1H ^b			^{31}P ^c	
$(\eta^5\text{-C}_5\text{H}_4)\text{-CH}_2\text{CH}_2\text{-O}_2\text{C-M(CO)}_2\text{PR}_3$						
M	R	$\text{C}_5\text{H}_4\text{R}$ (H_2 & H_5)	$\text{C}_5\text{H}_4\text{R}$ (H_3 & H_4)	$\text{-CH}_2\text{O}$	CpCH_2	
Mo, 2a	Ph ^d	5.46	4.30($J = 3.4$)	3.88	2.40	71.07(s)
W, 2b	Ph ^d	5.59	4.35($J = 3.4$)	3.86	2.43	39.98($J = 212.4$) ^e
Mo, 2c	p-tolyl	5.67	4.37($J = 3.2$)	3.78	2.37	71.61(s)
W, 2d	p-tolyl	5.84	4.42($J = 3.7$)	3.77	2.47	40.04($J = 217.3$) ^e
$(\eta^5\text{-C}_5\text{H}_5)\text{M(CO)}_2\text{PPh}_3\text{(-CO}_2\text{Me)}^b$						
		Cp		-CH_3		
Mo, 3a	<i>cis</i>	5.34(s)		2.57(s)		64.55(s)
	<i>trans</i>	5.15($d, J = 1.2$)		3.48(s)		73.36(s)
W, 3b	<i>cis</i>	5.47(s)		2.51(s)		35.54($J = 271.0$) ^e
	<i>trans</i>	5.25($d, J = 1.2$)		3.45(s)		42.94($J = 234.4$) ^e
$(\eta^5\text{-C}_5\text{H}_5)\text{W(CO)}_2\text{PPh}_3\text{(-CO}_2\text{Bz)}$						
				$\text{-CH}_2\text{-O}$		
W, 4	<i>trans</i>	5.29($d, J = 1.5$)		5.49		43.08($J = 227.1$) ^e

^a $(\text{CD}_3)_2\text{CO}$ solution. ^b Chemical shifts in ppm (δ), residual protons of acetone- d_6 used as reference (2.04 ppm). Coupling constants are in Hz. Unless otherwise noted, coupling patterns indicate an AA'BB' system, the coupling constants reported for the Cp protons are attributed to the ^{31}P nucleus. ^c Chemical shifts are in ppm relative to free phosphine under the same conditions. ^d CDCl_3 solution. ^e The signal is present as a singlet along with a small doublet due to coupling to the 14% abundance ^{183}W nucleus.

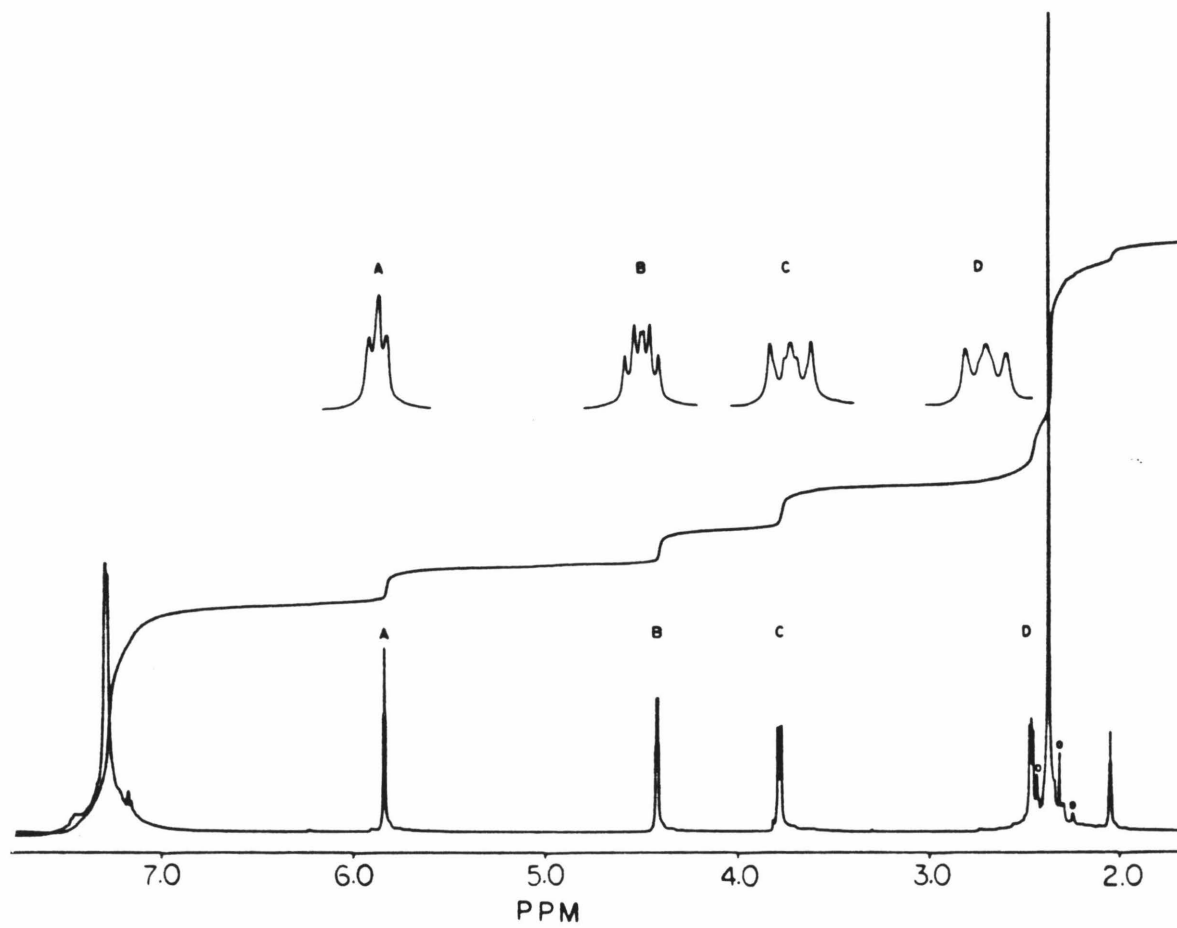


Figure 2.1. 500 MHz ^1H NMR spectrum of **2d**. Signals marked with small circles are spinning sidebands.

intense than the symmetric stretch in the IR, indicate that the single isomer formed is the *trans*,⁶ the chemical shifts and ^{183}W - ^{31}P coupling constants are consistent with this (Table 2.2).

Of particular interest with regard to the *trans* configuration of the ester and phosphine ligands is the complexity of the ^1H NMR signal at 4.30 to 4.42 ppm in **2** which appears to be a doublet of triplets (although not true binomial triplets). The signal at 5.46 to 5.84 ppm appears simply as a pseudo-triplet. These signals are due to the two pairs of protons on the substituted Cp ring. In a *trans* arrangement and with a tethered Cp ring, one pair will reside in much closer proximity to the aryl rings of the phosphine than the other and as such will display an NMR signal shifted upfield, much in the manner of Cp-ligand protons of an iron complex that has been reported.⁷

A difference Nuclear Overhauser Effect (NOE) experiment performed on **2d** is shown in Figure 2.2. The 4.42 ppm ^1H NMR signal is due to Cp protons situated much nearer to the phosphine ligand since an enhancement approximately four times greater than that for the 5.84 ppm signal is observed upon irradiation of the *ortho* protons of the tolyl phosphine. This suggests that the additional splitting of the signal is due to coupling with the ^{31}P nucleus.⁸ The coupling of more than 3 Hz is quite large in comparison to the couplings normally observed for *trans*-CpM(CO)₂LX compounds (1.0-1.5 Hz). This is presumably because rotation does not occur about the M-Cp axis and as such, the interaction between the ^{31}P and ^1H nuclei is greater for H₃ and H₄. Accordingly, the interaction between the phosphorus and H₂ and H₅ nuclei is small and no coupling is observed. This lends support in favor of the through-space coupling explanation of the ^1H and ^{31}P nuclei, since through-bond coupling does

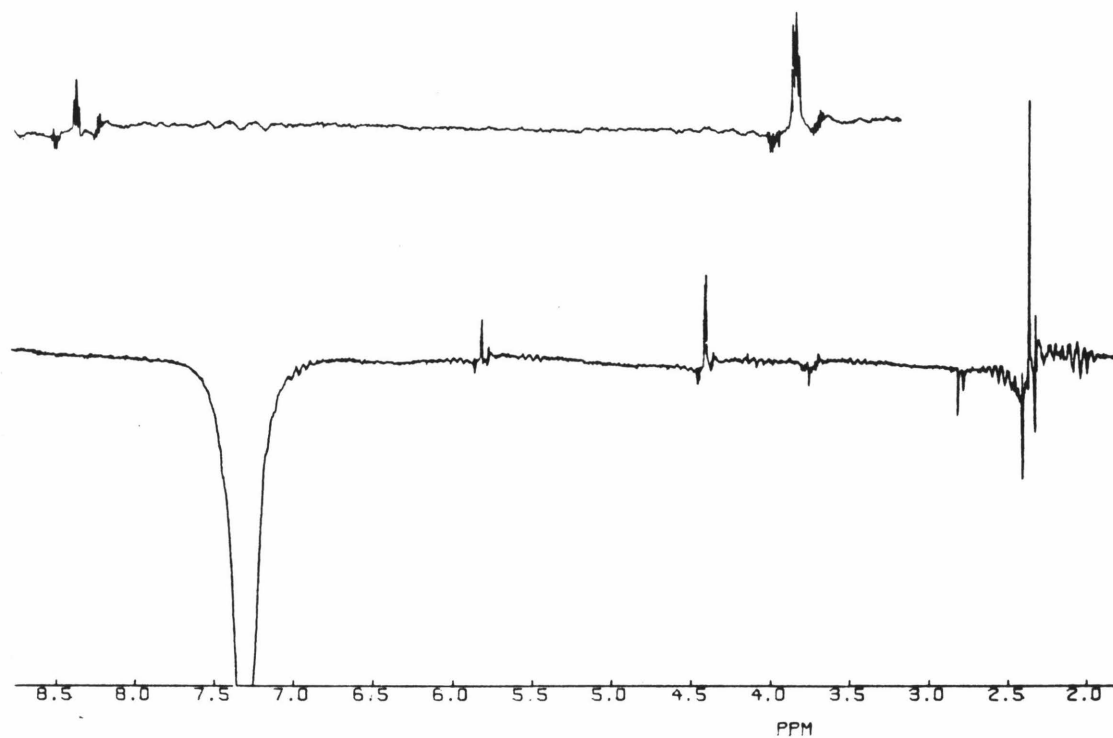


Figure 2.2. Difference NOE (500 MHz) spectrum of **2d** upon irradiation of *ortho* protons of the p-tolyl groups. Inset is an expansion of the region from approximately 4.0 to 6.0 ppm.

not explain the difference in the Cp protons as readily. The through-space mechanism has been proposed by some⁹ and disputed by others¹⁰ as an explanation of the doublet Cp ¹H NMR signal in *trans*-CpM(CO)₂LX compounds.

Isolation of **2b** as a crystalline product has permitted an x-ray structure determination. The *trans* configuration of the metalloester (Figure 2.3) confirms the spectroscopic assignments. The lack of *cis* isomer is most probably due to unfavorable steric interactions, since the arm bridging the Cp and carbonyl would be moved much closer to the carbonyls and the relatively bulky phosphine ligand. In the less bulky parent methyl ester complexes (**4**) the *trans* isomer predominates over the *cis* in solution by approximately 60:40. This predominance is significant when it is considered that there are two possible carbonyls that will yield a *cis* isomer upon methoxide attack.

Figure 2.4 shows the atom labeling scheme and bond lengths and angles are shown in Figures 2.5 and 2.6. The ester moiety is normal, with C–O bond lengths of 1.39(2) and 1.41(2) Å (C(1)–O(2), C(2)–O(2)) and a C=O bond length of 1.23(2) Å (C(1)–O(1)). While the ester carbonyl stretch is at lower than normal energy (1610 vs. 1750 cm⁻¹) the C(1)–O(1) bond length does not reflect this change.¹¹

Comparison of the W–CO bond lengths (1.94(1) and 1.96(2) Å for W–C(9) and W–C(10)), C≡O bond lengths (1.18(2) and 1.19(2) Å), and W–C–O angles (175.5(13) and 172.7(14)°) to other CpW compounds containing terminal carbonyls indicates that they are normal.^{12,13,14} The average distance from the W atom to the Cp ring carbons (2.361 Å) is quite similar to other reported values (2.366 Å¹³ and 2.336 Å¹⁴) as is the W–R (R≡ Cp centroid) distance (2.013 Å) to another reported value (2.04(1) Å).¹² Additionally, the angles between

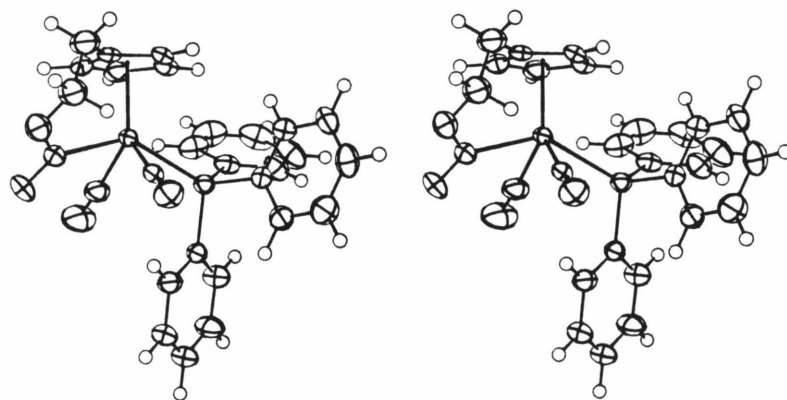


Figure 2.3. Stereoview ORTEP diagram of **2b**. Non-hydrogen atoms are represented by their 50 % probability ellipsoids.

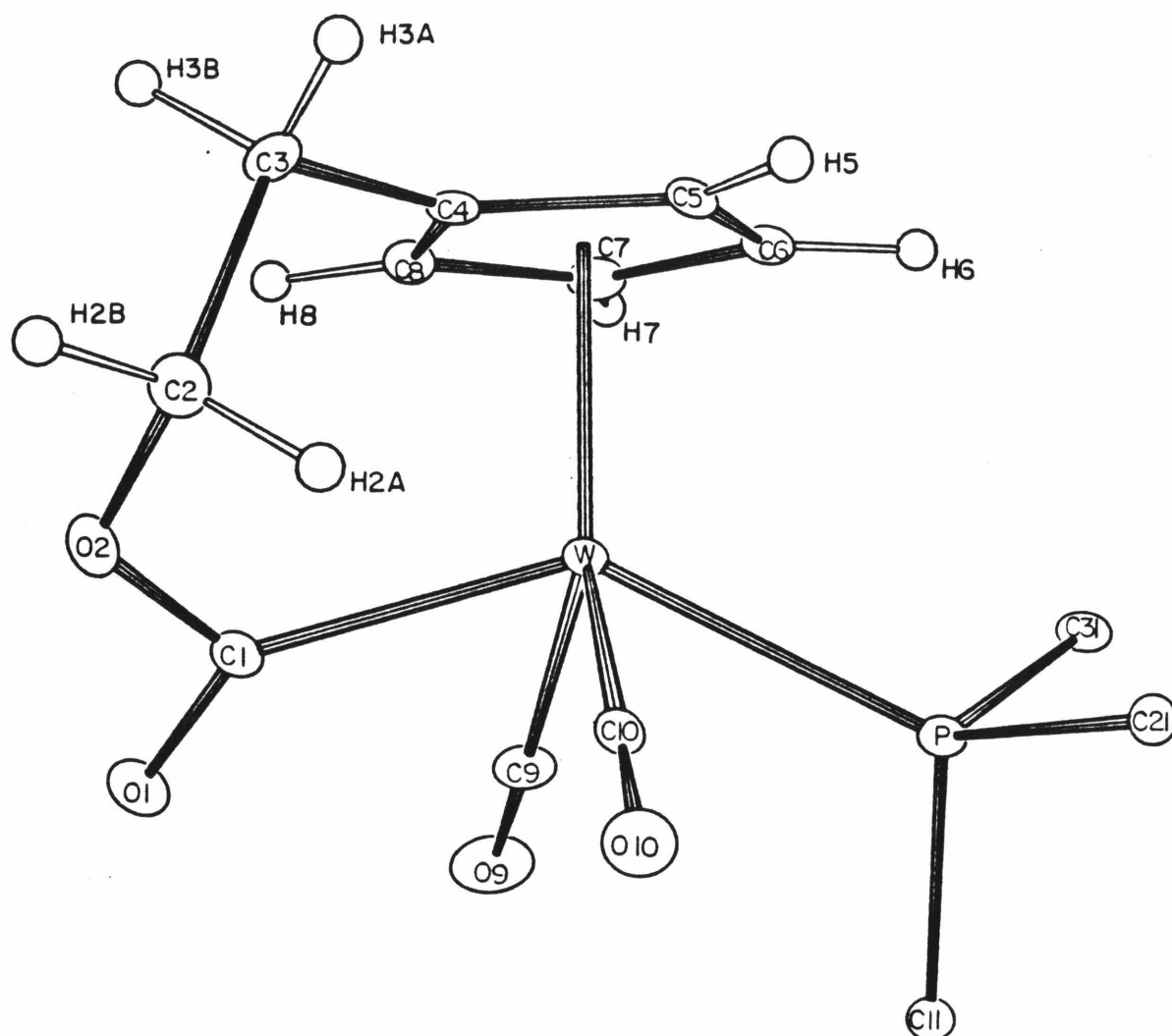


Figure 2.4. Atom labeling scheme for **2b**. A portion of the triphenylphosphine has been omitted for clarity.

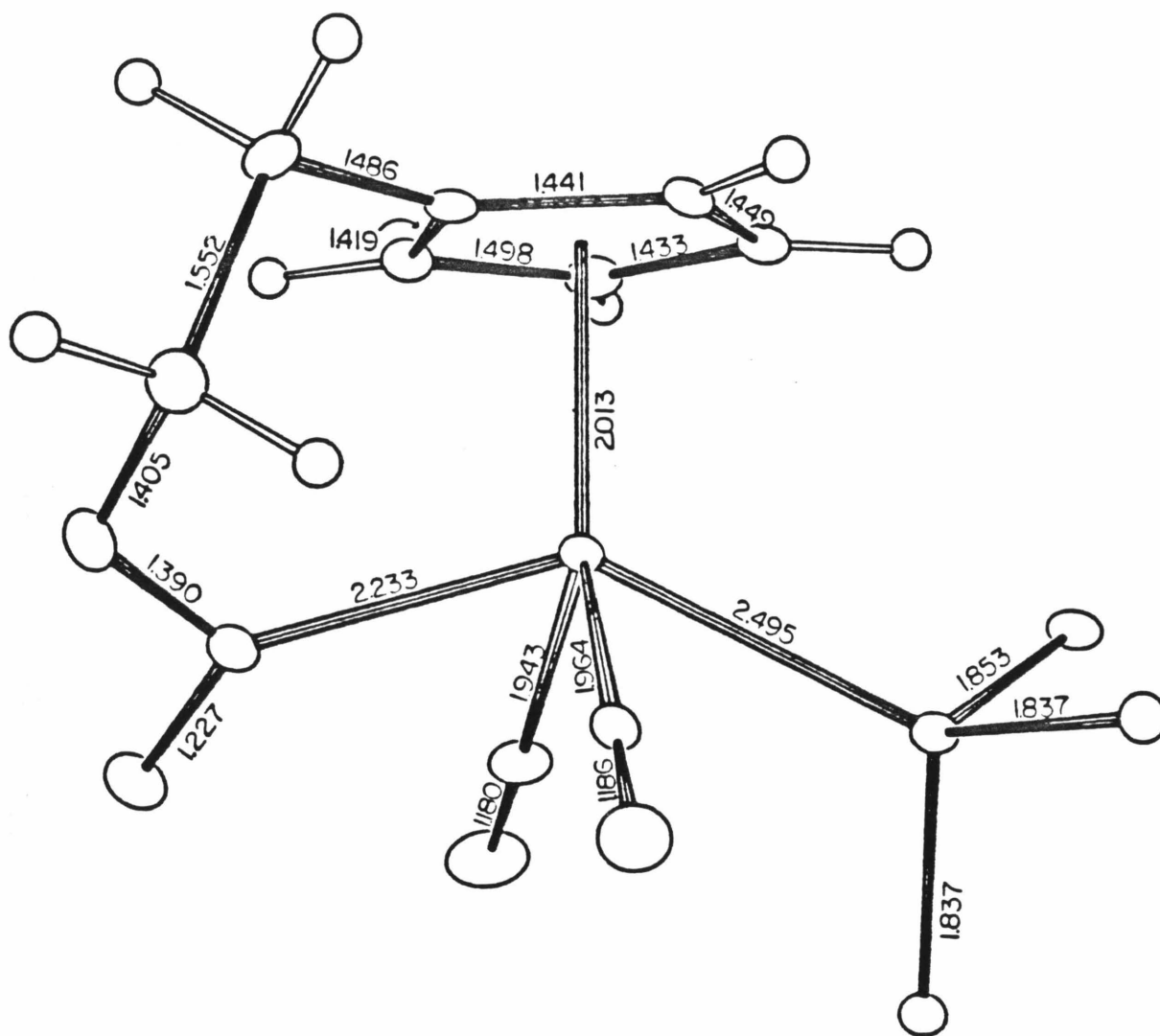


Figure 2.5. Selected bond lengths for **2b**. A portion of the triphenylphosphine has been omitted for clarity.

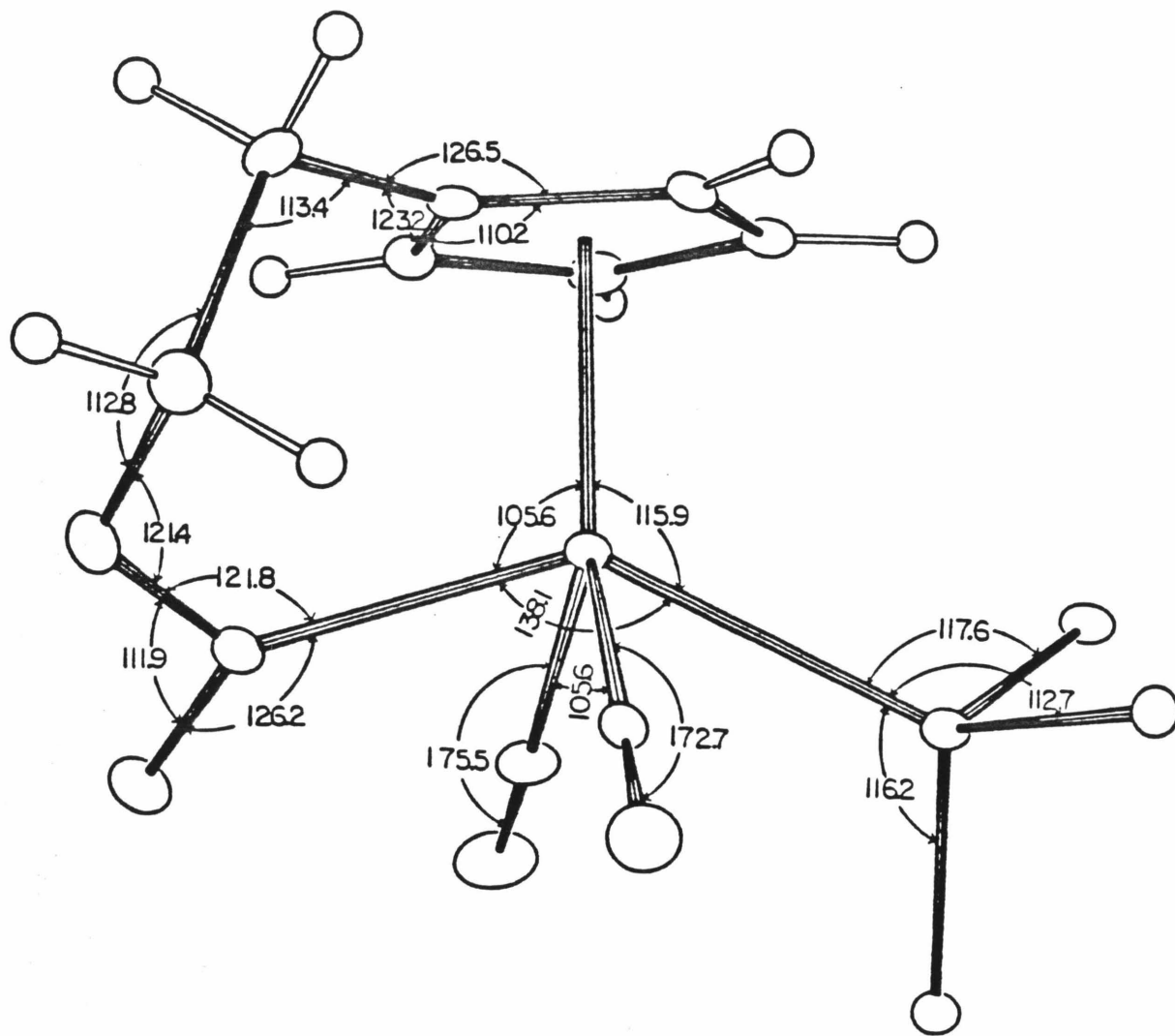


Figure 2.6. Selected bond angles for **2b**. A portion of the triphenylphosphine has been omitted for clarity.

the ligands *trans* to one another in the piano stool "legs" ($105.6(2)^\circ$ for C(9)–W–C(10) and $138.5(4)^\circ$ for C(1)–W–P) are reasonably similar to those reported for two four-legged Mo(II) complexes:

(a) for $\text{CpMo}(\text{CO})_2\text{PPh}_3(-\text{C}(\text{O})\text{CH}_3)$, C–Mo–P is $132.7(4)^\circ$ and OC–Mo–CO is $107.9(5)^\circ$,¹⁵ (b) for $\text{CpMo}(\text{CO})_2(-\text{GePh}_3)(=\text{C}(\text{OEt})\text{Ph})$, Ge–Mo–C is $131.8(3)^\circ$ and OC–Mo–CO is $105.1(5)^\circ$.¹⁶ The substituted-Cp molybdenum dimer, $[\text{Cp}(\text{CH}_2)_3\text{-OH Mo}(\text{CO})_3]_2$, has comparable angles; C(3)–Mo–Mo' is 127.9° and OC–Mo–CO is 105.8° . Additionally, a recent structure of a heterobimetallic complex containing a $\text{CpW}(\text{CO})_2(\overline{=\text{CO}-(\text{CH}_2)_3})$ fragment provides for further comparison: Mo–W=C is $136.1(5)^\circ$ and OC–W–CO is $99.5(18)^\circ$.¹⁷

The slightly enlarged C(1)–W–P angle of 138.5° in **2b** may indicate a small distortion due to the constraints imposed by the $-(\text{CH}_2)_2$ -bridging arm. The W–C(1) bond length of $2.233(15)\text{\AA}$ is somewhat longer than the carbene W double bond in the structure mentioned above ($1.977(17)\text{\AA}$). This is indicative of the lack of predominance of the carbenoid resonance form. Upon consideration of the bridging arm itself, no unusual bond lengths or angles are noted implying little or no strain upon coordination of the ester to W, although the O(2)–C(2)–C(3)–C(4) torsion angle of 60.6° (Table 2.3) indicates a *gauche* orientation rather than the staggered configuration of the unconstrained arm in the molybdenum dimer. However, the value of the torsion angle is quite similar to the corresponding value observed in structures containing analogous C–C–O fragments.¹⁸ Moreover, the Cp plane is roughly perpendicular to the W–R vector (deviation 3.91°), not unlike the coordination of Cp to other tungsten complexes.^{12,13,14,19} The individual deviation of atoms from the best least-squares plane (Table 2.3) is quite small, as is the displacement of C(3) from this plane ($.09\text{\AA}$), indicating

Table 2.3. Best Least Square Plane and Torsion Angles for 2b

Atom	Dev ^a
C(4)	0.006
C(5)	-0.014
C(6)	0.017
C(7)	-0.013
C(8)	0.004
W	2.013
C(3)	-0.089
C(2)	1.316

Atoms	Angle(°)
C(4)-C(3)-C(2)-O(2)	-60.6(17)
C(5)-C(4)-C(3)-C(2)	-96.6(17)
C(8)-C(4)-C(3)-C(2)	89.6(16)
C(3)-C(2)-O(2)-C(1)	72.8(17)
C(2)-O(2)-C(1)-W	-12.4(18)
C(2)-O(2)-C(1)-O(1)	169.5(13)
R-W-C(1)-O(1)	126.6(13)
R-W-C(1)-O(2)	-51.2(12)

^aDeviation in Å from best Cp plane (C(4) through C(8)).

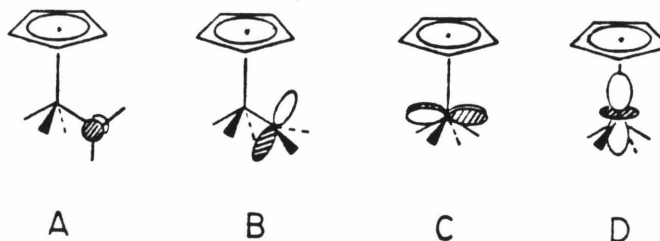
minimal strain at C(4). The Cp plane is tipped more with respect to the W-R vector than in the unconstrained of the Mo dimer (1.605°). This is a further indication of a slight distortion in the bridged system although the difference is not substantial. The ethylene bridge appears to be a reasonable length for linking the ester group and the Cp.

The non-bonding distances of the *ortho* phenyl protons to the H₂ & H₃ and H₃ & H₄ pairs can be calculated and an estimate of the NOE enhancement upon irradiation of the phenyl protons can be made. A ratio of 3 to 1 for the H₃ & H₄ pair over H₂ & H₃ is obtained. This is in good agreement with the observed value (*vide supra*). In a similar manner, calculation of the average distance between the phosphorus atom and the Cp proton pairs leads to a through-space coupling ratio of 2:1 for the H₃ & H₄ pair over H₂ & H₃.²⁰ Thus, while the coupling between phosphorus and H₂ & H₃ is expected to occur, it may simply be present at a value below the resolution of the NMR instrument (the calculated coupling constant based on these non-bonding distances is ≤ 1.5 Hz). The shape of the ¹H NMR signal arising from the H₂ & H₃ pair does not preclude such an explanation since it could quite easily be an unresolved doublet of pseudo-triplets.

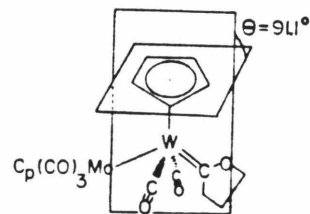
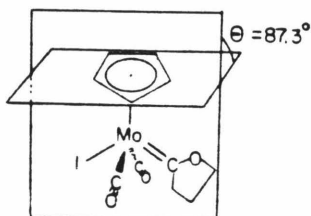
Regardless, the compounds have provided a unique opportunity to examine the putative through-space coupling mechanism. The tethering of the Cp ligand, however, thwarts to some extent an explanation of the difference in J_{HP} between the *cis* and *trans* CpM(CO)₂LX compounds since it has been suggested that the difference lies in the tipping of the Cp upon steric interaction with the phosphine and the *cis* or *trans* X ligand.²¹ As discussed above, the overriding factor involved in the configuration of the Cp in **2b** is most probably the

orientational requirement of the ethylene bridge.

Also of interest is the orientation of the $-\text{CO}_2\text{R}$ fragment about the $\text{W}-\text{C}(1)$ bond axis. Calculations indicate that for $\text{CpM}(\text{CO})_2\text{LL}'$ complexes, where L' is a π donor or acceptor, orientation **A** is preferred.²² Orientation **B** has been calculated to be 15 kcal higher in energy than **A** in the case of $[\text{CpMo}(\text{CO})_2\text{PH}_3(=\text{CH}_2)]^+$. This can be rationalized upon consideration of the overlap between the available orbitals on the transition-metal center, the d_{xy} and d_{z^2} (**C** and **D**), and the p orbital on the ligand; it is better in orientation **A** using the d_{xy} orbital.



Crystallographic data support the calculations. For example, the acyl complex, $\text{CpMo}(\text{CO})_2\text{PPh}_3(-\text{C}(\text{O})\text{Me})$, has a torsional angle for $\text{R}-\text{Mo}-\text{C}-\text{Me}$ of approximately 180° ¹⁵ as does the neutral carbene complex, $\text{CpMo}(\text{CO})_2(-\text{GePh}_3)(=\text{C}(\text{OEt})\text{Ph})$, for $\text{R}-\text{Mo}-\text{C}-\text{Ph}$ (where R is the Cp centroid in both cases).¹⁶ Similarly, two recent Mo and W carbene structures indicate angles between the planes defined by the Cp atoms and the $\text{M}=\text{C}(\text{O})-\text{C}$ atoms of 87.3° and 91.1° thus providing further evidence for a preference for the vertical orientation (**A**).^{17,23,24}



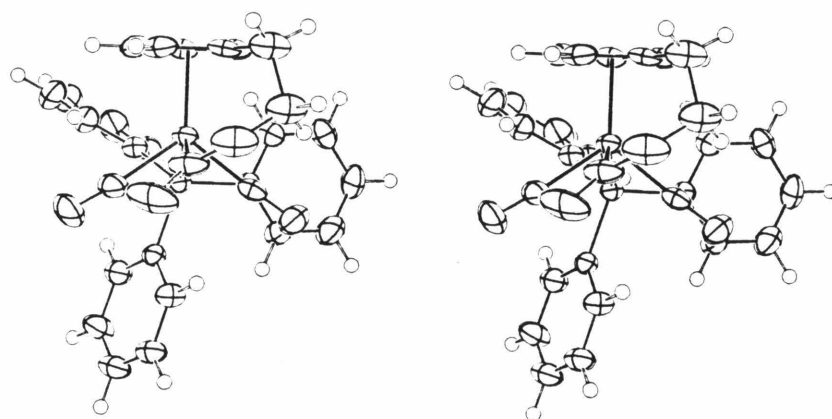


Figure 2.7. Stereoview ORTEP diagram of **2b** viewed along C(1)-W-P.

librium constants obtained are $1.65 \pm .30 \text{ M}^{-1}$ and $1.27 \pm .15 \text{ M}^{-1}$ for **2c** and **2d** respectively. However, measurements of ΔH° and ΔS° in acetone and THF indicate the probable existence of substantial solvent effects. Therefore, equilibrium measurements were obtained in benzene- d_6 in the hope of circumventing any major solvent participation. Figure 2.8 shows the van t'Hoff plot obtained for the process shown in eq 2.3, where M is tungsten and R is p-tolyl (**2d**). A similar plot is obtained for the molybdenum compound (**2c**). The values found for ΔH° and ΔS° are $-0.9 \pm .2 \text{ kcal/mole}$ and $4.5 \pm .6 \text{ eu}$ for W and $-1.1 \pm .6 \text{ kcal/mole}$ and $3.2 \pm 2.0 \text{ eu}$ for Mo. These correspond to ΔG° values of $-2.2 \pm .4$ and $-2.1 \pm 1.2 \text{ kcal/mole}$. Thus, it appears that in the absence of other effects, the process is favored slightly both entropically and enthalpically although both terms are admittedly small.

While it would seem that the entropy should decrease for the process as shown, the entropy gain upon dissociation of the intramolecular arm is apparently sufficiently high to balance the entropy loss associated with the binding of the external alcohol. An additional factor is the clustering of the methanol that is expected to occur in the solvent systems used. Therefore, the entropy of the free methanol may not be as great as would normally be encountered in more polar solvents. The change in enthalpy may be involved with an orientation change of the ester group upon loss of tethering. Presumably the methyl ester is able to attain a more favorable configuration with greater bond overlap than is feasible with the intramolecular ester. This is in general agreement with calculations using analogous systems (*vide supra*).

The system also offers the possibility of measuring the activation parameters, ΔG^\ddagger , ΔH^\ddagger and ΔS^\ddagger (Table 2.4).²⁵ As expected for a bimolecular process,

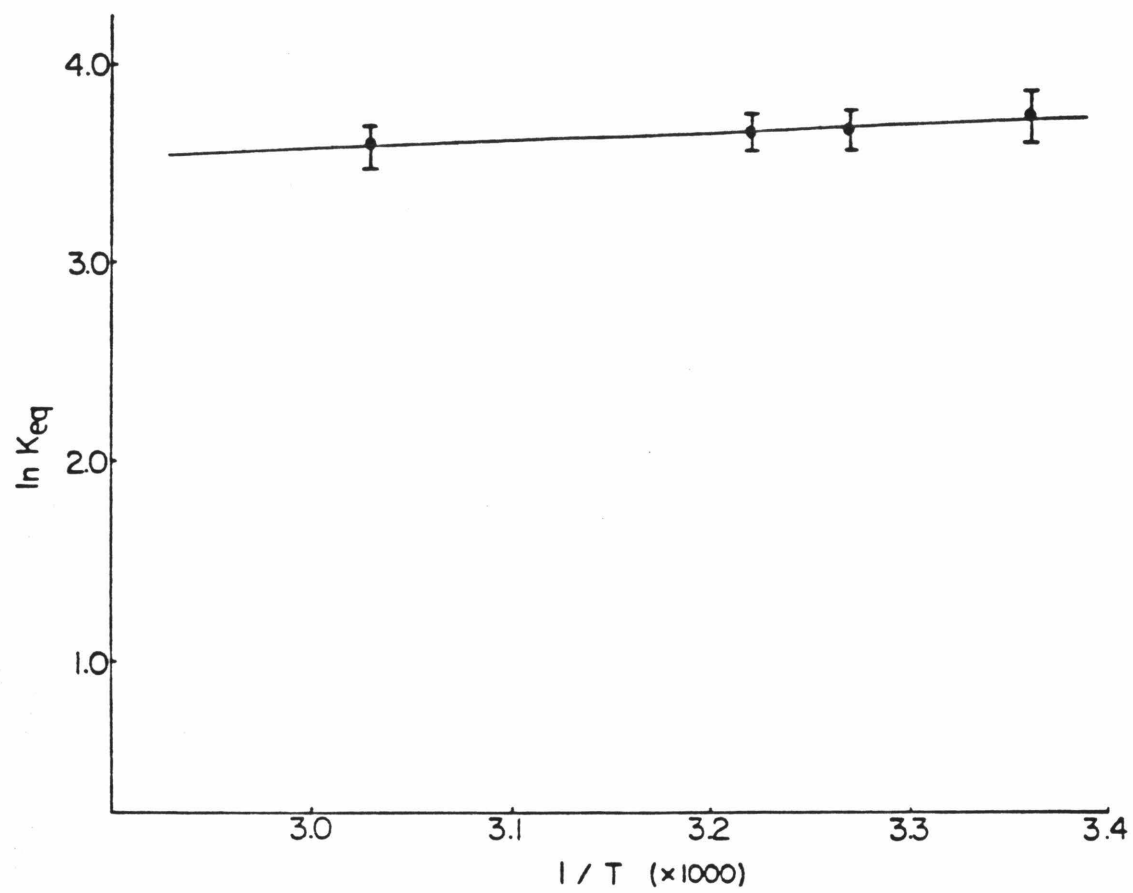


Figure 2.8. van t'Hoff plot for the equilibration of 2 with methanol. $M = W$ and $R = p\text{-tolyl}$ in C_6D_6 .

Table 2.4. Thermodynamic Parameters for Intra to Intermolecular Equilibration

M	R	<i>n</i>	$K_{eq}(M^{-1})^a$	$\Delta G^o(kcal)$	$\Delta H^o(kcal)$	$\Delta S^o(eu)$
W	Ph	1	$\leq 4.2(8)$	$\geq - .7(1)$
Mo	p-tolyl	2	17(3)	-1.7(1)	0.9(1)	8.7(4)
W	p-tolyl	2	40(12)	-2.2(2)	-0.9(2)	4.5(6)
Mo	Ph	3	$\geq 230(40)$	$\leq - 3.2(2)$
W	Ph	3	$\geq 117(19)$	$\leq - 2.8(1)$
With EtOH:						
W	p-tolyl	2	91(20)	-2.7(1)	-4(1)	-6(4)
				$\Delta G^\ddagger(kcal)$	$\Delta H^\ddagger(kcal)$	$\Delta S^\ddagger(eu)$
Mo	p-tolyl	2		20.2(3)	4(3)	-55(11)
W	p-tolyl	2		20.4(6)	5(2)	-53(8)

^a 25°C.

ΔS^\ddagger is negative and relatively large (-55 eu for Mo and -53 eu for W). ΔH^\ddagger on the other hand is positive and fairly small (4 and 5 kcal/mole). Therefore, it is apparent that ΔS^\ddagger is responsible for most of the positive ΔG^\ddagger (20.2 and 20.4 kcal/mole).

As a further study, the tungsten complex was equilibrated with ethanol at various temperatures. The resulting ΔH° and ΔS° values are -4 ± 1 kcal/mole and -6 ± 4 eu. The more negative ΔH° is difficult to rationalize since a number of factors may be responsible, for example, the ethyl group is more sterically demanding and will prefer a less crowded orientation. At the same time, ethanol should be less clustered in benzene solution. As a result, it is not wise to place too great an emphasis on comparison of ΔH and ΔS , however, the similarity in thermodynamics implies that there is relatively little difference between the reactions of the two alcohols with the intramolecular ester.

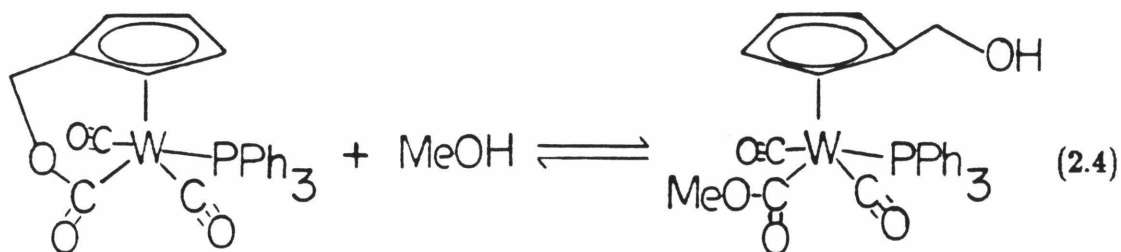
To further explore the requirements of intramolecular activation of CO, cationic complexes in which -OH was bound to the Cp by the trimethylene bridge were studied (1e and 1f). Treatment of these propanol compounds with methoxide affords only the methyl esters (5 e,f) unlike the ethanol complexes (see eq 2.2). Limiting values of the equilibrium constants for a process like that shown in eq 2.3 have been found to be $\geq 230 \text{ M}^{-1}$ for the Mo complex (5e) in acetone at 25°C and $\geq 117 \text{ M}^{-1}$ for W (5f) in benzene at 25°C . The corresponding ΔG° values are ≤ -3.2 and ≤ -2.8 kcal/mole. In actuality, the values are probably more negative since no intramolecular ester is observed in solution with minimal alcohol concentration. It appears then that the trimethylene bridge is unable to achieve the correct orientation, at least in competition with the methyl ester formation (other more sterically bulky bases form the analogous intermolecular

esters or carbamoyl compounds as well).²⁸ Molecular models indicate that while the trimethylene bridge is physically possible, steric interactions are expected to occur to a significant extent with the carbonyl ligands, in that the middle -CH₂- group appears to achieve close contact. It is also conceivable that the entropy loss may be prohibitively large for intra *versus* intermolecular ester formation.

Finally, since the -(CH₂)₂- arm appears suited to bridge the cyclopentadienyl and ester groups, and the -(CH₂)₃- appears to be unsuitable, the question arises whether shortening the arm will allow for intramolecular ester formation. To investigate this possibility, the hydroxymethyl derivative, $[(\eta^5\text{-C}_5\text{H}_4\text{CH}_2\text{OH})\text{M}(\text{CO})_3\text{PR}_3]^+\text{BF}_4^-$ (**1g**), was examined.

Treatment of **1g** with base affords the intramolecular metallaester (**2g**).²⁹ However, while treatment of the hydroxyethyl complexes (**1 a d**) with base yields the intramolecular metallaesters (**2 a d**) almost immediately, formation of **2g** requires several days under the same conditions. Additionally, the ester that is formed is stable in chloroform and acetone solution for days whereas the -(CH₂)₂- compound decomposes within hours in the same solvents. It appears that ester formation is slow but the overall process is more thermodynamically favored than for the hydroxyethyl derivative.

To understand this better, an intra *versus* intermolecular ester formation study was carried out. As before, methanol was added to a solution of the intramolecular metallaester, however, no methyl ester was observed. A limiting value of K_{eq} of $\leq 4.2 \pm 0.8 \text{ M}^{-1}$ was thus obtained for the process given in eq 2.4. This corresponds to $\Delta G \geq -0.7 \pm 0.1 \text{ kcal/mole}$. The source of the added stability, with reference to the -(CH₂)₂- metallaesters, may be better overlap between the carbenoid p and metal d_{xz} orbitals.

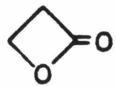
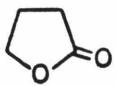
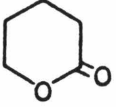
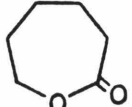


Consideration of molecular models as well as the bond distances obtained from the crystal structure of **2b** indicate that a single methylene should be quite suitable for bridging the distance between the cyclopentadienyl ring and the ester group. No significant distortion of the $-\text{CH}_2-$ out of the Cp ring plane should be encountered and the subsequent torsion about the W-C bond is expected to give more favorable π overlap (*vide supra*). This should give rise to additional stabilization. A lower limit of the difference in ΔG° for metallaester formation with the different bridging arms is 1.5 ± 0.4 kcal/mole with the $-(\text{CH}_2)-$ bridge providing the more stable complex.

An additional source of stability may simply be the effective ring size of the lactone-like intramolecular metallaester. It is known that γ -lactones are favored over their corresponding hydroxy-acids while the opposite is true of δ -lactones. This may also account for the lack of formation of the intramolecular metallaester bridged by the $-(\text{CH}_2)_3-$ group since ϵ -lactones are found to be almost completely disfavored in comparison to the hydroxy-acid (Table 2.5).³⁰

To better understand the source of the $-\text{CH}_2-$ bridged metallaester stability, a crystal was obtained and the x-ray structure determined.³¹ The structure is

Table 2.5. Lactone hydrolysis equilibria.

<u>LACTONE</u>	<u>AT EQUILIBRIUM</u>	
	<u>HYDROXY ACID</u>	<u>LACTONE</u>
β 	100	0
γ 	27	73
δ 	91	9
ϵ 	100	0

shown in Figure 2.9 where it is apparent that there are distinct similarities to the $-(\text{CH}_2)_2-$ bridged structure. The atom labeling scheme is shown in Figure 2.10 and bond distances and angles are presented in Figures 2.11 and 2.12.

It is apparent that some opening of the P-W-C(1) angle has occurred (139.5° *vs* 138.1° in **2d**) as well as a closing of the R-W-C(1) angle (103.1° *vs* 105.6°). A comparison of the bridging methylene, C(2) of **2g**, to C(3) of **2b** reveals that it has been pulled down out of the Cp plane ($.195 \text{ \AA}$, Table 2.6) a greater distance than the C(3) has been pushed up out of the plane ($.089 \text{ \AA}$) although neither of these distances is greatly disparate from that of the untethered substituted ring ($.136 \text{ \AA}$ for C(6) of the Mo dimer). The angle associated with the C(2) group of **2g** has closed to some extent (111.8° *vs* 113.4°). Also of interest is the R-W-P angle of 117.2° (*vs* 115.9°). The indications are that to accommodate the shorter bridging group, the W-R vector has tipped with respect to the C(1)-W-P moiety thus providing a shorter distance between the Cp and C(1) that must be spanned (Figure 2.13). Surprisingly, there is little difference between the two cases in the tip of the Cp with respect to the R-W vector (3.91° *vs* 3.75°). The untethered Cp of the Mo dimer (*vide supra*) has a tip of 1.61° .

The area in which a real difference is apparent is the O(2)-C(1)-W-R torsion angle. The $-\text{CH}_2-$ value is 26.4° (Figure 2.14) while the ethylene bridged complex has a value of 51.2° . Thus, the monomethylene complex more closely approaches the vertical orientation that is presumed to yield the better bonding arrangement (*vide supra*). The carbenoid resonance form may be more favored to some extent. In fact, the W-C(1) bond length is somewhat shorter ($2.207(7) \text{ \AA}$ as compared to $2.233(15) \text{ \AA}$) but the C(1)-O(1) and C(1)-O(2) bond lengths appear to be comparable at least upon consideration of the standard deviations. In

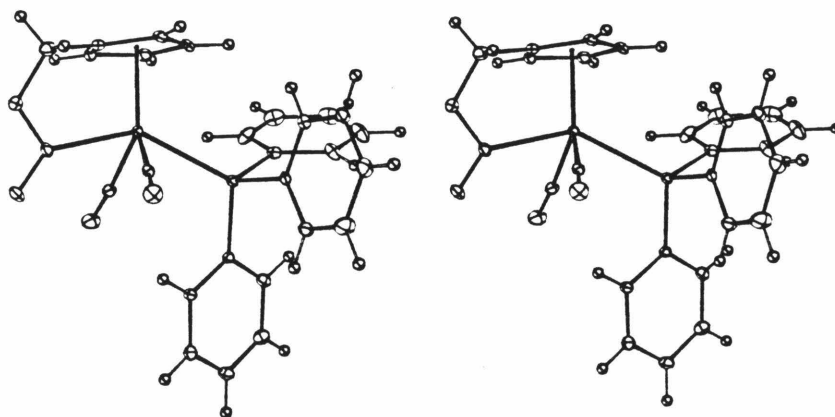


Figure 2.9. Stereoview ORTEP diagram of **2g**. Non-hydrogen atoms are represented by their 50 % probability ellipsoids.

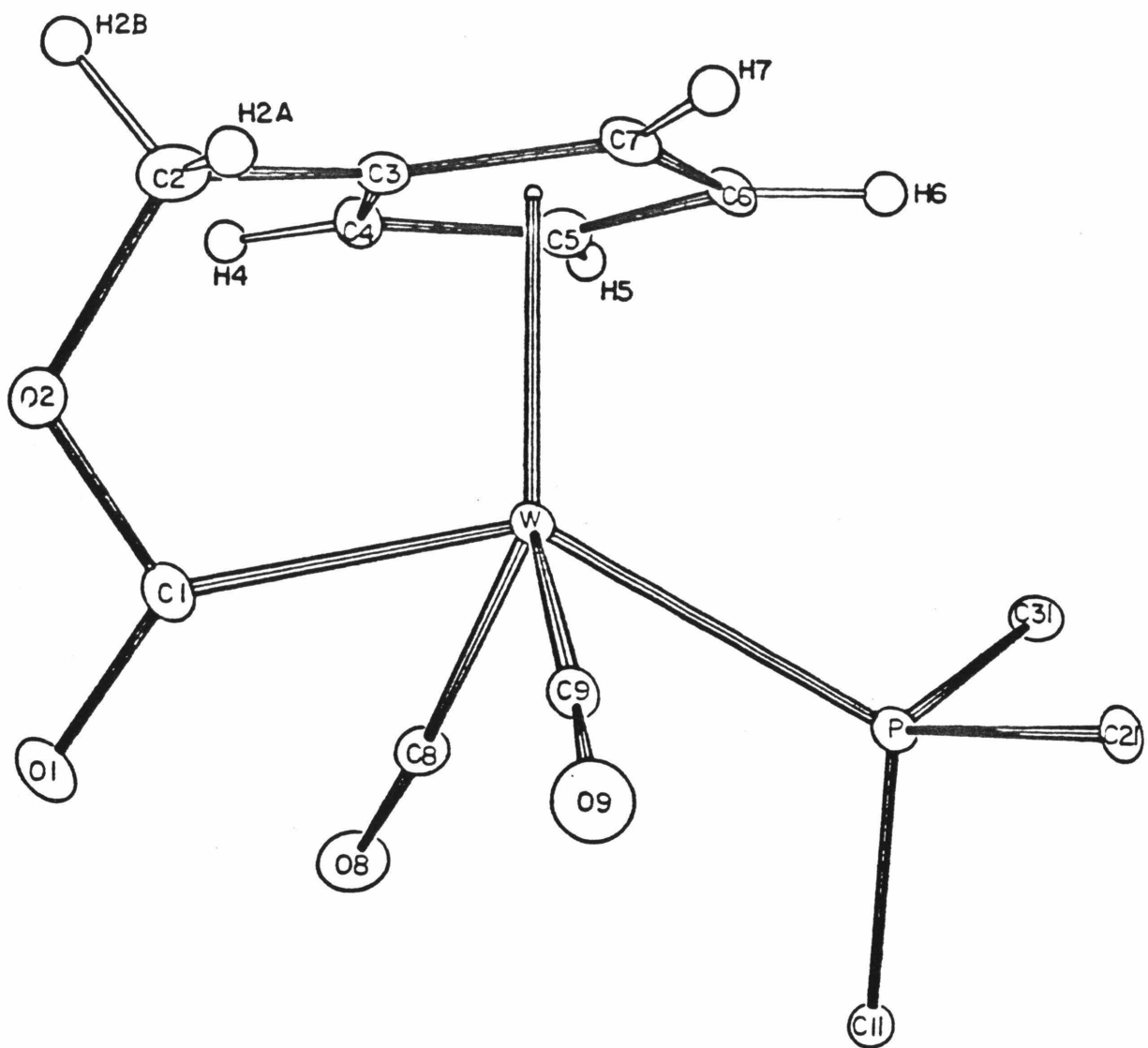


Figure 2.10. Atom labeling scheme for **2g**. A portion of the triphenylphosphine has been omitted for clarity.

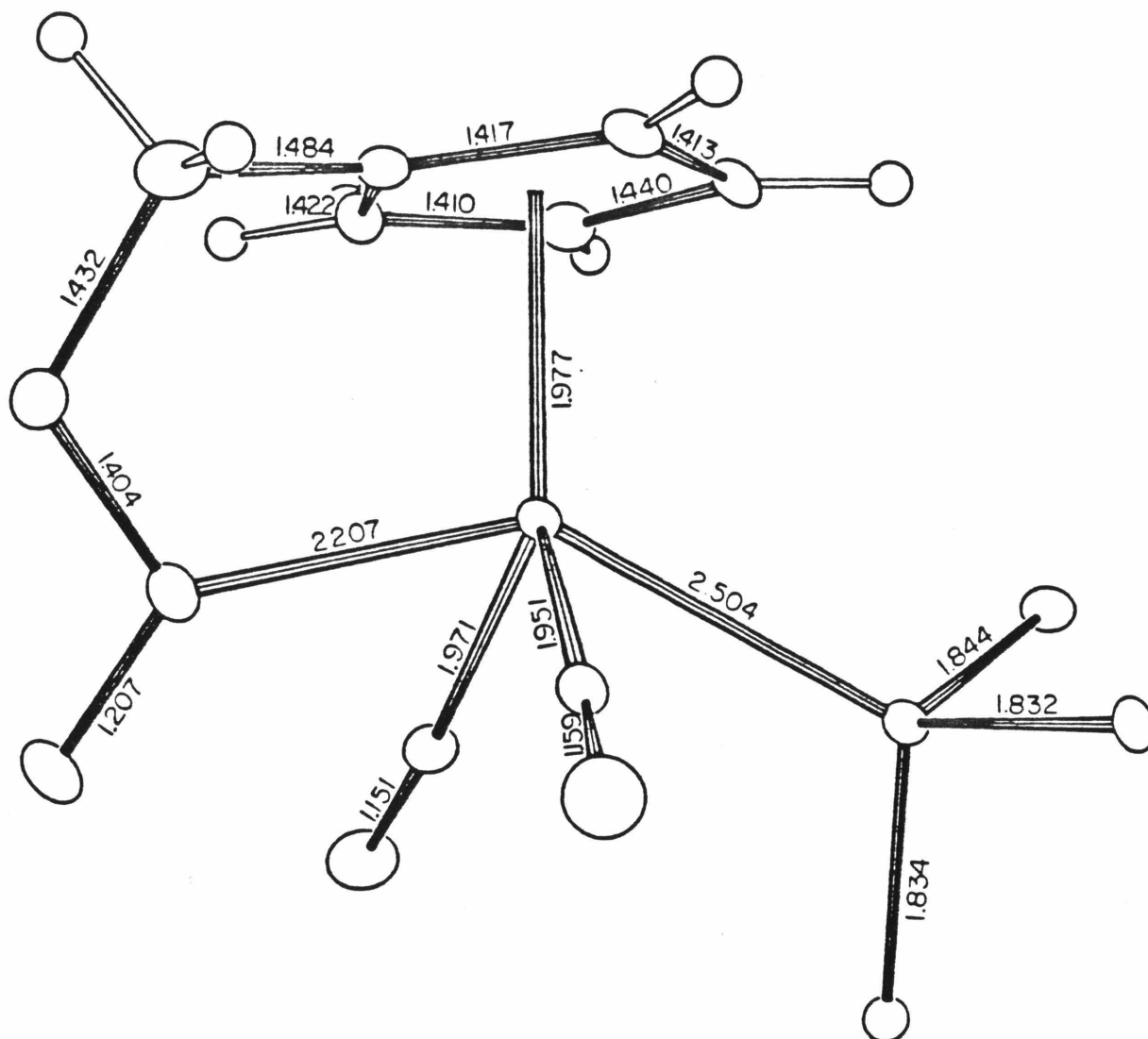


Figure 2.11. Selected bond lengths for **2g**. A portion of the triphenylphosphine has been omitted for clarity.

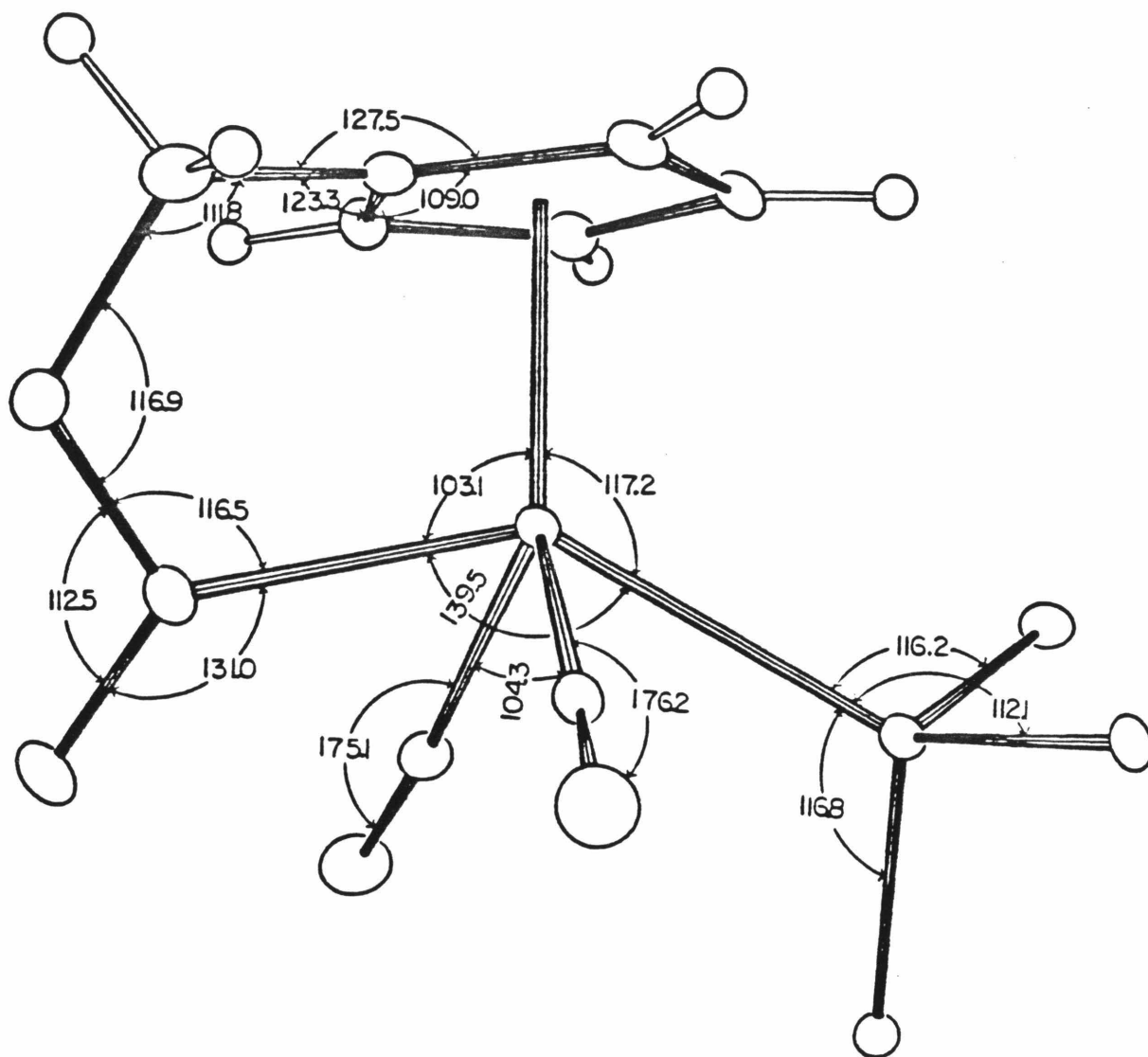


Figure 2.12. Selected bond angles for **2g**. A portion of the triphenylphosphine has been omitted for clarity.

Table 2.6. Best Least Square Plane and Torsion Angles for 2g

Atom	Dev ^a
C(3)	0.019
C(4)	-0.010
C(5)	-0.002
C(6)	0.014
C(7)	-0.020
W	1.977
C(2)	0.195

Atoms	Angle(°)
C(4)-C(3)-C(2)-O(2)	51.6(9)
C(7)-C(3)-C(2)-O(2)	-122.1(7)
C(3)-C(2)-O(2)-C(1)	23.1(8)
R-W-C(1)-O(1)	153.9(6)
R-W-C(1)-O(2)	-26.4(5)

^aDeviation in Å from best Cp plane (C(3) through C(7)).

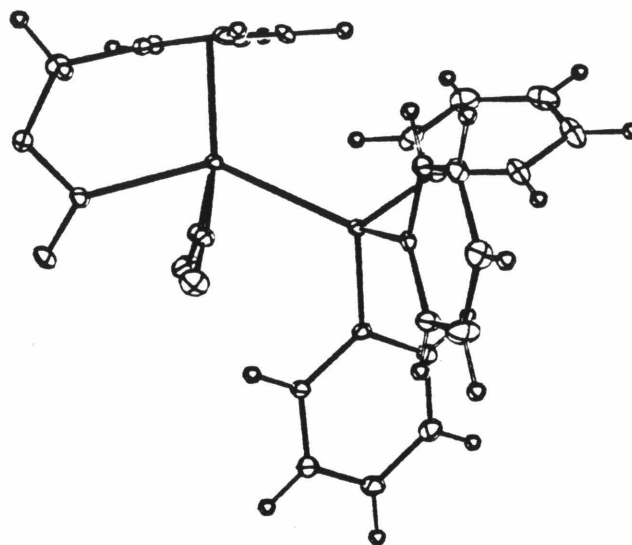


Figure 2.13. ORTEP diagram of **2g** showing the Cp orientation.

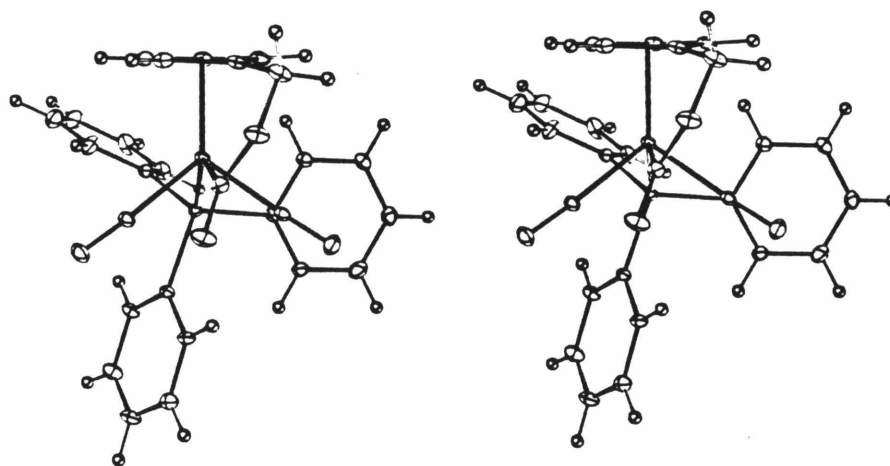
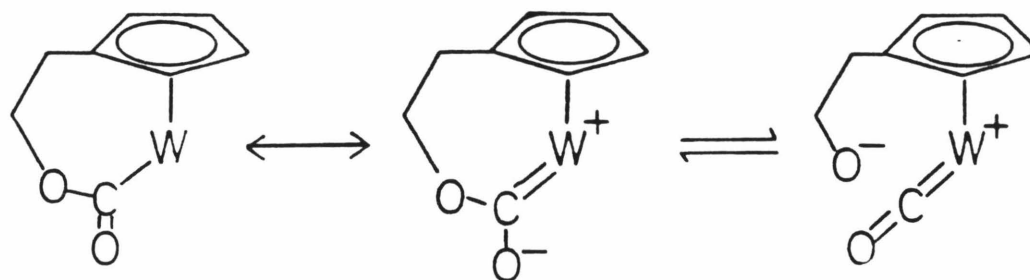


Figure 2.14. Stereoview of ORTEP diagram of **2g** viewed along C(1)-W-P.

comparison to other crystal structures containing free ester groups, the ketonic CO bond length is quite similar to these as well, e.g., recent Rh diester and cobalt ethyl ester complexes possess bond lengths of 1.185 Å and 1.196 Å.^{11,31}

It is of interest that the C=O infra-red stretch in the monomethylene case is slightly lower in energy than the ethylene bridged complex (1598 *vs.* 1610 cm^{-1}). This appears to lend support to a greater carbenoid predominance, but, the C=O stretches of the methyl and benzyl esters (Table 2.1) are also of higher energy. As a result, it appears that there is little dependence of the CO stretching frequency on the M-C torsion angle. It is possible that any effect is dampened by the buildup of electron density on the singly bonded oxygen in addition to the ketonic one, *via* the right hand tautomer:



The bond lengths are consistent with this; C(1)-O(2), 1.404(8) *vs.* 1.390(18) Å for **2g** and **2b**. However, there is the possibility that there is little significance to this difference upon consideration of the standard deviations.

In conclusion, though, it is clear that both $-\text{CH}_2-$ and $-(\text{CH}_2)_2-$ offer viable bridging groups.³³ It is also clear that these complexes provide a unique opportunity to explore the relationship between small changes in structure and their effect on the resulting stabilities.³⁴ Such an opportunity is quite relevant to the design of metal complexes containing two (or more) reactive functional groups.

Experimental

All reactions were carried out using standard Schlenk techniques. Argon used in Schlenk work was purified by passage through columns of BASF RS-11 (Chemalog) and Linde 4Å molecular sieves. Manipulations were also performed in a Vacuum Atmospheres dry box with nitrogen atmosphere. Toluene, benzene and THF were vacuum transferred from sodium-benzophenone ketyl. Methylene chloride was stirred over P₂O₅ and acetone was dried over 4Å molecular sieves prior to use. Infra-red spectra were obtained from a Perkin-Elmer 257 grating instrument and a Beckman model IR 4240 spectrometer referenced to the 1601 cm⁻¹ stretch of polystyrene. Continuous wave NMR spectra were recorded on a Varian EM-390 instrument with an ambient probe temperature of 34° C. Fourier transform ³¹P and ¹H spectra were taken on a JEOL FX-90Q spectrometer operating at 36.2 and 89.56 MHz respectively with a probe temperature of 25° C. All ³¹P NMR spectra were referenced to an external sample of the appropriate free phosphine in the relevant solvent. Difference NOE and 500 MHz ¹H NMR spectra were recorded on a Bruker WM-500 (500.13 MHz) at 25° C using the instrument of the Southern California Regional NMR Facility located at Caltech. Melting points were obtained from a Büchi melting point apparatus with all samples placed in glass capillaries under a nitrogen atmosphere and sealed. No temperature corrections were made. Elemental analyses were performed by Schwarzkopf Microanalytical of Woodside, New York, Dornis und Kolbe of Mannheim, West Germany, E & R Microanalytical of Corona, New York and the analytical facility of the California Institute of Technology.



The synthesis of the W complex is given below.

A mixture of $[(\text{CpCH}_2\text{CH}_2\text{OH})\text{W}(\text{CO})_3\text{PPh}_3]^+\text{BF}_4^-$ (108 mg, 0.15 mmol) and NaOMe (10 mg, 0.19 mmol) was placed in a Schlenk tube under nitrogen. Acetone (1.5 mL) was then added at room temperature at which point all of the material dissolved. Almost immediately, yellow solid precipitated. This was isolated by cannula filtration and remaining solvent was removed under reduced pressure leaving the product as a bright yellow solid (0.11 mmol, 70.1%):

2a: M=Mo MP=160 – 162°C (d); ^1H NMR (CDCl_3), PPh₃ 7.56 – 7.20 (m, 15H), CpR (H₂ & H₅) 5.46 (AA'XX', 2H), CpR (H₃ & H₄) 4.30 (m, 2H), -CH₂-O 3.88 (AA'XX', 2H), Cp-CH₂- 2.40 (AA'XX', 2H); ^{31}P NMR (CDCl_3), 71.07 (s); IR (CH_2Cl_2) νCO , 1970 (s), 1881 (vs), 1613 (m).

2b: M=W MP=170 – 175°C (d); ^1H NMR (CDCl_3), PPh₃ 7.53 – 7.31 (m, 15H), CpR (H₂ & H₅) 5.59 (AA'XX', 2H), CpR (H₃ & H₄) 4.35 (m, 2H), -CH₂-O 3.86 (AA'XX', 2H), Cp-CH₂- 2.43 (AA'XX', 2H); ^{31}P NMR (CDCl_3), 39.98 (s w/ small d, $J_{\text{WP}} = 212.4$ Hz); IR (CH_2Cl_2) νCO , 1961 (s), 1868 (vs), 1610 (m).



The same procedure was followed as that used for the triphenylphosphine complexes with the exception that the product did not precipitate from acetone

solution. Instead, solvent was removed under reduced pressure and the resulting material was extracted with benzene. Upon removal of solvent from the combined extracts, the product was obtained as a yellow, glassy solid (90%):

2c: M=Mo MP=95 – 99°C (d); ^1H NMR ($(\text{CD}_3)_2\text{CO}$), P(p-tolyl)₃ (aryl) 7.50 – 7.06 (m, 12H), CpR (H₂ & H₅) 5.67 (AA'XX', 2H), CpR (H₃ & H₄) 4.37 (m, 2H), -CH₂-O 3.78 (AA'XX', 2H), Cp-CH₂- 2.37 (AA'XX', 2H), -CH₃ 2.37 (s, 9H); ^{31}P NMR ($(\text{CD}_3)_2\text{CO}$), 71.61 (s); IR (CH_2Cl_2) νCO , 1968 (s), 1876 (vs), 1610 (m).

Anal. Calcd. for C₃₁H₂₉Mo₁O₄P₁: C 62.84; H 4.93. Found: C 62.68 ; H 5.08.

2d: M=W MP=100 – 105°C (d); ^1H NMR ($(\text{CD}_3)_2\text{CO}$), P(p-tolyl)₃ (aryl) 7.32 – 7.26 (m, 12H), CpR (H₂ & H₅) 5.84 (AA'XX', 2H), CpR (H₃ & H₄) 4.42 (m, 2H), -CH₂-O 3.77 (AA'XX', 2H), Cp-CH₂- 2.47 (AA'XX', 2H), -CH₃ 2.37 (s, 9H); ^{31}P NMR ($(\text{CD}_3)_2\text{CO}$), 40.04 (s w/ small d, $J_{WP} = 217.3$ Hz); IR (CH_2Cl_2) νCO , 1961 (s), 1870 (vs), 1610 (m).

Anal. Calcd. for C₃₁H₂₉O₄P₁W₁: C 54.72; H 4.30. Found: C 54.71; H 4.94.

$(\eta^5\text{-C}_5\text{H}_4)\text{CH}_2\text{O}_2\text{C W}(\text{CO})_2\text{PPh}_3$ (**2**)

The same procedure was followed as that for the -(CH₂)₂- bridged triphenylphosphine complexes. The reaction proceeded much more slowly, however, requiring three days at room temperature before the product formed as orange crystalline solids:

2g: MP=188 – 193°C (d); ^1H NMR ($(\text{CD}_3)_2\text{CO}$), PPh₃ 7.64 – 7.26 (m, 15H), CpR (H₂ & H₅) 6.26 (AA'XX', 2H), CpR (H₃ & H₄) 4.41 (m, 2H), -CH₂-O 4.12 (s); ^{31}P NMR ($(\text{CD}_3)_2\text{CO}$), 37.29 (s w/ small d, $J_{PW}=200.2$ Hz); IR

(CH₂Cl₂) ν CO, 1957 (s), 1882 (s), 1598 (m).

CpM(CO₂Me)(CO)₂PPh₃ (3)

(M=Mo, W)

The same procedure was followed as that used for the synthesis of (η^5 -C₅H₄)-CH₂CH₂-O₂C-M(CO)₂P(p-tolyl)₃ with the substitution of the parent Cp compound instead of the substituted tri-p-tolyl cation. The product (a mixture of the *cis* and *trans* isomers) was obtained as a glassy orange solid (56%). Thermal instability has precluded elemental analysis:

3a: M=Mo ¹H NMR ((CD₃)₂CO), PPh₃ 7.60 – 7.28 (m), Cp *cis* 5.34 (s), Cp *trans* 5.15 (d, J=1.2 Hz), -CH₃ *trans* 3.48 (s), -CH₃ *cis* 2.57 (s); ³¹P NMR ((CD₃)₂CO), *trans* 73.36 (s), *cis* 64.55 (s); IR (CH₂Cl₂) ν CO, 1960 (s), 1875 (s), 1610 (m).

3b: M=W ¹H NMR ((CD₃)₂CO), PPh₃ 7.54 – 7.29 (m), Cp *cis* 5.47 (s), Cp *trans* 5.25 (d, J=1.2 Hz), -CH₃ *trans* 3.45 (s), -CH₃ *cis* 2.51 (s); ³¹P NMR ((CD₃)₂CO), *trans* 42.94 (s w/ small d, J_{WP} = 234.4 Hz), *cis* 35.54 (s w/ small d, J_{WP} = 271.0 Hz); IR (CH₂Cl₂) ν CO, 1950 (s), 1863 (vs), 1608 (m).

CpW(CO₂Bz)(CO)₂PPh₃ (4)

The same procedure was followed as that used for the synthesis of (η^5 -C₅H₄)-CH₂CH₂-O₂C-M(CO)₂P(p-tolyl)₃ with the substitution of the parent Cp compound instead of the substituted tri-p-tolyl cation as well as PhCH₂OLi for NaOMe. The product was obtained as a glassy yellow solid (45%):

4: MP: 172-173°C :¹H NMR (C₆D₆), Ph 7.40 – 6.89 (m, 20H), -CH₂- 5.44 (s,

2H), Cp 4.94 (d, J=1.0 Hz); ^{31}P NMR (C_6D_6), 44.29 (s w/ small d, $J_{\text{WP}}=224.6$ Hz); IR (CH_2Cl_2) νCO , 1957 (s), 1866 (s), 1610 (m).

Anal. Calcd. for $\text{C}_{33}\text{H}_{27}\text{O}_4\text{P}_1\text{W}_1$: C 55.84; H 3.66. Found: C 55.87; H 4.00.

X ray Structure Determinations

2b

A thin crystalline plate of $(\eta^5\text{-C}_5\text{H}_4\text{-})\text{-CH}_2\text{CH}_2\text{-O}_2\text{C-W}(\text{CO})_2\text{PPh}_3$ ($0.062 \times 0.266 \times 0.628\text{mm}$), obtained after layering pentane on top of a methylene chloride solution and cooling to -20°C for 2 days, was mounted approximately along the a -axis in a glass capillary under N_2 . A series of oscillation and Weissenberg photographs indicated monoclinic symmetry and the space group $P2_1/n$ ($0k0$ absent for k odd, $h0l$ absent for $h+l$ odd); data were collected on a locally-modified Syntex $P2_1$ diffractometer with graphite monochromator and $\text{MoK}\alpha$ radiation. The unit cell parameters (Table 2.7) were obtained by least-squares refinement of fifteen reflections ($30^\circ < 2\theta < 34^\circ$). The three check reflections indicated no decomposition. The data were corrected for absorption ($0.3 < \mu l < 0.7$) and reduced to F_o^2 ; the form factors for H were from Stewart *et al.*³⁵ and those for the other atoms were from the *International Tables for X-Ray Crystallography*³⁶. The values for W and P were corrected for anomalous dispersion. The details of data collection are included in Table 2.7.

The position of the W was derived from the Patterson map, and the Fourier map phased on W revealed the remainder of the complex. All H-atoms were

introduced into the model with fixed coordinates at idealized positions and isotropic $U = 0.076 \text{ \AA}^2$. Least-squares refinement of the non-hydrogen atoms with anisotropic U_{ij} 's, minimizing $\Sigma w[F_o^2 - (F_c/k)^2]^2$,³⁷ using all the data (5728 reflections) led to S (Goodness of fit) = 1.27 and $R_F = 0.043$; final shift/errors < 0.01. The maximum deviations found in the $\Delta\rho$ map are close to W and are about $1.2 e \text{ \AA}^{-3}$. All calculations were carried out on a VAX 11/780 computer using the CRYRM system of programs. Tables of bond lengths and angles (2.8), non-H atom coordinates (2.9) and Gaussian amplitudes (2.10) and H-atom coordinates (2.11) follow.

2g

A crystal of $(\eta^5\text{-C}_5\text{H}_4\text{-})\text{-CH}_2\text{-O}_2\text{C-W(CO)}_2\text{PPh}_3$ ($0.175 \times 0.194 \times 0.456 \text{ mm}$), obtained from $(\text{CD}_3)_2\text{CO}$ solution after allowing the reaction mixture of the cation **1g** and NaOMe to sit at room temperature for three weeks was mounted in a glass capillary under N_2 . Oscillation and Weissenberg photographs indicated monoclinic symmetry and the space group $P2_1/n$ ($0k0$ absent for k odd, $h0l$ absent for $h+l$ odd); data were collected on an Enraf-Nonius CAD 4 diffractometer with graphite monochromator and $\text{MoK}\alpha$ radiation. The unit cell parameters (Table 2.12) were obtained by least-squares refinement of twenty reflections ($5^\circ < 2\theta < 60^\circ$). Three check reflections indicated minimal decomposition. The data were reduced to F_o^2 ; the form factors for H were from Stewart *et al.*³⁵ and those for the other atoms were from the *International Tables for X-Ray Crystallography*.³⁶ The values for W and P were corrected for anomalous dispersion. The details of data collection are included in Table 2.12.

The position of the W was derived from the Patterson map, and the Fourier map phased on W revealed the remainder of the complex. All H-atoms were introduced into the model with fixed coordinates at idealized positions and isotropic $U = 0.076 \text{ \AA}^2$. Least-squares refinement of the non-hydrogen atoms with anisotropic U_{ij} 's, minimizing $\Sigma w[F_o^2 - (F_c/k)^2]^2$,³⁷ using all the data (4079 reflections) led to S (goodness of fit) = 2.80 and $R_F = 0.047$; final shift/errors < 0.01. The maximum deviations found in the $\Delta\rho$ map are close to W and are about $3 e \text{ \AA}^{-3}$. The residual electron density and an S of 2.80 are due to errors introduced by the twinning in the crystal. All calculations were carried out on a VAX 11/750 computer using the CRYRM system of programs. Tables of bond lengths and angles (2.13), non-H atom coordinates (2.14) and Gaussian amplitudes (2.15) and H-atom coordinates (2.16) follow.

Equilibrium Studies

Initial concentrations of **2** were based on the integrated peak areas with respect to added alcohol at time, $t=0$. Subsequent concentrations of **2** and **5** were established by the percentage of the integrated signal intensities of the relevant Cp proton signals in relation to that of the total Cp integration. Temperatures were determined by measurement of $\Delta\nu$ MeOH using the equation:

$$T(\text{K}) = 406.0 - 0.551 |\Delta\nu| - 63.4 \left(\frac{\Delta\nu}{100}\right)^2$$

$\Delta\nu$ is the difference in Hz between the chemical shifts of the OH and CH₃ signals.

The above equation is for 60 MHz values; 90 MHz values must be corrected accordingly.³⁸

Table 2.7. Summary of Data Collection and Refinement Parameters of 2b

Formula	$C_{28}H_{23}O_4PW$	
Formula weight	638.32	
Space group	$P2_1/n$	
a	8.1273(17)Å	
b	16.823(5)Å	
c	17.623(3)Å	
β	101.980(16)°	
V	2357.1(10)Å ³	
Z	4	
D_{calc}	1.799 g/cm ³	
Crystal size	0.062 × 0.266 × 0.628 mm	
λ	0.71073Å	
μ	5.10 mm ⁻¹	
2 θ limits	4 — 36°	35 — 56°
Scan rate	4.88°/min	2.02°/min
Bkgrd-to-scan time ratio	1.0	0.5
Scan width	1.1°	1.2° above $K\alpha_2$
	1.1°	1.2° below $K\alpha_1$
Number of reflections	3657	9066
Total number of averaged data	5728	
Final agreement ^a		
R_F	0.043 (5335)	
R'_F	0.027 (4085)	
S	1.27 (5728)	

^aDefined in footnote 37; number of reflections given in parentheses.

Table 2.8. Bond Lengths and Angles for 2b

Bonds	Å	Angles	deg
W-P	2.495(3)	P-W-C(1)	138.5(4)
W-C(1)	2.233(15)	R-W-P	115.9
C(1)-O(1)	1.227(19)	R-W-C(1)	105.6
C(2)-O(2)	1.405(20)	W-C(1)-O(1)	126.2(11)
C(1)-O(2)	1.390(18)	O(1)-C(1)-O(2)	111.9(13)
C(2)-C(3)	1.552(23)	W-C(1)-O(2)	121.8(10)
C(3)-C(4)	1.486(21)	C(1)-O(2)-C(2)	121.4(12)
C(4)-C(5)	1.441(19)	O(2)-C(2)-C(3)	112.8(13)
C(5)-C(6)	1.449(19)	C(3)-C(4)-C(5)	126.5(12)
C(6)-C(7)	1.433(20)	C(3)-C(4)-C(8)	123.2(12)
C(7)-C(8)	1.498(19)	C(4)-C(5)-C(6)	107.1(11)
C(4)-C(8)	1.419(18)	C(8)-C(4)-C(5)	110.2(11)
W-C(9)	1.943(14)	C(7)-C(8)-C(4)	106.7(11)
W-C(10)	1.964(17)	C(5)-C(6)-C(7)	108.6(4)
C(9)-O(9)	1.180(19)	C(6)-C(7)-C(8)	108.3(4)
C(10)-O(10)	1.186(20)	R-W-C(9)	126.7
P-C(11)	1.837(13)	R-W-C(10)	127.9
P-C(21)	1.837(13)	C(9)-W-C(10)	105.6(2)
P-C(31)	1.853(14)	W-C(9)-O(9)	175.5(13)
W-R ^a	2.013	W-C(10)-O(10)	172.7(14)
W-C(4)	2.328(13)	W-P-C(11)	116.2(4)
W-C(5)	2.385(13)	W-P-C(21)	112.7(4)
W-C(6)	2.371(14)	W-P-C(31)	117.6(4)
W-C(7)	2.381(14)	W-R-C(4)	88.7(6)
W-C(8)	2.339(12)	W-R-C(5)	91.4(6)
		W-R-C(6)	90.7(7)
		W-R-C(7)	90.9(7)
		W-R-C(8)	88.5(6)

^aR ≡ ring centroid of Cp-ring.

Table 2.9. Atom Coordinates ($\times 10^4$) and U_{eq} 's (\AA^2 , $\times 10^4$)
for 2b

	x	y	z	U_{eq}
W	2845.2(2)	1740.4(1)	973.9(1)	316
P	1804.3(13)	2923.5(7)	1591.7(5)	314
C(1)	5278(5)	1121(4)	996(3)	509
O(1)	6568(4)	1414(3)	885(3)	783
C(2)	4196(6)	-148(3)	1376(3)	576
O(2)	5432(4)	306(3)	1119(2)	635
C(3)	2592(6)	-247(3)	761(3)	571
C(4)	1779(5)	521(3)	482(2)	389
C(5)	459(5)	919(3)	751(2)	374
C(6)	33(5)	1608(3)	304(2)	406
C(7)	1062(6)	1649(3)	-255(2)	451
C(8)	2151(5)	993(3)	-148(2)	468
C(9)	4306(6)	2600(3)	705(2)	520
O(9)	5076(6)	3085(3)	498(2)	842
C(10)	3658(5)	1539(3)	2078(2)	349
O(10)	4126(4)	1382(2)	2733(2)	540
C(11)	3400(5)	3660(3)	2008(2)	334
C(12)	5000(5)	3412(3)	2397(2)	414
C(13)	6213(5)	3965(3)	2719(3)	447
C(14)	5867(6)	4772(3)	2640(3)	492
C(15)	4304(6)	5023(3)	2246(3)	526
C(16)	3082(6)	4469(3)	1941(2)	438
C(21)	805(5)	2654(3)	2402(2)	327
C(22)	-701(5)	2243(3)	2234(2)	388
C(23)	-1451(6)	1975(3)	2828(3)	453
C(24)	-687(7)	2107(3)	3585(3)	534
C(25)	804(7)	2518(4)	3758(3)	586
C(26)	1563(6)	2785(3)	3171(2)	440
C(31)	179(5)	3535(3)	974(2)	387
C(32)	178(7)	3612(3)	190(3)	504
C(33)	-1016(8)	4074(4)	-284(3)	644
C(34)	-2202(7)	4461(4)	23(3)	668
C(35)	-2215(7)	4411(3)	804(3)	628
C(36)	-1017(6)	3938(3)	1277(3)	485

Table 2.10. Gaussian amplitudes ($\times 10^4$) for 2b

	U_{11}	U_{22}	U_{33}	U_{12}	U_{13}	U_{23}
W	246(1)	426(1)	284(1)	-92(1)	71(0)	-101(1)
P	296(5)	377(6)	264(4)	-60(5)	40(4)	-22(4)
C(1)	275(22)	729(40)	527(27)	-71(24)	91(19)	-293(25)
O(1)	311(18)	1037(35)	1067(30)	-207(20)	290(18)	-444(25)
C(2)	419(27)	537(34)	719(32)	83(25)	-6(23)	-132(26)
O(2)	320(17)	715(28)	831(25)	108(19)	25(16)	-253(21)
C(3)	442(27)	489(31)	720(33)	9(25)	-27(24)	-184(25)
C(4)	269(19)	391(26)	479(23)	-126(18)	10(17)	-184(19)
C(5)	222(18)	430(27)	463(22)	-103(19)	50(16)	-108(19)
C(6)	299(19)	425(30)	464(22)	-96(19)	7(16)	-97(19)
C(7)	456(23)	552(31)	311(18)	-122(25)	0(17)	-86(20)
C(8)	343(22)	650(35)	397(22)	-86(23)	44(18)	-247(22)
C(9)	522(28)	708(37)	360(22)	-276(28)	158(20)	-149(22)
O(9)	983(32)	1018(38)	628(22)	-621(29)	402(22)	-123(22)
C(10)	245(18)	351(27)	465(22)	-74(17)	102(16)	-80(17)
O(10)	555(20)	640(23)	392(17)	-1(18)	18(14)	20(15)
C(11)	317(20)	425(25)	270(17)	-80(19)	80(15)	-42(16)
C(12)	385(22)	401(29)	430(21)	-26(20)	24(17)	-73(18)
C(13)	324(22)	529(31)	464(24)	-73(22)	20(18)	-75(21)
C(14)	393(24)	518(32)	552(26)	-155(23)	67(20)	-127(23)
C(15)	492(28)	399(30)	660(30)	-142(24)	56(23)	-52(23)
C(16)	419(24)	405(28)	458(23)	-50(21)	16(19)	-4(20)
C(21)	319(20)	352(24)	317(18)	3(18)	82(15)	-24(16)
C(22)	374(22)	384(26)	412(22)	-37(20)	94(17)	-36(18)
C(23)	374(23)	447(29)	587(27)	-7(20)	209(20)	53(21)
C(24)	584(31)	659(35)	424(25)	34(27)	251(22)	132(23)
C(25)	620(32)	805(41)	336(22)	-90(31)	105(21)	4(23)
C(26)	397(24)	583(32)	336(21)	-26(22)	66(18)	-34(20)
C(31)	357(21)	420(25)	345(20)	-92(19)	-23(16)	7(17)
C(32)	646(31)	446(28)	384(22)	-88(25)	18(21)	42(20)
C(33)	857(42)	597(37)	397(25)	-80(33)	-63(26)	113(24)
C(34)	564(33)	627(40)	697(35)	-80(30)	-140(27)	247(29)
C(35)	430(27)	617(36)	809(39)	33(28)	62(26)	218(28)
C(36)	383(24)	557(32)	502(25)	5(23)	57(20)	81(22)

Table 2.11. Atom Coordinates ($\times 10^3$) of Hydrogen Atoms of 2b

	<i>x</i>	<i>y</i>	<i>z</i>
H(2A)	3908	122	1837
H(2B)	4669	-687	1529
H(3A)	1777	-569	986
H(3B)	2874	-535	308
H(5)	-73	739	1185
H(6)	-847	2003	368
H(7)	1018	2074	-657
H(8)	3030	872	-453
H(12)	5270	2831	2442
H(13)	7339	3782	3010
H(14)	6746	5170	2867
H(15)	4054	5604	2180
H(16)	1946	4657	1667
H(22)	-1254	2138	1681
H(23)	-2549	1685	2702
H(24)	-1213	1905	4012
H(25)	1345	2625	4312
H(26)	2662	3074	3302
H(32)	1052	3330	-34
H(33)	-1010	4125	-849
H(34)	-3078	4787	-324
H(35)	-3072	4710	1026
H(36)	-1024	3890	1843

Table 2.12. Summary of Data Collection and Refinement Parameters of 2g

Formula	$C_{27}H_{21}O_4PW$
Formula weight	624.29
Space group	$P2_1/n$
a	7.8673(12)Å
b	17.083(4)Å
c	17.768(7)Å
β	100.959(28)°
V	2344.4(11)Å ³
Z	4
D_{calc}	1.769 g/cm ³
Crystal size	0.175 × 0.194 × 0.456 mm
λ	0.71073Å
μ	5.10 mm ⁻¹
2 θ limits	4 – 50°
Scan rate	≤ 2°/min
Bkgrd-to-scan time ratio	0.5
Scan width	0.8° above $K\alpha_2$ 0.8° below $K\alpha_1$
Number of reflections	9263
Total number of averaged data	4079
Final agreement ^a	
R_F	0.047 (3771)
R'_F	0.037 (3146)
S	2.80 (4079)

^aDefined in footnote 37; number of reflections given in parentheses.

Table 2.13. Bond Lengths and Angles for 2g

Bonds	Å	Angles	deg
W-P	2.504(2)	P-W-C(1)	139.5(2)
W-C(1)	2.207(7)	R-W-P	117.2
C(1)-O(1)	1.207(8)	R-W-C(1)	103.1
C(2)-O(2)	1.432(9)	W-C(1)-O(1)	131.0(5)
C(1)-O(2)	1.404(8)	O(1)-C(1)-O(2)	112.5(6)
C(2)-C(3)	1.484(10)	W-C(1)-O(2)	116.5(4)
C(3)-C(4)	1.422(10)	C(1)-O(2)-C(2)	116.9(5)
C(4)-C(5)	1.410(9)	O(2)-C(2)-C(3)	111.8(6)
C(5)-C(6)	1.440(9)	C(2)-C(3)-C(4)	123.3(6)
C(6)-C(7)	1.413(9)	C(2)-C(3)-C(7)	127.5(6)
C(3)-C(7)	1.417(10)	C(3)-C(4)-C(5)	107.8(6)
W-C(8)	1.971(7)	C(7)-C(3)-C(4)	109.0(6)
W-C(9)	1.951(6)	C(6)-C(7)-C(3)	107.2(6)
C(8)-O(8)	1.151(8)	C(4)-C(5)-C(6)	107.8(6)
C(9)-O(9)	1.159(8)	C(5)-C(6)-C(7)	108.6(7)
P-C(11)	1.834(6)	R-W-C(8)	127.9
P-C(21)	1.832(6)	R-W-C(9)	125.9
P-C(31)	1.844(6)	C(8)-W-C(9)	104.3(3)
W-R ^a	1.977	W-C(8)-O(8)	175.1(6)
W-C(3)	2.236(7)	W-C(9)-O(9)	176.2(6)
W-C(4)	2.286(7)	W-P-C(11)	116.8(2)
W-C(5)	2.351(7)	W-P-C(21)	112.1(2)
W-C(6)	2.362(7)	W-P-C(31)	116.2(2)
W-C(7)	2.343(7)	W-R-C(3)	85.9
		W-R-C(4)	88.2
		W-R-C(5)	91.8
		W-R-C(6)	92.7
		W-R-C(7)	91.2

^aR ≡ ring centroid of Cp-ring.

Table 2.14. Atom Coordinates ($\times 10^4$) and U_{eq} 's ($\text{\AA}^2, \times 10^4$)
for 2g

	x	y	z	U_{eq}
W	2829.1(3)	1613.1(1)	975.1(1)	285
P	1874.5(20)	2832.8(9)	1565.4(9)	302
C(1)	5129(9)	848(4)	1080(4)	401
O(1)	6658(6)	998(3)	1247(3)	590
C(2)	3036(10)	-196(4)	758(5)	591
O(2)	4813(6)	46(3)	935(3)	526
C(3)	1866(9)	462(4)	457(4)	427
C(4)	2129(9)	949(4)	-163(4)	451
C(5)	930(8)	1573(4)	-223(4)	435
C(6)	-96(8)	1459(4)	361(4)	428
C(7)	450(9)	758(4)	760(4)	457
C(8)	4648(9)	2323(4)	747(4)	416
O(8)	5728(7)	2699(3)	573(3)	646
C(9)	3549(9)	1376(4)	2067(4)	356
O(9)	3965(8)	1190(3)	2704(3)	611
C(11)	3570(8)	3543(3)	1956(3)	327
C(12)	5185(8)	3279(4)	2356(4)	398
C(13)	6396(9)	3810(4)	2698(4)	463
C(14)	6088(10)	4608(5)	2628(4)	553
C(15)	4534(11)	4863(4)	2227(5)	588
C(16)	3262(9)	4339(4)	1898(4)	456
C(21)	880(8)	2617(3)	2397(3)	303
C(22)	1576(9)	2856(4)	3132(4)	446
C(23)	857(12)	2619(5)	3747(4)	693
C(24)	-587(11)	2133(5)	3636(4)	559
C(25)	-1316(9)	1891(4)	2908(4)	453
C(26)	-594(9)	2132(4)	2288(4)	409
C(31)	245(8)	3440(4)	938(3)	379
C(32)	347(13)	3533(4)	182(4)	603
C(33)	-823(14)	3996(5)	-301(5)	715
C(34)	-2126(14)	4363(5)	-54(6)	791
C(35)	-2231(11)	4292(5)	744(6)	726
C(36)	-1024(9)	3824(4)	1222(4)	524

Table 2.15. Gaussian amplitudes ($\times 10^4$) for 2g

	U_{11}	U_{22}	U_{33}	U_{12}	U_{13}	U_{23}
W	215(1)	351(2)	308(1)	-46(2)	70(1)	-69(1)
P	246(9)	364(10)	319(9)	-40(8)	75(7)	-38(8)
C(1)	274(43)	554(50)	411(44)	19(36)	111(34)	-60(37)
O(1)	252(32)	620(37)	886(44)	4(28)	49(29)	-87(32)
C(2)	485(54)	387(44)	888(68)	-82(40)	46(47)	-96(44)
O(2)	394(33)	429(32)	758(38)	35(26)	53(28)	-178(29)
C(3)	294(41)	393(43)	561(48)	-81(33)	46(34)	-189(36)
C(4)	301(41)	575(50)	438(45)	-16(37)	85(34)	-180(38)
C(5)	385(42)	566(47)	374(39)	-65(42)	32(31)	-100(38)
C(6)	194(35)	514(50)	579(47)	-19(33)	30(32)	-101(38)
C(7)	283(38)	568(52)	557(49)	-156(37)	99(37)	-147(40)
C(8)	400(46)	507(47)	401(42)	-156(37)	197(36)	-131(35)
O(8)	670(44)	749(43)	625(38)	-330(35)	333(33)	-109(32)
C(9)	261(38)	400(42)	401(42)	-76(30)	135(31)	-74(32)
O(9)	651(42)	722(40)	411(34)	5(33)	90(29)	87(29)
C(11)	292(37)	364(43)	354(36)	-88(30)	118(29)	-103(29)
C(12)	283(38)	488(47)	407(40)	-55(35)	37(31)	-124(35)
C(13)	382(47)	613(53)	458(46)	-26(40)	140(37)	-114(40)
C(14)	390(50)	609(58)	693(57)	-188(42)	117(42)	-222(45)
C(15)	578(59)	395(47)	780(61)	-70(43)	136(48)	-129(44)
C(16)	333(45)	444(46)	602(51)	-73(36)	119(38)	-53(38)
C(21)	240(37)	311(36)	373(38)	38(29)	109(29)	8(30)
C(22)	349(44)	678(56)	335(41)	-89(40)	95(34)	-78(37)
C(23)	733(69)	987(76)	371(46)	-173(59)	96(45)	-83(47)
C(24)	526(56)	732(61)	453(50)	-41(47)	249(42)	51(44)
C(25)	328(42)	497(45)	577(50)	-37(36)	206(37)	-12(39)
C(26)	358(44)	455(46)	450(43)	-23(35)	126(35)	-65(35)
C(31)	369(40)	376(39)	383(38)	-47(36)	5(30)	-7(35)
C(32)	962(77)	487(55)	349(44)	118(48)	77(45)	-2(37)
C(33)	916(85)	682(65)	545(60)	-48(62)	-17(57)	97(50)
C(34)	767(79)	634(63)	798(75)	-17(57)	-264(62)	293(58)
C(35)	438(55)	670(61)	1085(88)	107(48)	174(58)	317(57)
C(36)	359(47)	568(52)	673(56)	61(40)	108(41)	189(43)

Table 2.16. Atom Coordinates ($\times 10^3$) of Hydrogen Atoms of 2g

	<i>x</i>	<i>y</i>	<i>z</i>
H(2A)	2722	-395	1213
H(2B)	2933	-601	382
H(4)	2975	872	-478
H(5)	809	1990	-585
H(6)	-986	1801	460
H(7)	-58	529	1157
H(12)	5426	2733	2388
H(13)	7465	3628	2990
H(14)	6940	4973	2859
H(15)	4326	5414	2167
H(16)	2179	4525	1630
H(22)	2551	3198	3217
H(23)	1376	2783	4251
H(24)	-1095	1974	4061
H(25)	-2305	1557	2823
H(26)	-1116	1969	1783
H(32)	1239	3270	-15
H(33)	-740	4055	-827
H(34)	-2923	4680	-339
H(35)	-3101	4553	943
H(36)	-1082	3776	1756

Notes and References

- (1) Generally there is a correlation between the CO stretching frequency and the tendency for a nucleophile to attack at the CO carbon (the cutoff being $\leq 2000\text{cm}^{-1}$): Angelici, R.J.; Blacik, L.J. *Inorg. Chem.* **1972**, *11*, 1754.
- (2) Jetz, W.; Angelici, R.J. *J. Am. Chem. Soc.* **94**, *94*, 3799.
- (3) A significant proportion of this material has been submitted for publication: Coolbaugh, T.S.; Santarsiero, B.D.; Grubbs, R.H. *J. Am. Chem. Soc.* *submitted*.
- (4) Model studies further reinforced this optimism.
- (5) Other intramolecular metallaesters have been synthesized but without utilizing a Cp ligand as the means for anchoring the oxygen nucleophile prior to ester formation. See for example: (a) Heck, R.F.; Boss, C.R. *J. Am. Chem. Soc.* **1964**, *86*, 2580. (b) Murdoch, H.D. *Helv. Chim. Acta* **1947**, *47*, 936. (c) Klemarczyk, P.; Price, T.; Priester, W.; Rosenblum, M. *J. Organomet. Chem.* **1977**, *190*, C25. (d) Knoth, W.H. *Inorg. Chem.* **1975**, *14*, 1566.
- (6) Craig, P.J.; Edwards, J. *J. Less Comm. Met.* **1974**, *96*, 193.
- (7) Treichel, P.M.; Shubkin, R.L. *Inorg. Chem.* **1967**, *6*, 1328.
- (8) The ^1H NMR spectrum in which H_3 & H_4 were decoupled from H_2 & H_5 displays only a doublet for the signal ($J = 3.7$ Hz) while the decoupled H_2 & H_5 signal is a singlet. Thus the additional coupling does not arise from the ring protons and is most probably due to P-H coupling. Further support is obtained from the ^{31}P NMR spectrum in which the aryl protons have been selectively decoupled; the ^{31}P signal shape is consistent with a somewhat broad signal

approximating a triplet.

- (9) George, T.A.; Turnipseed, C.D. *Inorg. Chem.* **1973**, *12*, 394.
- (10) Kennedy, J.D.; McFarlane, W.; Rycroft, D.S. *Inorg. Chem.* **1973**, *12*, 2742.
- (11) A recent crystal structure of $\text{Cp}^*\text{Rh}(\text{CO})(\text{CO}_2\text{Me})_2$ displays quite similar ester bond lengths and angles; the only difference is in the C=O bond length of 1.185(6) Å vs 1.227(19) Å for **2b** although upon consideration of the esd's the difference may not be significant: Burk, P.L.; Engen, D.V.; Campo, K.S. *Organometallics* **1984**, *3*, 493.
- (12) Petersen, R.B.; Stezowski, J.J.; Wan, C.; Burlitch, J.M.; Hughes, R.E. *J. Am. Chem. Soc.* **1971**, *93*, 3532.
- (13) Greaves, W.W.; Angelici, R.J.; Helland, B.J.; Klima, R.; Jacobson, R.A. *J. Am. Chem. Soc.* **1979**, *101*, 7618.
- (14) Conway, A.J.; Gainsford, G.J.; Schrieke, R.R.; Smith, J.D. *J. C. S. Dalton* **1975**, 2499.
- (15) Churchill, M.R.; Fennessey, J.P. *Inorg. Chem.* **1968**, *7*, 953.
- (16) Chan, L.Y.Y.; Dean, W.K.; Graham, W.A.G. *Inorg. Chem.* **1977**, *16*, 1067.
- (17) Bailey, N.A.; Chell, P.L.; Manuel, C.P.; Mukhopadhyay, A.; Rogers, D.; Tabbron, H.E.; Winter, M.J. *J. Chem. Soc. Dalton* **1983**, 2397.
- (18) (a) Villa, A.C.; Coghi, L.; Manfredotti, A.G.; Guastini, C. *Cryst. Struct. Commun.* **1974**, *3*, 543. (b) Mikuriya, M.; Torihara, N.; Okawa, H.; Kida, S. *Bull. Chem. Soc. Jpn.* **1981**, *54*, 1063. (c) Rémy, G.; Cottier, L.; Descotes, G.; Faure, R.; Loiseleur, H.; Thomas-David, G. *Acta Cryst.* **1980**, *B36*, 873.
- (19) Sieber, W.; Wolfgruber, M.; Neugebauer, D.; Orama, O.; Kreißl, F.R. *Z.*

Naturforsch. **1983**, *38B*, 67.

(20) NOE enhancement falls off as $1/r^6$ whereas through-space coupling decreases as $1/r^3$.

(21) Barnett, K.W.; Beach, D.L.; Gaydos, S.P.; Pollman, T.G. *J. Organomet. Chem.* **1974**, *69*, 121.

(22) Kubáček, P.; Hoffmann, R.; Havlas, Z. *Organometallics* **1982**, *1*, 180.

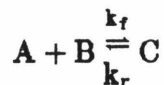
(23) Adams, H.; Bailey, N.A.; Winter, M.J. *J. Chem. Soc. Dalton* **1984**, 273.

(24) Spectroscopic evidence has also been given for the preference for the vertical orientation in $\text{Cp}(\text{CO})_2\text{LW}=\text{CH}_2^+$. The carbene protons exhibit different chemical shifts as would not be expected in the horizontal orientation: Kegley, S.E.; Brookhart, M.; Husk, G.R. *Organometallics* **1982**, *1*, 760.

(25) ΔH^\ddagger may be obtained from a plot of $\ln(k_f/T)$ vs $1/T$ and ΔG^\ddagger may be calculated using the equation:²⁶

$$\Delta G^\ddagger = -RT \ln \frac{k_f h}{k_B T}$$

where k_f is calculated for the process:



using the equation:²⁷

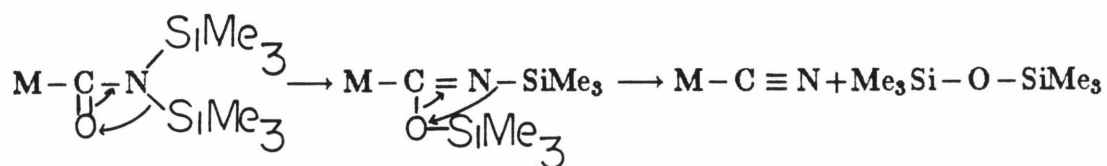
$$k_f = \frac{K_{\text{eq}}}{t(2K_{\text{eq}}[\text{A}]_\infty + 1 + K_{\text{eq}}\Delta)} \ln \frac{([\text{A}] + [\text{A}]_\infty + 1/K_{\text{eq}} + \Delta)([\text{A}]_0 - [\text{A}]_\infty)}{([\text{A}]_0 + [\text{A}]_\infty + 1/K_{\text{eq}} + \Delta)([\text{A}] - [\text{A}]_\infty)}$$

where $[B]_0 > [A]_0$, $[C]_0 = 0$, and $\Delta = [B]_0 - [A]_0$.

(26) Berry, R.S.; Rice, S.A.; Ross, J., "Physical Chemistry"; Wiley: New York (1980), 1154.

(27) Espenson, J.H., "Chemical Kinetics and Reaction Mechanisms"; McGraw-Hill: New York (1981).

(28) In fact, treatment with $(TMS)_2N^-Na^+$ yields the carbamoyl complex which decomposes to give the CN complex *via* the mechanism:



This reaction has been observed in a number of cases: (a) Wannagat, U.; Seyfert, H. *Angew. Chem. Int. Ed. Engl.* **1965**, *4*, 438. (b) King, R.B. *Inorg. Chem.* **1967**, *6*, 25.

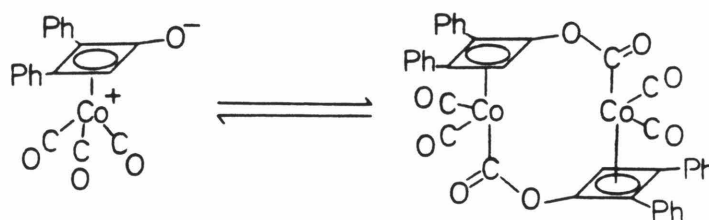
(29) H_3 & H_4 display an ^1H NMR signal similar to that of the ethylene bridged complex (a doublet of pseudo-triplets, $J = 3.4$ Hz).

(30) Streitwieser, A., Jr.; Heathcock, C.H., "Introduction to Organic Chemistry"; Macmillan: New York (1976).

(31) The crystal was found to be twinned but no serious difficulties arose from this other than a slightly high value for the goodness-of-fit (see experimental section).

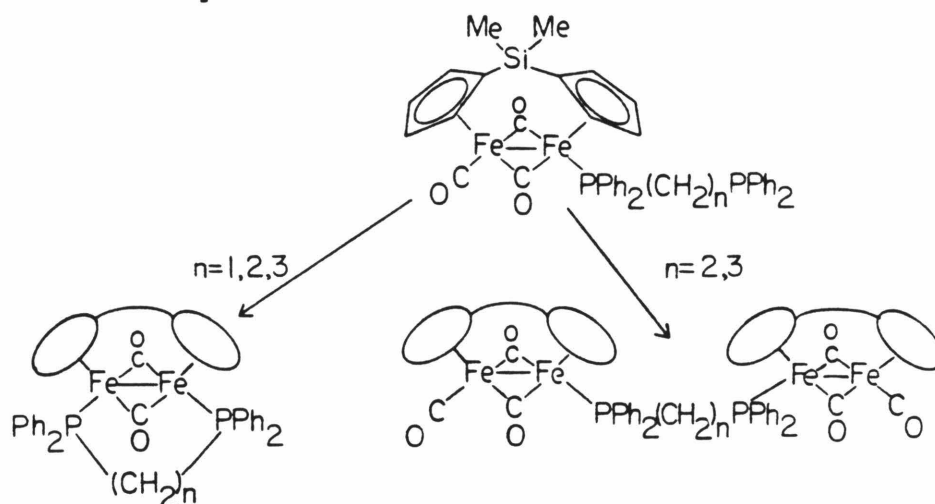
(32) Milstein, D.; Huckaby, J.L. *J. Am. Chem. Soc.* **1982**, *104*, 6150.

(33) While the compound with no methylene groups between the Cp and OH functionalities would be of academic interest, it would be expected to yield an intermolecular ester akin to the example given by the cyclobutenonyl complex:



Chidsey, C.E.; Donaldson, W.A.; Hughes, R.P.; Sherwin, P.F. *J. Am. Chem. Soc.* **1979**, *101*, 233.

(34) An interesting system that also displays a direct relationship between the bridging arm length and intramolecular stability is the iron dimer containing a diphosphine ligand connected by $-(\text{CH}_2)_n-$ where $n = 1, 2$ or 3 . When $n = 1$, only the dinuclear complex is formed while $n = 2$ or 3 yields increasing amounts of the tetranuclear species:



Wright, M.E.; Mezza, T.M.; Nelson, G.O.; Armstrong, N.R.; Day, V.W.; Thompson, M.R. *Organometallics* **1983**, *2*, 1711.

(35) Stewart, R.F.; Davidson, E.R.; Simpson, W.T. *J. Chem. Phys.* **1965**, *42*, 3175.

(36) "International Tables for X-ray Crystallography"; Kynoch Press: Birmingham, England, 1974; Vol. IV.

(37) The weights, $w = [s + r^2b + (.02 \times s)^2]^{-1} (Lp/k^2)^2$, s = scan counts, r =

scan-to-background time ratio, total background counts, k = scale factor of F ;
 $R_F = \Sigma |F_o - |F_c|| / \Sigma |F_o|$ (sums of reflections with $I > 0$); $R'_F = R_F$ (sums of
reflections with $I > 3\sigma_I$); $S = [\Sigma w(F_o^2 - (F_c/k)^2)^2 / (n - v)]^{1/2}$, n = number of
reflections, v = number of parameters.

(38) Gordon, A.J.; Ford, R.A. "*The Chemist's Companion*"; Wiley: New York,
1972.

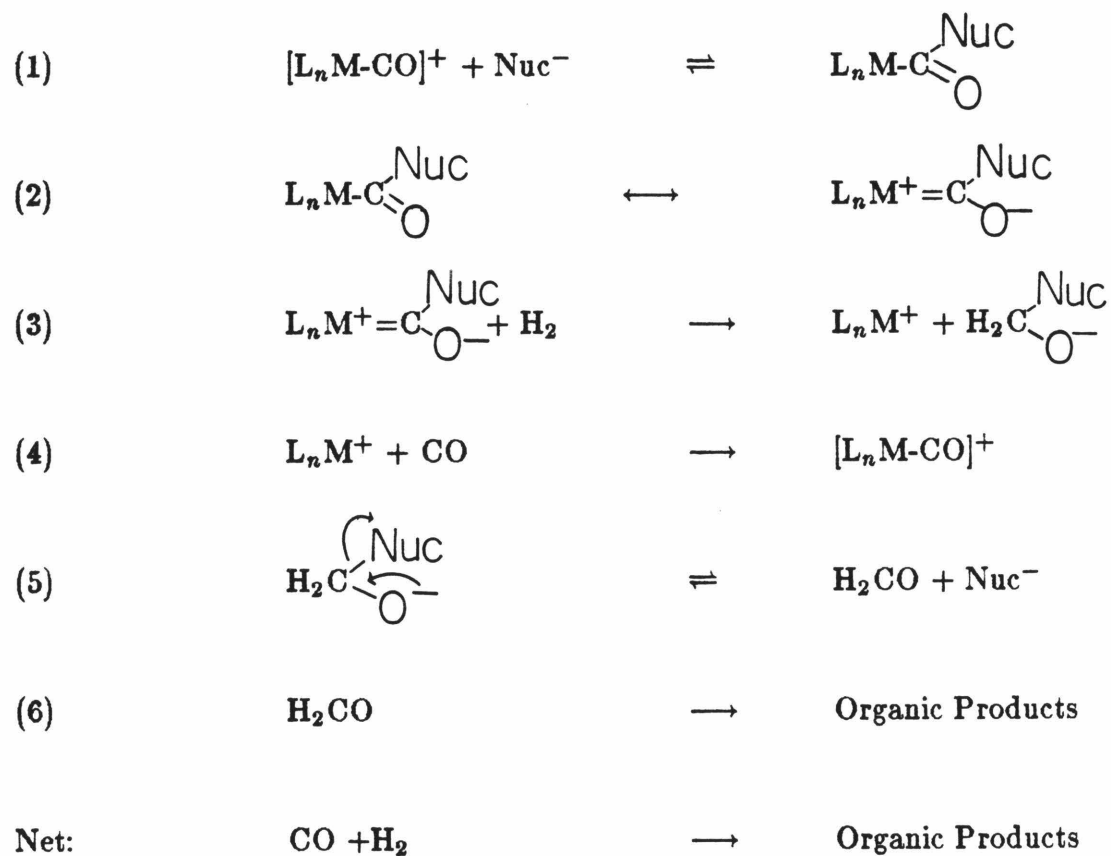
Chapter 3

**Reactivity of Group VI B Intramolecular
Metallaesters**

Introduction

It has been shown that the first step of the scheme shown below (Scheme 3.1) may be achieved using intramolecular nucleophiles.¹ In the absence of exogenous nucleophiles, the equilibrium of (1) lies completely to the right as was desired.

Scheme 3.1



While it is clear that the right hand resonance form of (2) does contribute it is not clear whether it is more predominant in the intramolecular case than

the intermolecular one. In fact, the non-zero torsion angle of the Cp centroid-W-C-O in the case of Cp-(CH₂)_n-O₂C-M(CO)₂PR₃ complexes (where n= 1,2) may result in non-optimal bond overlap in the carbenoid form.¹ Nevertheless, the C=O infra-red stretch is essentially the same for the tethered and free complexes, perhaps suggesting that other factors are involved as well.

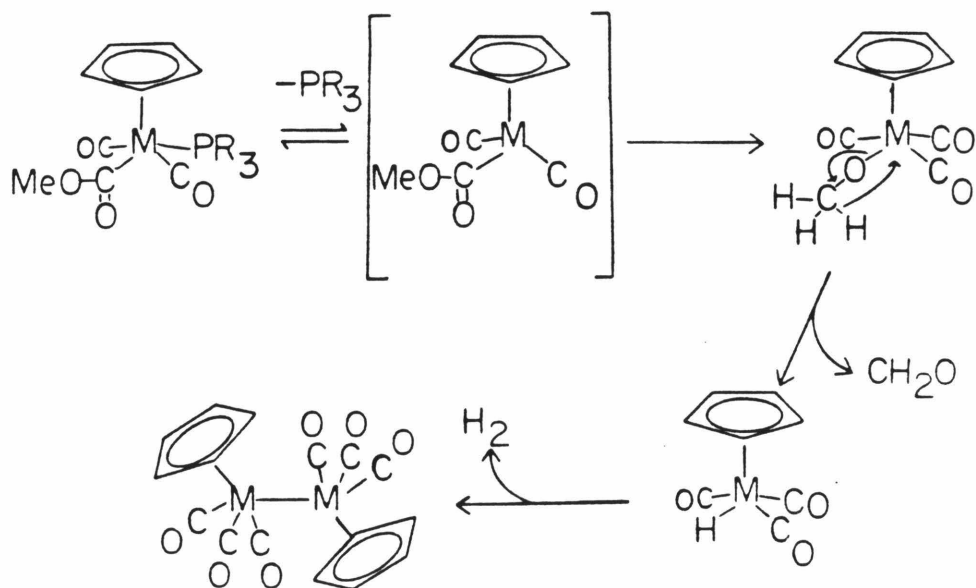
At this point it is of interest to consider the reactivities of the intramolecular metallaesters with hydrogen, both from molecular and stoichiometric sources. In this manner, the latter part of the scheme may be explored.

Results and Discussion

Investigation of the metallaesters was initiated with $n=2$. These compounds were found to be slightly less stable than the $n=1$ compounds ($\Delta\Delta G^\circ \geq 1\text{kcal}$) and it is quite often the case that some degree of destabilization is desirable in a catalyst since overly stable complexes tend not to be active catalysts. The reaction conditions employed were 100°C and 50 psi of a 1:1 CO/H_2 mixture in benzene- d_6 . In comparison to most syngas reactions, these are quite mild conditions and are similar to those used in hydrogenation of a Cr carbene complex to produce dimethylformamide.²

Nonetheless, volatile products were not obtained and, even though the reaction mixture did remain homogeneous, the metallaester decomposed, as evidenced by the appearance of a red color. This is generally indicative of metal dimer formation. In general, the methyl ester rapidly turns red in solution; a possible mechanism for dimer production is shown in Scheme 3.2.

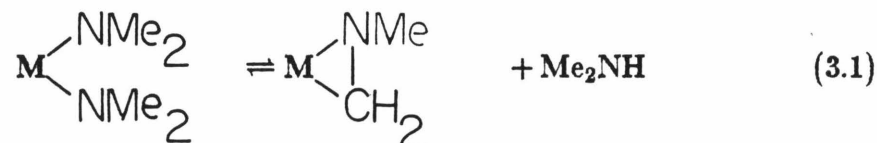
Scheme 3.2



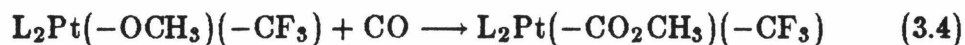
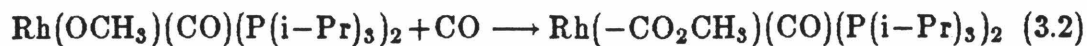
Quite recently a molybdate cluster containing methoxy groups was found to decompose thermally and photolytically to produce formaldehyde. The possibility exists, however, that proton transfer to a molybdenum oxide rather than β -hydride to molybdenum occurs prior to formaldehyde formation.³

While formaldehyde is generally produced by dehydrogenation of methanol it is usually over a heterogeneous catalyst at fairly high temperatures. Usually these reactions are carried out oxidatively, but direct dehydrogenation has been studied as well.⁴ For example, a recent study used silver as the catalyst at 670° C and .1 MPa pressure to give approximately a 40 % yield of formaldehyde upon 50 % conversion of methanol.⁴ Methoxy species on a copper surface, on the other hand, have been found to decompose at 100° C to yield formaldehyde.⁵ On metal surfaces with high heats of CO and hydrogen chemisorption (for example, Ru, Ni, Pd, Pt), decomposition of methoxy species to CO and hydrogen is generally observed.^{6,7,8,9}

Of interest with respect to the possible β -hydride route is the report that dimethylamino compounds may undergo cyclometalation at the methyl group (eq 3.1).¹⁰



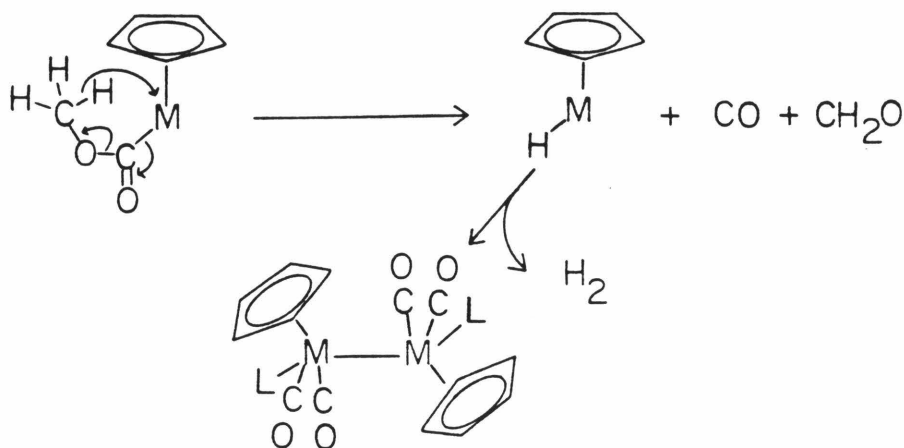
A difficulty that is associated with Scheme 3.2 is the formal deinsertion of carbon monoxide to yield a metal alkoxide species. While this reaction is not to be found in the literature, several examples of the reverse reaction are known

(eqs 3.2–3.4).^{11,12,13}

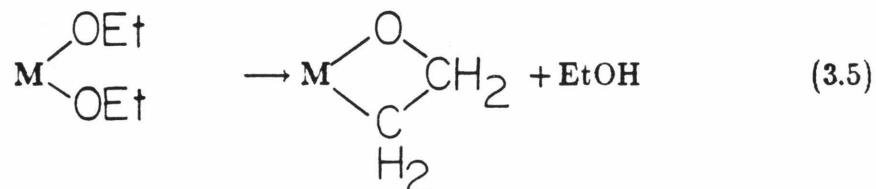
These reactions have been found to proceed at ambient temperatures under one atmosphere of CO pressure. The reversibility of the reaction has not been demonstrated.

The possibility exists for a concerted mechanism employing γ -hydride-like abstraction from the methyl group followed by extrusion of CO and formation of formaldehyde (Scheme 3.3):

Scheme 3.3



Bis ethoxy compounds have been reported that undergo cyclometalation reactions at solely the methyl groups, thus making the requirements of Scheme 3.3 at least plausible (eq 3.5).¹⁰

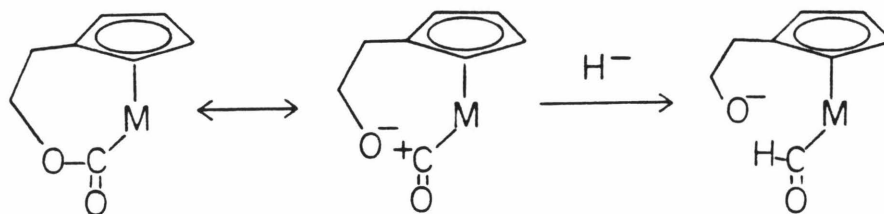


Thermolysis of the ethylene bridged W ester shows formation of an untethered Cp ligand as well as an NMR signal at 8.02 ppm, the indication being that a formate is formed, giving the metal-hydride which subsequently dimerizes (the red color of the dimer becomes apparent). Reaction of the W ester under CO and H₂, as described above for the Mo case, yields no volatile products either. The red color that becomes apparent again implicates the thermolysis as proposed.¹⁴

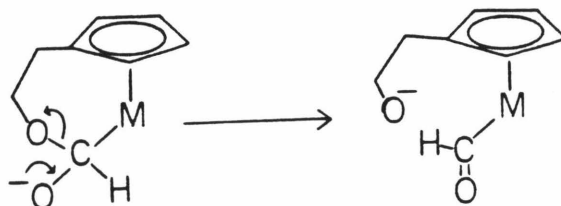
To enhance the possibility of the reaction with hydrogen, the utilization of a cocatalyst was explored. A sample of the ethylene bridged molybdenum ester in benzene containing one tenth of an equivalent of Pd on carbon was pressured up as before. After reaction for 48 hours, the only identifiable product (by IR and ³¹P NMR) was Mo(CO)₅P(p-tolyl)₃.¹⁵ Thus, it appears that Pd facilitated hydrogenation of the Cp ligand and subsequent substitution by CO ligands occurs. Because of these unpromising results with molecular hydrogen, a more enlightening avenue was sought.

Upon reaction of $\text{Cp}-(\text{CH}_2)_2-\text{O}_2\text{C}-\text{Mo}(\text{CO})_2\text{P}(\text{p-tolyl})_3$ with LiEt_3BH at room temperature in benzene, the only product observed was the hydride complex $\text{Cp}-(\text{CH}_2)_2\text{OLiMo}(\text{CO})_2\text{P}(\text{p-tolyl})_3\text{H}$ as evidenced by ^1H and ^{31}P NMR. A reasonable mechanism entails the initial formation of the formyl complex thus freeing the bridging arm as the alkoxide. Subsequent decarbonylation of the thermally unstable formyl yields the hydride.¹⁶ Upon changing solvents to toluene- d_8 and going to a lower temperature (-40°C), it is possible to observe the formyl resonance in the proton NMR (14.78 ppm). However, while formyl complexes are of interest with respect to CO reduction, they are readily made without the use of intramolecular compounds. As such, they are not of primary importance, although a formyl complex containing an intramolecular alkoxide group is unique.¹⁷

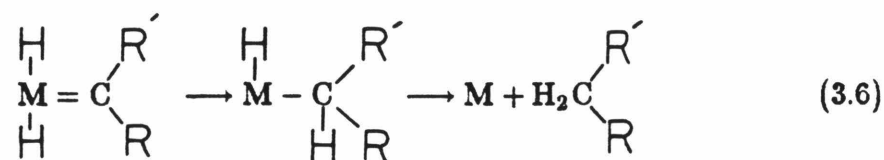
It is of interest, however, to understand the mechanism of formyl formation. Two possibilities are readily apparent: (1) The ester may exist in equilibrium with the alkoxide carbonyl and the hydride simply adds at the carbonyl carbon,



or (2) the hydride may attack at the carbonyl to yield a deprotonated hemiacetal-like compound which then decomposes to the formyl and the alkoxide.



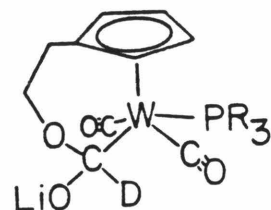
The question is whether or not the intermediate may be detected. The possible intermediate is interesting in that it is quite similar to the product obtained in the first step of a two step mechanism that may be proposed for the hydrogenation of a carbene (eq 3.6):



In fact, the hemiacetal anion is the product expected to result from the reaction of an anionic carbene with one-half of an equivalent of hydrogen. Therefore, the possible intermediacy of a compound of this form is quite intriguing.

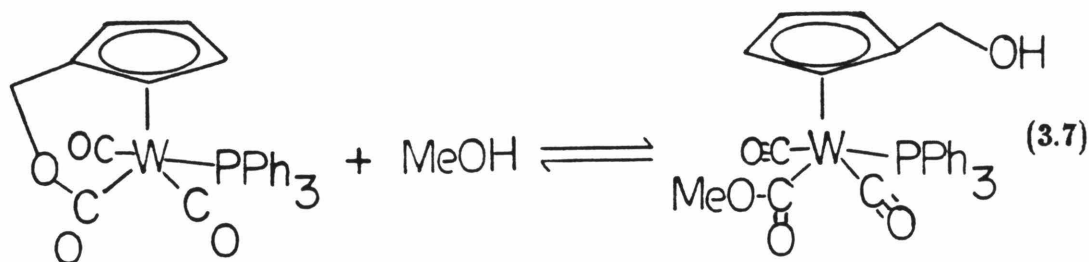
The main difficulty in the NMR monitoring of this species is the number of protons with chemical shifts in the region of interest. The problem is that the hydride is delivered using LiEt_3BH , 1M in THF. To circumvent this, the switch was made to the deuteride and the reaction was monitored by ^2H NMR. This change proved to be fortunate.

Treatment of the ethylene bridged tungsten ester with one equivalent of LiEt_3BD at -50°C in methylene chloride gave rise to a signal in the deuterium NMR at 6.12 ppm.^{18,19} With time at -50°C , the formyl signal became apparent at 15.53 ppm. Attempts to trap the intermediate by reaction with acetic acid to form the hemiacetal at low temperature yielded the hydride complex as well as the tricarbonyl phosphine cation upon warming to room temperature.²⁰ If the hemiacetal was formed, it is unstable at room temperature. The results are indicative of a process in which hydride first adds to the ester carbon to yield a compound of the form:²¹



This then loses alkoxide to produce the formyl.

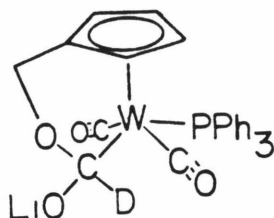
It was considered that the function of alkoxide as a leaving group in formyl formation and the stability of the bridging group to which the oxygen is bound may be related. It was observed earlier that a marked difference in stability may occur upon relatively small structural changes. Removal of one methylene group from the bridging arm in the intramolecular metallaesters is sufficient to force the equilibrium shown below (eq 3.7) almost (if not) completely to the left ($K_{eq} \leq 4 \text{ M}^{-1}$ when $n=1$):



It is conceivable, then, that similar differences would be observed in the reaction with hydride.

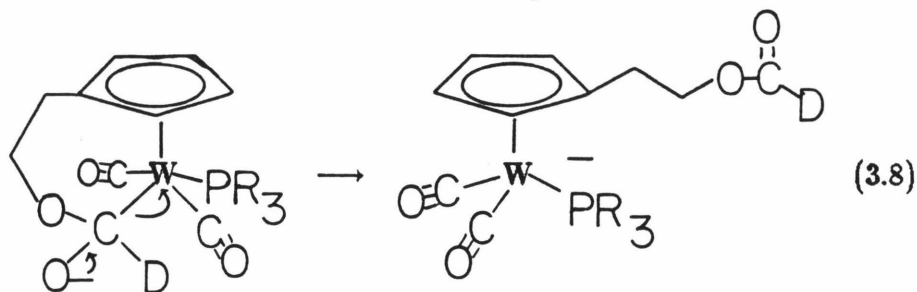
With this in mind, the monomethylene bridged species was reacted with LiEt_3BD under the same conditions as above. A deuterium NMR signal appears at 6.05 ppm. No other signals are present even after two weeks at -50°C except for a signal at 3.6 which is attributed to CH_2DCl from reaction of LiEt_3BD with the solvent. Subsequent warming of the reaction mixture reveals that the

compound is stable for a period of days at room temperature. The infra-red stretches at 1925 and 1832 cm^{-1} indicate an increase of the electron density as would be expected for the new complex. The starting ester has IR stretches at 1957 and 1882 as well as 1598 cm^{-1} . The stretch near 1600 had disappeared altogether. The methylene and Cp proton NMR signals broaden significantly upon formation of the complex. This is consistent with formation of a chiral complex, as the hemiacetal anion is expected to be.



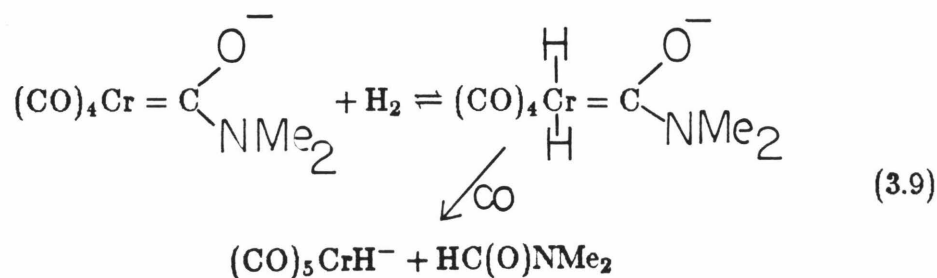
In an attempt to determine how important a role the W-C torsion angle plays in the stability, the reaction with an untethered ester was investigated. Reaction of LiEt_3BD with $\text{CpW}(\text{CO})_2\text{PPh}_3(-\text{CO}_2\text{CH}_2\text{Ph})$ was carried out under the same conditions. As before, a signal at 6.34 was observed in the deuterium NMR yet after being warmed to room temperature for two hours, the hydride signal was observed as well (-6.67 ppm). The indication is that while the torsion does have an effect, there is the intra *vs.* intermolecular effect of the alkoxide to consider as well. Based on the three results, a reasonable explanation of the remarkable stability of the monomethylene bridged species is that it possesses an advantageous mixture of both small torsion angle and intramolecularity. An example of the effect that intramolecularity may impart can be observed in the reaction of hydride with the intramolecular esters. The ethylene bridged complex routinely gave an additional NMR signal at 8.22 ppm

and on one occasion, the methylene bridged compound displayed an additional signal at 8.18 ppm. In the latter case, the Cp-CH₂- signals were indicative of the untethered CpRW(CO)₂PPh₃⁻ complex.²² The benzyl ester did not display any unusual NMR signals upon reaction with hydride. A possible mechanism for the production of a formate ester is shown in eq 3.8.²³



While loss of alkoxide is apparently the favored route with the ethylene bridged and the benzyl esters, the close proximity of the tethered alkoxide that results in the ethylene bridged case allows for the possibility of the secondary reaction to occur. This leads to production of a formate while once PhCH₂O⁻ is formed, it is lost to solution. The methylene bridged ester also offers the opportunity for formate formation even though cleavage is not the favored route of the hemiacetal anion.

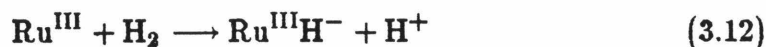
The formate ester-substituted cyclopentadienyl W(CO)₂L anion is quite analogous to the product obtained upon hydrogenation of an anionic chromium carbene (eq 3.9).² However, in this case, hydride is delivered intermolecularly and the product formate remains bound in the metal complex *via* the cyclopentadienyl ring.



It is apparent that two different types of products are possible upon reaction of the esters with hydride; cleaved and cyclic. The amounts of cleaved dicarbonyl phosphine anion and formyl produced are dependent on several factors, including bridging arm length and reaction temperature. Treatment of these compounds with H^+ should produce $W-H$ and $O-H$ bonds respectively.

The production of the uncleaved hydride reduced species is indicative of the type of compound that might be expected from the reaction of a metal hydrido carbene complex upon transfer of one hydride ligand to the organic fragment. It is, however, apparent that further reaction with hydride does not occur, this being clear from the presence of excess unreacted $LiEt_3BD$. Therefore, in this instance, the use of an external hydride reagent may differ from the reaction of a complex that incorporates hydride intramolecularly, where it might be anticipated that a second hydride ligand will not be as hydridic as the first.

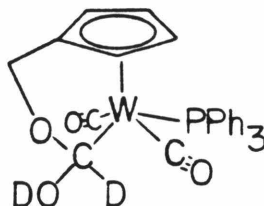
A number of transition-metals have been observed to promote the heterolytic cleavage of hydrogen (eqs 3.10–3.12):^{24,25,26}



Few group VI systems are known, however, although a molybdenum tin system has been used in the reduction of ethylene.²⁷ A proposed step during the process is shown in eq 3.13.

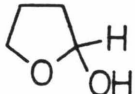
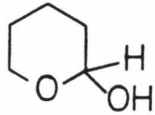
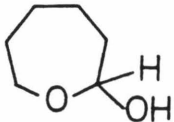


Sequential hydride, proton reaction should be viable and in order to mimic a reaction in which the reaction of H_2 may be considered to occur heterolytically, the compound obtained from hydride reduction of the monomethylene ester was reacted with a proton source, CH_3COOD . Immediately a new signal appeared in the deuterium spectrum at 4.10 ppm. This may be assigned to the -OD group of the metalla-hemiacetal compound:

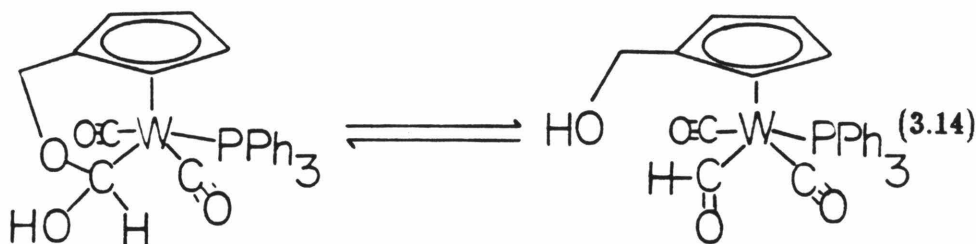


Cyclic organic hemiacetals are known to exist in equilibrium with the open hydroxy-aldehydes. In both the five and six membered ring compounds, the equilibrium favors the hemiacetal, but in the seven membered ring, the open compound is preferred (Table 3.1).²⁸ It has been demonstrated that the in-

Table 3.1. Hemiacetal to Hydroxy Aldehyde Equilibria.

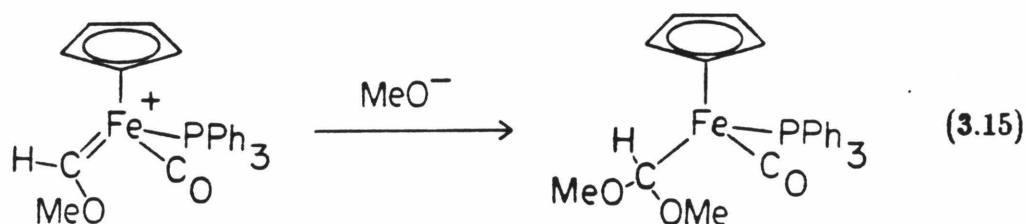
HEMIACETAL \rightleftharpoons HYDROXY ALDEHYDE	% FREE ALDEHYDE	K_{eq}
	11	.124
	6	.064
	85	5.667

tramolecular metallaesters possess stabilities that mimic those observed in lactones (γ more stable than δ , much more stable than ϵ).¹ Unfortunately, it is not possible to examine the trend exhibited by the metalla-hemiacetals. At temperatures where the ethylene bridged complex opens to form the hydroxy-substituted Cp metal-formyl, the formyl decarbonylates irreversibly. However, in the case of the methylene bridged complex, a limiting value of K_{eq} and ΔG may be calculated for the process shown in eq 3.14:



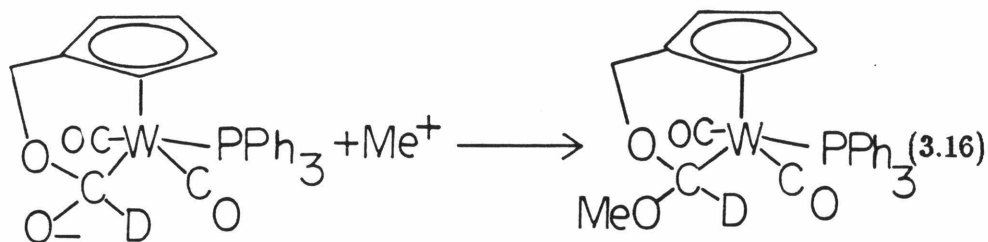
The values obtained are $\leq .100 \pm .013$ and $\geq 1.4 \pm .1$ kcal/mole respectively. Thus, the metalla-hemiacetal is at least as stable as the five and six membered cyclic hemiacetals.

Recently, iron acetal complexes have been synthesized by methoxide attack on a cationic carbene species (eq 3.15).²⁹

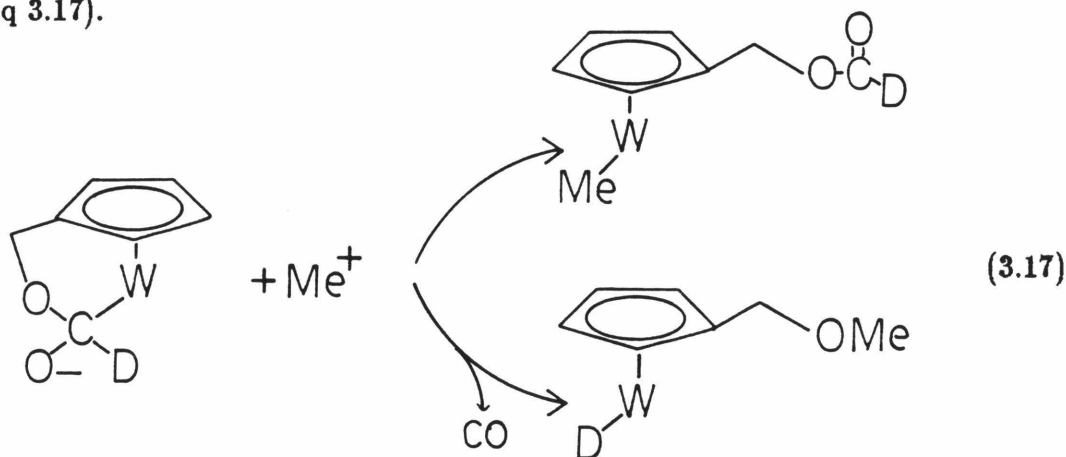


This represents an analogous approach but using methoxide as the nucleophile rather than hydride.

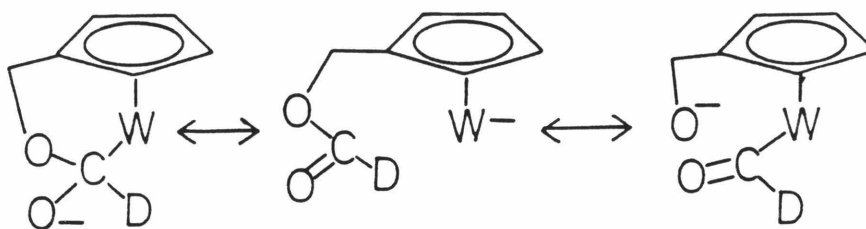
Reaction of the tungsten hemiacetal anion, containing the methylene bridge, with Me^+ yields the tungsten acetal (eq 3.16). NMR and IR spectroscopy provide data consistent with this. The Cp and methylene signals broaden further upon acetal formation, suggesting greater asymmetry is associated with the compound.



Not surprisingly, side reactions occur as well, yielding several products in which the intramolecular bridge has been cleaved. Among the products are a tungsten-methyl complex as well as a methyl ether substituted-Cp compound (eq 3.17).

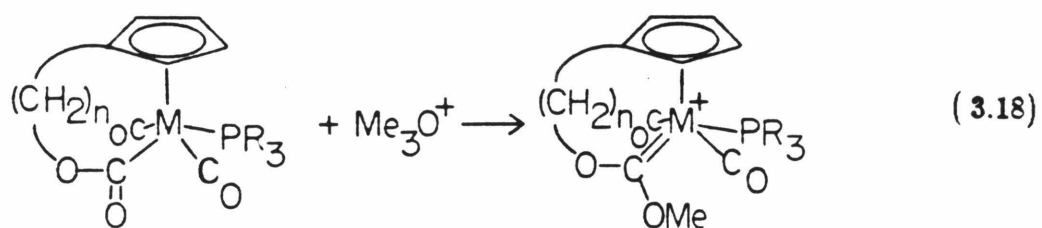


In the deuterium NMR, signals at 8.7 and -6.8 ppm confirm the presence of tungsten-deuteride and formate compounds. These results are consistent with the presence of substantial electron density on both oxygens as well as on the tungsten:



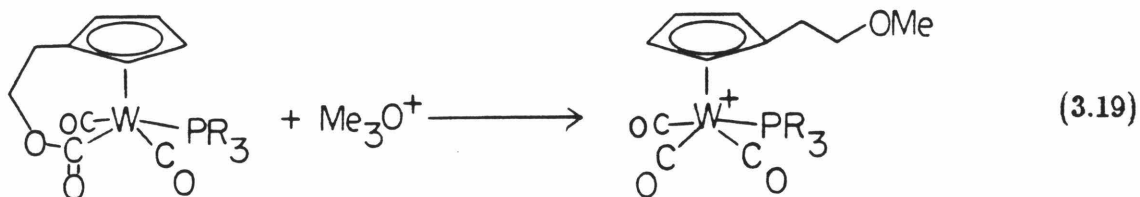
In any event, a model for the H_2 reduction of a metallaester to the corresponding metalla-hemiacetal and to the cleaved formate metal-hydride products has been obtained using H^- and H^+ sequentially as the hydrogen source.

Another interesting reaction would be the combination of metallaesters with alkyl cations in the hope of generating dioxy carbenes. While it has become apparent that the carbenoid resonance is not predominant, it is clear that the ester carbon possesses positive charge as evidenced by reactions with hydride. As such, it is expected that the carbonyl oxygen may possess some negative charge and reaction with Me^+ would be expected to yield the methoxy-intramolecular alkoxy cationic carbene (eq 3.18).³⁰

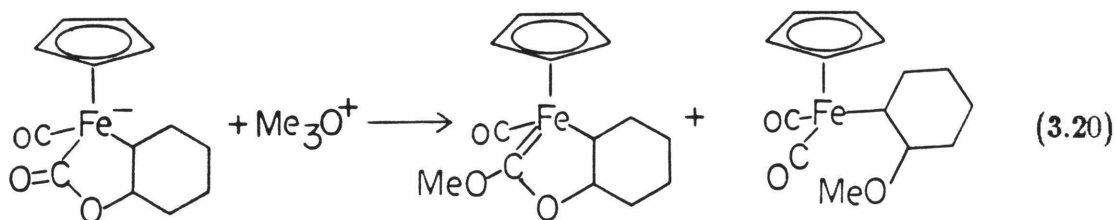


Difficulties may however be encountered because of the torsion about the M-C bond. As has been discussed, when $n = 2$, a disadvantageous torsion angle of 51.2° is obtained.¹ Metal-carbon π bonding is expected to be seriously weakened in such an orientation and indeed, reaction of the ethylene bridged ester with trimethyloxonium leads solely to the cleavage of the intramolecular bridge and the generation of the tricarbonyl phosphine cation along with the

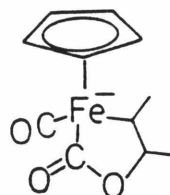
methyl ether substituted cyclopentadienyl ligand (eq 3.19).³¹



It has been observed in the case of an anionic iron intramolecular metal-ester that treatment with Me_3OBF_4 yields an approximately equal mixture of the carbene and the cleaved methyl ether (eq 3.20):³²



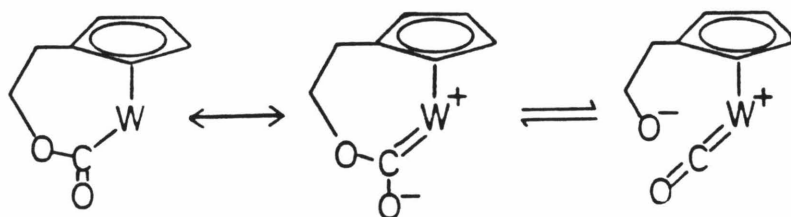
In the analogous situation where the ester shown below is treated with trimethyloxonium, none of the carbene is obtained.³²



A possible explanation is that the cyclohexyl ring serves to better maintain the necessary close proximity of the alkoxide oxygen to the carbonyl, thus making electrophilic attack at the ketonic oxygen competitive with cleavage to form the methyl ether.

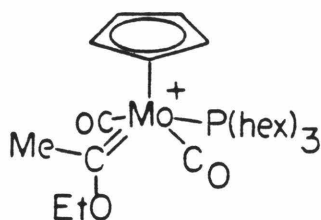
Perhaps not surprisingly then, reaction of the benzyl ester, $\text{CpW}(\text{CO})_2\text{-PPh}_3\text{-}(\text{-CO}_2\text{CH}_2\text{Ph})$, with trimethyloxonium produces the cleaved products as well, the tricarbonylphosphine cation and benzylmethylether. It was with some surprise however, that the monomethylene bridged tungsten ester was observed to react with Me^+ at -50°C to give a cleaved methyl ether- substituted cyclopentadienyl cation similar to that obtained with the ethylene bridged compound.

It is apparent then that instead of a predominance of negative charge residing on the ketonic oxygen, the singly bonded oxygen must have a δ^- associated with it. It may be that reaction of Me^+ at the negatively charged oxygen of the right hand tautomer given below may account for the products. It was expected then that treatment with H^+ should regenerate the starting cationic complex and in fact, treatment with HBF_4 did just that at -50°C .³³



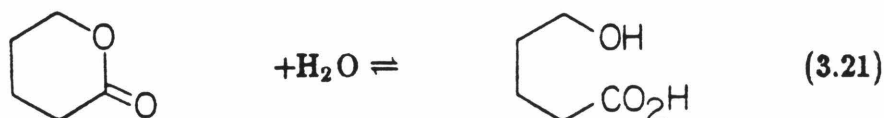
It is known that electrophilic addition to metal acyls to form alkoxy carbenes is dependent on the electron density on the metal center. For example $\text{CpFe}(\text{CO})\text{PPh}_3\text{-}(\text{-C}(\text{O})\text{Me})$ reacts with Me^+ to form the methoxymethyl carbene, but $\text{CpFe}(\text{CO})_2\text{-}(\text{-C}(\text{O})\text{-}p\text{-C}_6\text{H}_4\text{F})$ will not react.³⁵ There are two contributing factors; the more electron withdrawing carbonyl ligand (instead of PPh_3) and the *para*-fluoro phenyl acyl group.

A carbene more closely related to the complexes under investigation is the molybdenum complex:³⁶



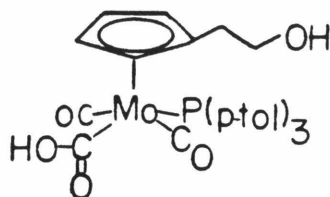
In this case a more basic phosphine is employed thus increasing the electron density on the metal center and facilitating electrophilic attack at the acyl oxygen. The compounds in the current investigation, however, possess less basic aryl phosphines as well as an ester group that is able to accept electron density onto the additional oxygen. These factors contribute to a situation that disfavors carbene formation.³⁷

Finally, since it was shown that the intramolecular metallaesters look and act at least superficially like lactones, their reaction with water to form hydroxy-acid compounds may be possible (eq 3.21).



In this manner, an interesting means of forming metallacarboxylic acids may be encountered. The compound of choice in this reaction is of course the ethylene bridged metallaester since the monomethylene bridged compound has shown little propensity for cleavage by alcohols.

Subsequently, a sample of $\text{Cp}-(\text{CH}_2)_2-\text{O}_2\text{C}-\text{Mo}(\text{CO})_2\text{P}(\text{p-tolyl})_3$ was dissolved in benzene- d_6 and water was introduced. At 25°C little reaction was observed although new signals appeared in the ^1H and ^{31}P NMR that may be assigned to the metallacarboxylic acid ($K_{eq} = .7 \text{ M}^{-1}$):



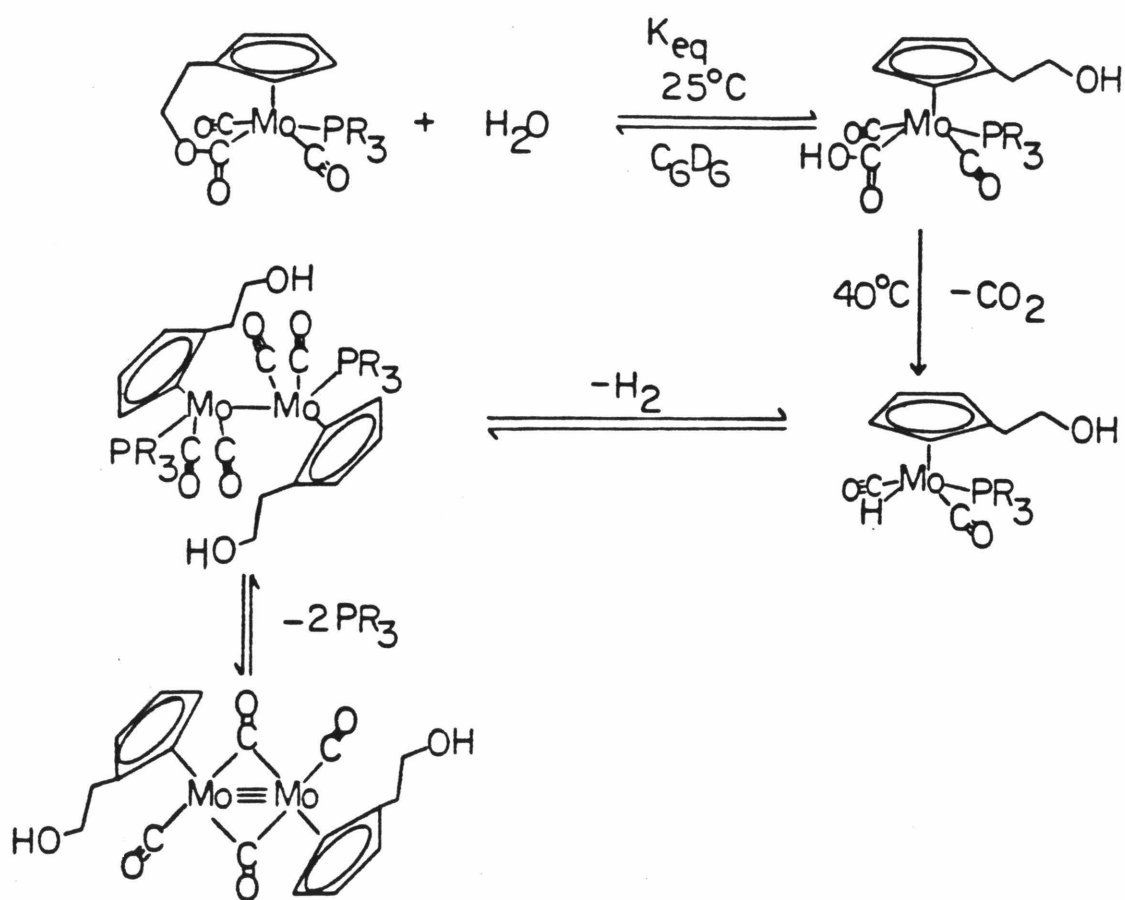
Upon warming to 40°C, the starting material began to disappear and the carboxylic acid was no longer apparent. In their places, two new phosphine containing products as well as free phosphine grew in. A plausible scheme for the reaction is given below (Scheme 3.4).

Independent syntheses of $\text{CpMo}(\text{CO})_2\text{PPh}_3\text{H}$ and $[\text{CpMo}(\text{CO})_2\text{PPh}_3]_2$ confirm the presence of the hydroxyethyl analogs in the reaction mixture. Additionally, the evolution of CO_2 , as evidenced by infra-red spectroscopy, confirms the likelihood of the formation of the metallacarboxylic acid which apparently decarboxylates at 40°C.³⁸

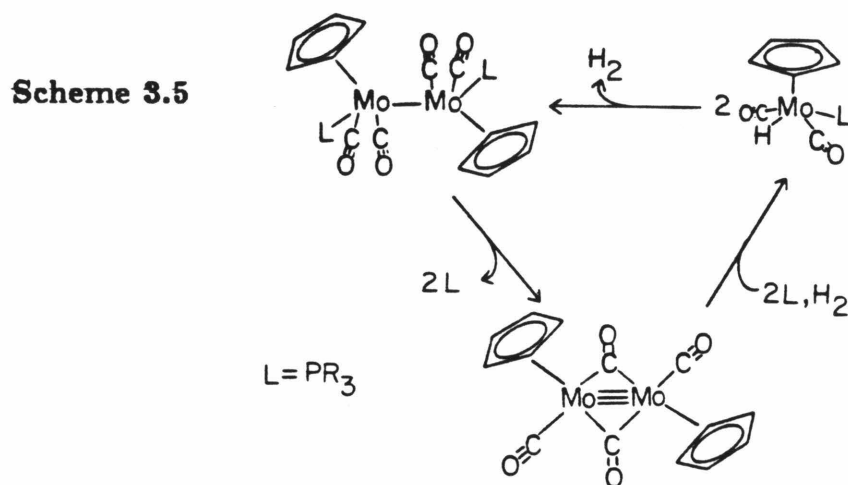
An intriguing result is that with time, the ^1H NMR signal due to the hydride does not completely disappear nor does that of the singly bonded dimer. The indication is that with dihydrogen present as well as free phosphine, equilibria are established. It is known however that $[\text{CpMo}(\text{CO})_3]_2$ does not react with H_2 to form the tricarbonyl hydride at least under conditions not too far removed from those used in this case.³⁹

To test the validity of our proposal of the formation of the hydride from the dicarbonyl phosphine dimer, a sample of $[\text{CpMo}(\text{CO})_2\text{PPh}_3]_2$ (contaminated with $[\text{CpMo}(\text{CO})_2]_2$ and free PPh_3) was sealed in an NMR tube in benzene- d_6 under 600 torr of H_2 . Upon warming, the hydride resonances became apparent. Of particular interest is the result that upon sitting for an extended period of time at room temperature, all of the Mo containing compounds were converted

Scheme 3.4



to the dicarbonyl phosphine hydride.⁴⁰ Thus, not only is the formation of the hydride possible, it is favored under fairly low hydrogen pressures and low temperatures. Of course, rather than the equilibria indicated in Scheme 3.4, it may be that the formation of the hydride occurs *via* the triply bonded dimer (Scheme 3.5).⁴²



This may explain why $[\text{CpMo}(\text{CO})_3]_2$ does not react with hydrogen since the formation of the triply bonded dimer requires elevated temperatures (100–120°C).⁴³ It has been shown that under the conditions necessary for formation of the triply bonded dimer from the single bonded carbonyl complex, homolytic Mo–Mo cleavage occurs. This is followed by CO loss and recombination to form the product dimer.⁴⁴ Presumably, the conditions used in the present study are not vigorous enough for Mo–Mo cleavage and the difference in reactivity is due to an alternate low energy pathway. In any event, Scheme 3.5 may represent an effective tripartite equilibrium.

The scheme as a whole (Scheme 3.4) represents in effect a stoichiometric water-gas shift reaction (WGSR), since coordinated carbon monoxide is oxidized to CO_2 and the protons from water are converted to H_2 at 50% efficiency.

While the process shown is of little practical utility (there is no simple means of recycling the final organometallic products to the starting ester), it is of interest that the reaction proceeds under such mild conditions.³⁸ Typically, the mildest conditions employed entail the use of 100°C and approximately 1 atm of H₂.⁴⁵

An advantage of low temperatures lies in the equilibrium constant associated with the WGSR (eq 3.22):



At 127°C, $K_{eq} = 1.45 \times 10^5$ while at elevated temperatures the value decreases substantially (e.g., $K_{eq} = 26.9$ at 327°C).⁴⁶

In conclusion, it is quite apparent that the intramolecular metallaesters possess properties and reactivities that make them of interest in a number of areas. They are of use in the model studies of the reduction of bound carbon monoxide, they react with water under mild conditions to produce water-gas shift products and they allow for a detailed investigation of the relationship between structural changes and the resulting thermodynamic stabilities. They have proven their usefulness in the area of bifunctional catalyst design. Since the syntheses and properties of the group VI compounds are fairly well worked out, the opportunity exists to synthesize other esters of more reactive transition metals. The possibilities for a number of exciting systems are quite broad and an investigation of these should prove to be extremely valuable and fruitful.

Experimental

LiEt₃BH, LiEt₃BD (both as 1M solutions in THF) and HBF₄-Me₂O were purchased from Aldrich. CH₃COOD (98 atom % D), Me₃OBF₄ and MeO₂CCF₃ were purchased from Alfa. CO/H₂ (certified 50.6 % CO) was purchased from Scott Specialty Gases.

All reactions were carried using standard Schlenk techniques. Argon used in Schlenk work was purified by passage through BASF RS-11 (Chemalog) and Linde 4 Å molecular sieves. Benzene-d₆ and toluene-d₈ were vacuum transferred from sodium benzophenone ketyl prior to use. Methylene chloride-d₂ was stirred over CaH₂ and CH₂Cl₂ was stirred over P₂O₅ and both were vacuum transferred prior to use. Infra-red spectra were obtained on a Beckman IR 4240 spectrometer referenced to the 1601 cm⁻¹ stretch of polystyrene. Fourier transform ³¹P, ¹H and ²H NMR spectra were taken on a JEOL FX-90Q operating at 36.2, 89.56 and 13.70 MHz respectively. All ³¹P spectra were referenced to an external sample of the appropriate free phosphine in the relevant solvent. ²H NMR spectra utilized an internal lithium lock and were referenced to (CD₃)₂CO (2.04 ppm).

The parent compounds, CpMo(CO)₂PPh₃H ⁴¹ and [CpMo(CO)₂PPh₃]₂ ⁴⁴ were prepared using literature methods.

Pressure Bottle Reactions

Pressure bottle reactions were carried out using a glass pressure bottle topped with a pressure head equipped with a pressure gauge, inlet valve, safety valve set to release at 100 psi and a ball valve fitted with a septum to allow for

gas sampling.

Generally, the sample being investigated was loaded into an NMR tube under nitrogen, dissolved in 400 μL of the appropriate solvent (usually C_6D_6) and placed in the pressure bottle. Ten mL of the solvent were then added to the pressure bottle to serve as heat transfer agent. The pressure head was then fitted and tightened, being sealed using a Teflon O-ring. The bottle was then flushed three times with 50 psi of the CO/H_2 mixture and finally pressured up to 50 psi. The temperature was then raised to 90° or 100° C using an oil bath.

The reaction was monitored by gas chromatography of both vapor and liquid samples on a Varian 1400 GC equipped with N_2 carrier gas and a flame ionization detector, using either an 18 foot 20 % CW20M/ Chromosorb P or a 9 foot Porapak Q column at 150° C. The reaction was also monitored by occasional NMR; pressure would be released, the tube removed under argon followed by reintroduction to the pressure bottle after the spectrum was obtained. Finally, the sample was analyzed by infra-red.

Hydride Reactions

All hydride (and deuteride) reactions were carried out in the following manner: The sample to be reacted was loaded into an NMR tube under N_2 , the tube then being sealed with a septum. The appropriate solvent (usually CD_2Cl_2 or CH_2Cl_2) was then introduced (either *via* syringe or by vacuum transfer) and the solution was cooled to -50° C before injection of one equivalent of the hydride (or deuteride) as a 1M solution in THF. The reactions were then monitored by NMR at the appropriate probe temperature, this being varied as the reaction

progressed.

Tungsten (Methylene bridge): ^2H NMR (CH_2Cl_2), W-CD 6.05; ^{31}P NMR, 38.90; IR (CH_2Cl_2), νCO , 1925 (m), 1832 (s).

Starting the reaction at room temperature: ^2H NMR (CH_2Cl_2), W-CDO 15.25, $-\text{O}_2\text{CD}$ 8.15, W-CD 6.09.

Tungsten (Ethylene bridge): ^2H NMR (CH_2Cl_2), W-CDO 15.53, $-\text{O}_2\text{CD}$ 8.22, W-CD 6.16.

Trimethyloxonium Reactions

In the cases of the ethylene bridged and the benzyl tungsten metalloesters, reaction was carried out in C_6D_6 in an NMR tube under nitrogen. One equivalent of Me_3OBF_4 was added and the mixture was warmed to 50°C . Starting material was observed to decrease with concurrent precipitation of a yellow solid which was isolated and redissolved in CD_2Cl_2 . NMR indicated the presence of the tricarbonylphosphine cations and the methyl ethers.

Ethylene bridge: ^1H NMR $(\text{CD}_3)_2\text{CO}$, p-tol 7.73-7.14 (m, 12H), CpR H_2 & H_5 6.23 (AA'BB', 2H), CpR H_3 & H_4 5.91 (AA'BB', 2H), $-\text{CH}_2-\text{O}$ 3.72 (t, 2H), $-\text{OMe}$ 3.20 (s, 3H), CpCH₂ 2.73 (t, 2H), $-\text{Me}$ 2.44 (s, 9H); ^{31}P NMR $(\text{CD}_3)_2\text{CO}$, 19.79 (s w/ small d, $J=188\text{ Hz}$).

Benzyl ester: ^1H NMR $(\text{CD}_3)_2\text{CO}$, Ph 7.79-7.23 (m, 21H), Cp 6.21 (s, 5H), $-\text{CH}_2-$ 4.61 (s, 2H), $-\text{Me}$ 2.80 (s, 3H); ^{31}P NMR $(\text{CD}_3)_2\text{CO}$, 19.79 (s w/ small d, $J=188\text{ Hz}$).

In the case of the monomethylene bridged tungsten metalloester, reaction be-

tween one equivalent of the ester and Me_3OBF_4 was carried out at -50°C in CD_2Cl_2 under argon. The methyl ether-substituted-cyclopentadienyl tungsten tricarbonyl phosphine cation was the sole product.

^1H NMR (CD_2Cl_2), CpR H_2 & H_5 5.96 (AA'BB', 2H), CpR H_3 & H_4 5.42 (AA'BB', 2H), $-\text{CH}_2\text{O}$ 4.42 (s, 2H), O-Me 3.20 (s, 3H).

Reaction with Fluoroboric Acid

To an NMR tube containing approximately 5 mg of $\text{CpCH}_2\text{O}_2\text{C-W}(\text{CO})_2\text{-PPh}_3$ in CD_2Cl_2 at -50°C under argon was added 2 μL of $\text{HBF}_4\text{-Me}_2\text{O}$. Formation of only $[\text{CpCH}_2\text{OH}(\text{CO})_3\text{PPh}_3]^+$ was observed. ^1H NMR (CD_2Cl_2), CpR H_2 & H_5 5.93 (AA'BB', 2H), CpR H_3 & H_4 5.47 (AA'BB', 2H), $-\text{CH}_2\text{O}$ 4.43 (s, 2H), $-\text{OH}$ not observed.

Metallohemiacetal

To the product obtained from reaction of $\text{CpCH}_2\text{O}_2\text{C-W}(\text{CO})_2\text{PPh}_3$ and LiEt_3BD in CH_2Cl_2 was added one equivalent of CH_3COOD under argon, at room temperature in an NMR tube. The reaction was monitored by ^2H NMR: ^2H NMR (CH_2Cl_2): C-D 5.91, $-\text{OD}$ 4.10.

Metalloacetal

10 mg of the methylene bridged ester (.016 mmol) were loaded into an NMR tube under nitrogen and dissolved in 350 μL of methylene chloride. After

cooling to -50°C , one equivalent of LiEt_3BD (1M in THF) was added and the mixture was left at -50°C for 12 h. Deuterium NMR indicated the presence of the hemiacetal anion. The mixture was then warmed to room temperature and solvent was removed under reduced pressure. The material was redissolved in $350\text{ }\mu\text{L}$ of CD_2Cl_2 and again cooled to -50°C at which point 5mg of Me_3OBF_4 was added.

During reaction, the NMR signals of the starting anion broadened substantially and dimethyl ether was observed to grow in. After 2 h, the mixture was warmed to room temperature and solvent was removed under reduced pressure. ^1H NMR (CD_2Cl_2 , tethered Cp 5.86 and 4.54 (broad m), untethered Cp 5.15 and 4.95 (m), $-\text{CH}_2\text{-O}$ (untethered) 4.13 (s), W-COCH_3 3.27 (s), $-\text{OMe}$ 2.88 (s), W-CH_3 .41 (d, $J=3$ Hz); ^{31}P NMR (CD_2Cl_2), 46.77, 27.59; ^2H NMR (toluene), O_2CD 8.68, W-D -6.80 ; ^2H NMR (CH_2Cl_2), W-CD 6.02; IR (CH_2Cl_2), νCO , 1960(s), 1915(ms), 1880(m), 1850(sh).

$\text{CpW}(\text{CO})_2\text{PPh}_3\text{Me}^{47}$: ^1H NMR (CDCl_3), Cp 4.82 (d, $J=1.8$ Hz), Me .54 (d, $J=2.8$ Hz); IR (CH_2Cl_2), νCO , 1927(s), 1842(s).

$\text{CpW}(\text{CO})_2\text{PPh}_3\text{H}^{41}$: ^1H NMR (CDCl_3), Cp 5.25 (s), $-\text{H}$ -6.00 (d, $J=54$ Hz); IR (C_6H_{12}), νCO , 1962(s), 1876(s).

$\text{Cp}(\text{CH}_2)_2\text{O}_2\text{C Mo}(\text{CO})_2\text{P}(\text{p tolyl})_3 + \text{H}_2\text{O}$

Twenty mg of the metalloester (.034 mmol) were loaded into an NMR tube under N_2 and dissolved in $350\text{ }\mu\text{L}$ of C_6D_6 . The reaction was monitored by NMR.

At 25° C one new ^{31}P NMR signal at 84.00 was observed. Upon warming to 40° C this disappeared and was replaced by additional signals (including free phosphine):

$\text{Cp}(\text{CH}_2)_2\text{OHMo}(\text{CO})_2\text{P}(\text{P-tolyl})_3\text{H}$: ^{31}P NMR 77.74; ^1H NMR -H -4.98 (d, $J_{\text{PH}} = 49$ Hz).

$[\text{Cp}(\text{CH}_2)_2\text{OHMo}(\text{CO})_2\text{P}(\text{p-tolyl})_3]_2$: ^{31}P NMR 80.56 (s).

These compare quite well with authentic samples of the unsubstituted compounds:

$\text{CpMo}(\text{CO})_2\text{PPh}_3\text{H}$: ^{31}P NMR (C_6D_6), 78.34; ^1H NMR (C_6D_6), -H -4.96 (d, $J_{\text{PH}} = 49$ Hz).

$[\text{CpMo}(\text{CO})_2\text{PPh}_3]_2$: ^{31}P NMR (C_6D_6), 80.50 (s).

Synthesis of $\text{CpMo}(\text{CO})_2\text{PPh}_3\text{H}$ Using H_2

A mixture containing $[\text{CpMo}(\text{CO})_2\text{PPh}_3]_2$, $[\text{CpMo}(\text{CO})_2]_2$ and PPh_3 was loaded into an NMR tube under N_2 . The solid was dissolved in 350 μL of C_6D_6 giving a red solution. The NMR tube was then placed on a Schlenk line by means of a Teflon adapter fitted with O-ring seals. The solution was frozen with liquid nitrogen and evacuated. The tube was then back filled with 600 torr of hydrogen and flame sealed (Caution).

After heating at 40° C for 15 h, hydride resonances were observed at -4.99 ppm (d, $J = 50$ Hz). Upon sitting at room temperature for one month, the color of the solution had changed to yellow and only the hydride product was obtained:

$\text{CpMo}(\text{CO})_2\text{PPh}_3\text{H}$: ^1H NMR (C_6D_6), Cp 4.74 (s, 5H), -H -5.12 (1H, d, $J = 50$

Hz); ^{31}P NMR (C_6D_6), 78.48 (s).

Notes and References

- (1) See Chapter 2, this thesis.
- (2) 130° C and 35 psi of hydrogen: Doxsee, K.M.; Grubbs, R.H. *J. Am. Chem. Soc.* **1981**, *103*, 7696-7698.
- (3) McCarron, E.M., III; Harlow, R.L. *J. Am. Chem. Soc.* **1983**, *105*, 6179-6181.
- (4) Aneke, L.E.; den Ridder, J.J.J.; van den Berg, P.J. *Recl. Trav. Chim. Phys.-Bas.* **1981**, *100*, 236-240.
- (5) Sexton, B.A. *Surf. Sci.* **1979**, *88*, 299.
- (6) Luth, H.; Rubloff, G.W.; Grobman, W.D. *Surf. Sci.* **1977**, *63*, 325.
- (7) Rubloff, G.W.; Demuth, J.E. *J. Vac. Sci. Technol.* **1977**, *14*, 419.
- (8) Egelhoff, W.F.; Linnett, J.W.; Perry, D.L. *Faraday Dis. Chem Soc.* **1975**, *60*, 127.
- (9) Sexton, B.A. *Surf. Sci.* **1981**, *102*, 271-281.
- (10) Nugent, W.A.; Ovenall, D.W.; Holmes, S.J. *Organometallics* **1983**, *2*, 161-162.
- (11) Yoshida, T.; Okano, T.; Ueda, Y.; Otsuka, S. *J. Am. Chem. Soc.* **1981**, *103*, 3411.
- (12) Bennett, M.A.; Yoshida, T. *J. Am. Chem. Soc.* **1978**, *100*, 1750.
- (13) Michelin, R.A.; Napoli, .; Ros, R. *J. Organomet. Chem.* **1979**, *175*, 239.
- (14) Reaction under 50 psi of H₂ yields decomposition products similar to those obtained in the thermolysis; no volatile organic products were in evidence.
- (15) Mo(CO)₅PPh₃ displays a ³¹P NMR signal at 31.5 ppm downfield from free

PPh_3 in methylene chloride and IR CO stretches at 2074(m), 1987(vw) and 1950(vs) in cyclohexane: Grim, S.O.; Wheatland, D.A.; McFarlane, W. *J. Am. Chem. Soc.* **1967**, *89*, 5573-5577.

(16) In a manner similar to that reported by: Tam, W.; Wong, W.-K.; Gladysz, J.A. *J. Am. Chem. Soc.* **1979**, *101*, 1589-1591.

(17) Good yields of the parent formyl compound have recently been reported: Gibson, D.H.; Owens, K.; Ong, T.-S. *J. Am. Chem. Soc.* **1984**, *106*, 1125-1127.

(18) In retrospect, a singlet was present in the earlier ^1H NMR spectrum at 6.04 ppm.

(19) Molybdate clusters containing acetal functionalities have been reported to display proton resonances at 6.12, 6.05 and 5.83 ppm in CD_2Cl_2 : Day, V.W.; Thompson, M.R.; Day, C.S.; Klemperer, W.G.; Liu, R.-S. *J. Am. Chem. Soc.* **1980**, *102*, 5973-5974.

(20) Presumably from cleavage of the intermediate and unreacted starting metalloester.

(21) In a manner similar to L-selectride reduction of organic ketones to alcohols: Brown, H.C.; Krishnamurthy, S. *J. Am. Chem. Soc.* **1972**, *94* 7159.

(22) ^1H NMR signals are at: 4.96 (CpR H_2 & H_5), 4.67 (CpR H_3 & H_4), 3.54 (- CH_2 -).

(23) This is similar to the decomposition pathway observed for hydroxy carbenes, Ref 33.

(24) Wilmarth, W.K.; Kapanan, A.F. *J. Am. Chem. Soc.* **1956**, *78*, 1308.

(25) Harrod, J.F.; Ciccone, S.; Halpern, J. *Can. J. Chem.* **1961**, *39*, 1372.

(26) Krushch, A.P.; Shilov, A.E. *Kinet. Catal. (USSR)* **1970**, *11*, 67.

(27) Chatt, J.; Halpern, J., in "Catalysis: Progress in Research," Basolo, F.;

Burwell, R.L. Jr., eds., Plenum: London (1973).

(28) Streitwieser, A., Jr.; Heathcock, C.H., "Introduction to Organic Chemistry"; Macmillan: New York (1976).

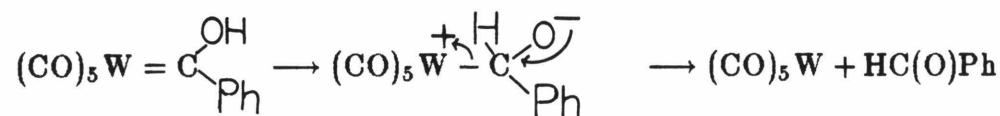
(29) Casey, C.P.; Tukada, H.; Miles, W.H. *Organometallics*, **1982**, *1*, 1083-1084.

(30) Priester, W.; Rosenblum, M. *J. Chem. Soc., Chem. Commun.* **1978**, 26.

(31) Kubáček, P.; Hoffmann, R.; Havlas, Z. *Organometallics* **1982**, *1*, 180.

(32) Klemarczyk, P.; Price, T.; Priester, W.; Rosenblum, M. *J. Organomet. Chem.* **1977**, *139*, C25-C28.

(33) While hydroxycarbenes are known,³⁴ if a hydroxycarbene were made it might be expected to be additionally unstable because of the availability of the decomposition route observed in other hydroxycarbenes:



Fischer, E.O.; Kiener, V. *J. Organomet. Chem.* **1970**, *23*, 215.

(34) (a) Fischer, E.O.; Maasböl, A. *Angew. Chem. Intl. Ed. Engl.* **1964**, *3*, 580. (b) Fischer, E.O.; Kreis, G.; Kreissl, F.R. *J. Organomet. Chem.* **1973**, *56*, C37.

(35) Treichel, P.M.; Wagner, K.P. *J. Organomet. Chem.* **1975**, *88*, 199-206.

(36) Green, M.L.H.; Mitchard, L.C.; Swanwick, M.G. *J. Chem. Soc. A* **1971**, 794.

(37) Dioxocarbenes are known, but frequently employ either cyclic carbene groups or basic ligands. See for example: (a) Motschi, H.; Angelici, R.J. *Organometallics* **1982**, *1*, 343-349. (b) ref. 30.

(38) The iron carboxylic acid, $\text{CpFe}(\text{CO})_2\text{COOH}$ decomposes at room temper-

ature to yield H₂ and CO₂: Crice, N.; Kau, S.C.; Pettit, R. *J. Am. Chem. Soc.* **1979**, *101*, 1627.

(39) Bergman, R.G. *personal communication*.

(40) In fact, this process may be of interest as a synthetic means of obtaining CpMo(CO)₂PR₃H since it entails fewer steps than that of the literature method⁴¹ and is apparently quantitative with time.

(41) Bainbridge, A.; Craig, P.J.; Green, M. *J. Chem. Soc. A.* **1968**, 2715-2718.

(42) Merola, J. *personal communication*.

(43) Klingler, R.; Butler, W.M.; Curtis, M.D. *J. Am. Chem. Soc.* **1975**, *97*, 3535.

(44) Curtis, M.D.; Klingler, R.J. *J. Organomet. Chem.* **1978**, *161*, 23-37.

(45) See for example, a number of studies described in "Catalytic Activation of Carbon Monoxide", Ford, P.C., ed., American Chemical Society: Washington, D.C. (1981).

(46) Kassel, L.S. *J. Amer. Chem. Soc.* **1934**, *56*, 1838-1842.

(47) Barnett, K.W.; Treichel, P.M. *Inorg. Chem.* **1967**, *6*, 294.